



(51) International Patent Classification:

A61K 35/741 (2015.01) *A61K 35/744* (2015.01)
A61K 35/742 (2015.01) *A61K 35/745* (2015.01)

(21) International Application Number:

PCT/US2016/053073

(22) International Filing Date:

22 September 2016 (22.09.2016)

(25) Filing Language:

English

(26) Publication Language:

English

(30) Priority Data:

62/222,034 22 September 2015 (22.09.2015) US

(71) Applicant: MAYO FOUNDATION FOR MEDICAL
EDUCATION AND RESEARCH [US/US]; 200 First
Street S.W., Rochester, Minnesota 55905 (US).

(72) Inventors; and

(71) Applicants : KASHYAP, Purna C. [IN/US]; 2126 Glen-
view Ln N.E., Rochester, Minnesota 55906-8398 (US).
BATTAGLIOLI, Eric J. [US/US]; 419 15th Street S.W.,
Rochester, Minnesota 55902-2152 (US). HALE, Vanessa
L. [US/US]; 1912 10th Street N.E., Rochester, Minnesota
55906-7168 (US).(74) Agents: WILLIS, Margaret S. J. et al.; Fish & Richard-
son P.C., PO Box 1022, Minneapolis, Minnesota 55440-
1022 (US).(81) Designated States (unless otherwise indicated, for every
kind of national protection available): AE, AG, AL, AM,

AO, AT, AU, AZ, BA, BB, BG, BH, BN, BR, BW, BY,
BZ, CA, CH, CL, CN, CO, CR, CU, CZ, DE, DK, DM,
DO, DZ, EC, EE, EG, ES, FI, GB, GD, GE, GH, GM, GT,
HN, HR, HU, ID, IL, IN, IR, IS, JP, KE, KG, KN, KP, KR,
KW, KZ, LA, LC, LK, LR, LS, LU, LY, MA, MD, ME,
MG, MK, MN, MW, MX, MY, MZ, NA, NG, NI, NO, NZ,
OM, PA, PE, PG, PH, PL, PT, QA, RO, RS, RU, RW, SA,
SC, SD, SE, SG, SK, SL, SM, ST, SV, SY, TH, TJ, TM,
TN, TR, TT, TZ, UA, UG, US, UZ, VC, VN, ZA, ZM,
ZW.

(84) Designated States (unless otherwise indicated, for every
kind of regional protection available): ARIPO (BW, GH,
GM, KE, LR, LS, MW, MZ, NA, RW, SD, SL, ST, SZ,
TZ, UG, ZM, ZW), Eurasian (AM, AZ, BY, KG, KZ, RU,
TJ, TM), European (AL, AT, BE, BG, CH, CY, CZ, DE,
DK, EE, ES, FI, FR, GB, GR, HR, HU, IE, IS, IT, LT, LU,
LV, MC, MK, MT, NL, NO, PL, PT, RO, RS, SE, SI, SK,
SM, TR), OAPI (BF, BJ, CF, CG, CI, CM, GA, GN, GQ,
GW, KM, ML, MR, NE, SN, TD, TG).

Declarations under Rule 4.17:

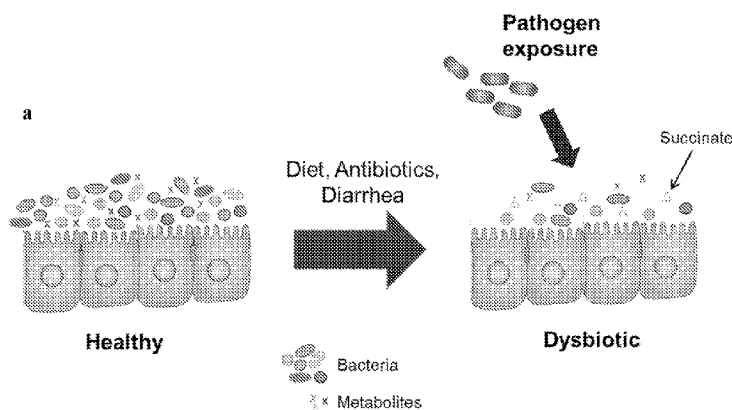
- as to applicant's entitlement to apply for and be granted a patent (Rule 4.17(ii))
- as to the applicant's entitlement to claim the priority of the earlier application (Rule 4.17(iii))

Published:

- with international search report (Art. 21(3))

(54) Title: METHODS AND MATERIALS FOR USING BIOMARKERS WHICH PREDICT SUSCEPTIBILITY TO *CLOSTRIDIUM DIFFICILE* INFECTION

FIG. 1



(57) **Abstract:** This document relates to biomarkers of gut microbiota dysbiosis. Bacteria that are increased or decreased in gut microbiota dysbiosis can be used as biomarkers to predict dysbiosis in patients with diarrhea and/or to predict susceptibility to *Clostridium difficile* infection (CDI). In addition, provided herein are compositions including at least three bacteria that are decreased in gut microbiota dysbiosis which can be used, for example, to restore healthy gut microbiota (e.g., by probiotic or by fecal microbiota transplant) to treat CDI.

METHODS AND MATERIALS FOR USING BIOMARKERS WHICH PREDICT SUSCEPTIBILITY TO *CLOSTRIDIUM DIFFICILE* INFECTION

CROSS-REFERENCE TO RELATED APPLICATIONS

This application claims priority to U.S. Application Serial No. 62/222,034, filed
5 on September 22, 2015. The disclosure of the prior application is considered part of the
disclosure of this application, and is incorporated in its entirety into this application.

BACKGROUND

1. Technical Field

This document relates to biomarkers of gut microbiota dysbiosis which can
10 predict dysbiosis and/or predict susceptibility to *Clostridium difficile* infection, as well as
compositions and methods for treating and/or preventing *C. difficile* infection.

2. Background Information

Hospital-acquired infections are a major cause of morbidity and mortality. *C.*
15 *difficile* infections cause nearly half a million illnesses each year, and 1 in 11 people 65
and older died within a month of *C. difficile* infection diagnoses (Lessa et al. 2015 *N Engl*
J Med 372:825-834). However, antibiotics reduce gut microbiome diversity, alter the
metabolic landscape (Theriot et al. 2014 *Nat Commun* 5:3114-3114), and enable pathogen
invasion – indicating that disturbances increase ecosystem vulnerability. Notably, risk
20 factors associated with *C. difficile* infection (CDI) in humans extend beyond antibiotic use
and include altered motility states such as diarrhea (Ferreyra et al. 2014 *Cell Host*
Microbe 16:770-777).

SUMMARY

This document relates to biomarkers of gut microbiota dysbiosis. For example,
25 this document provides biomarkers which predict susceptibility to CDI and targeted
therapeutics to prevent CDI. Enteric pathogens can induce diarrhea (one of the most
common symptoms of gastrointestinal disorders such as CDI), and can significantly
remodel the gut microenvironment.

As described herein, a subset of patients with diarrhea has an altered gut
30 microbiota (*i.e.*, dysbiosis) relative to healthy individuals, but a gut microbiome that is
similar to individuals with *C. difficile* infection. Bacteria that are increased or decreased

in gut microbiota dysbiosis can be used as biomarkers to predict dysbiosis in patients with diarrhea and/or to predict susceptibility to CDI. In addition, provided herein are compositions including bacteria that are decreased in dysbiosis which can be used, for example, to restore healthy gut microbiota (*e.g.*, by probiotic or by fecal microbiota transplant (FMT)) to prevent and/or treat CDI. For example, prophylactic FMT with a healthy microbial community restructured the metabolic landscape, restoring colonization resistance to *C. difficile*. A lack of colonization resistance, defined with simple stool metabolic parameters, can be an inherent phenotype of the microbiome, and can be corrected by introducing a diverse microbial community. The ability to identify at-risk individuals using simple noninvasive metrics and restore colonization resistance through FMT represents a novel approach to the prevention of diseases like CDI, especially among hospitalized and immunocompromised patients.

In general, one aspect of this document features a method for predicting dysbiosis in a mammal with diarrhea. The method includes, or consists essentially of, determining the amount of at least one biomarker of gut microbiota dysbiosis in a fecal sample obtained from the mammal and identifying the mammal as having dysbiosis if the amount of the at least one biomarker of gut microbiota is altered relative to a mammal without diarrhea. The alteration in gut microbiota can be a decrease in at least one of *Roseburia*, *Faecalibacterium*, *Akkermansia*, *Bacteroides*, or *Blautia*. The alteration in gut microbiota can be an increase in at least one of *Escherichia*, *Shigella*, *Enterobacter*, *Enterococcus*, or *Parasutterella*. In some cases, the alteration in gut microbiota can include both a decrease in at least one of *Roseburia*, *Faecalibacterium*, *Akkermansia*, *Bacteroides*, or *Blautia* and an increase in at least one of *Escherichia*, *Shigella*, *Enterobacter*, *Enterococcus*, or *Parasutterella*. The mammal can be a human. The human can exhibit at least one clinical biomarker of dysbiosis (*e.g.*, current/recent hospitalization, immune suppression, recent/current antibiotic use, and prior *C. difficile* infection).

In another aspect, this document features a method for predicting susceptibility to *C. difficile* infection in a mammal with diarrhea. The method includes, or consists essentially of, determining the amount of at least one biomarker of gut microbiota dysbiosis in a fecal sample obtained from the mammal and identifying the mammal as having increased susceptibility to *C. difficile* infection if the amount of the at least one biomarker of gut microbiota is altered relative to a mammal without diarrhea. The alteration in gut microbiota can be a decrease in at least one of *Roseburia*,

Faecalibacterium, *Akkermansia*, *Bacteroides*, or *Blautia*. The alteration in gut microbiota can be an increase in at least one of *Escherichia*, *Shigella*, *Enterobacter*, *Enterococcus*, or *Parasutterella*. In some cases, the alteration in gut microbiota includes both a decrease in at least one of *Roseburia*, *Faecalibacterium*, *Akkermansia*, *Bacteroides*, or *Blautia* and an increase in at least one of *Escherichia*, *Shigella*, *Enterobacter*, *Enterococcus*, or *Parasutterella*. The mammal can be a human. The human can exhibit at least one clinical biomarker of dysbiosis (e.g., current/recent hospitalization, immune suppression, recent/current antibiotic use, and prior *C. difficile* infection).

In another aspect, this document features a method for treating *C. difficile* infection in a mammal. The method includes, or consists essentially of, administering to the mammal a composition comprising at least three bacteria that are decreased in gut microbiota dysbiosis, wherein the at least three bacteria that are decreased in gut microbiota dysbiosis are selected from the group consisting of *Roseburia*, *Faecalibacterium*, *Akkermansia*, *Bacteroides*, *Blautia*, and *Bacteroides*. In some cases, the at least two bacteria that are decreased in gut microbiota dysbiosis include *Roseburia feacis*, *Faecalibacterium prausnitzii*, and optionally *Akkermansia muciniphila*. The method can include identifying said mammal as having said *C. difficile* infection prior to said administration. The mammal can be a human. The human can exhibit at least one clinical biomarker of dysbiosis (e.g., current/recent hospitalization, immune suppression, recent/current antibiotic use, and prior *C. difficile* infection).

Another aspect of this documents is a composition comprising at least two bacteria that are decreased in gut microbiota dysbiosis (e.g., *Roseburia*, *Faecalibacterium*, *Akkermansia*, *Bacteroides*, *Blautia*, and *Bacteroides*). In some cases, the at least three bacteria that are decreased in gut microbiota dysbiosis include *Roseburia feacis*, *Faecalibacterium prausnitzii*, and optionally *Akkermansia muciniphila*. The composition can be a pill, tablet, capsule, or enema. The composition is configured to deliver said at least three bacteria to the intestines of said mammal.

In another aspect, this document features a method for predicting susceptibility to *C. difficile* infection in a mammal with diarrhea. In some embodiments, the method includes, or consists essentially of, determining a level of at least one free amino acid in a fecal sample obtained from the mammal, and identifying the mammal as having increased susceptibility to *C. difficile* infection if the level of the at least one amino acid is altered relative to a mammal without diarrhea. The alteration in the free amino acid level can be an increase in the at least one amino acid. The at least one amino acid can include

proline, alanine, glycine, histidine, isoleucine, leucine, methionine, phenylalanine, threonine, tryptophan, tyrosine, and/or valine. In some cases, the at least one amino acid is proline. In some embodiments, the method includes, or consists essentially of, determining a clinical risk factor profile, and identifying the mammal as having increased susceptibility to *C. difficile* infection if the mammal has at least one clinical risk factor. The at least one clinical risk factor can include current/recent hospitalization, immune suppression, current/recent antibiotic use, and/or prior *C. difficile* infection. In some embodiments, the method includes, or consists essentially of, determining a level of at least one short chain fatty acid (SCFA) in a fecal sample obtained from the mammal, and identifying the mammal as having increased susceptibility to *C. difficile* infection if the level of the at least one SCFA is altered relative to a mammal without diarrhea. The alteration in the SCFA level can be a decrease in the at least one SCFA. In some embodiments, the method includes, or consists essentially of, determining a level of at least one bile acid (BA) in a fecal sample obtained from the mammal, and identifying the mammal as having increased susceptibility to *C. difficile* infection if the level of the at least one BA is altered relative to a mammal without diarrhea. The BA can be cholic acid (CA), deoxycholic acid (DCA), lithocholic acid (LCA), or ursodeoxycholic acid (UDCA). The determining a level of at least one BA can include determining a level of CA, and determining a level of DCA, can further include determining a ratio of CA/DCA. The alteration in the BA level can be an increase in the ratio of CA/DCA.

In another aspect, this document features a method for preventing *C. difficile* infection in a mammal. The method includes, or consists essentially of, administering to the mammal a composition comprising at least two bacteria that are decreased in gut microbiota dysbiosis, where the at least two bacteria that are decreased in gut microbiota dysbiosis are selected from the group consisting of *Roseburia*, *Faecalibacterium*, *Akkermansia*, *Bacteroides*, *Blautia*, and *Bacteroides*. The at least two bacteria that are decreased in gut microbiota dysbiosis can include *Roseburia feacis* and *Faecalibacterium prausnitzii*. The composition can be administered by fecal microbiota transplant (FMT). The FMT can be administered by enema, colonoscope, nasogastric tube, or nasoduodenal tube. The method also can include identifying said mammal as having increased susceptibility to *C. difficile* infection prior to said administration (e.g., using any of the methods described herein). The mammal can be a human.

Unless otherwise defined, all technical and scientific terms used herein have the same meaning as commonly understood by one of ordinary skill in the art to which this

disclosure belongs. Methods and materials are described herein for use in the present disclosure; other, suitable methods and materials known in the art can also be used. The materials, methods, and examples are illustrative only and not intended to be limiting. All publications, patent applications, patents, sequences, database entries, and other references mentioned herein are incorporated by reference in their entirety. In case of conflict, the present specification, including definitions, will control. In addition, the materials, methods, and examples are illustrative only and not intended to be limiting.

The details of one or more embodiments of the invention are set forth in the accompanying drawings and the description below. Other features, objects, and advantages of the invention will be apparent from the description and drawings, and from the claims.

DESCRIPTION OF DRAWINGS

Figure 1 shows that alterations in gut microbiota can result in diarrhea. (A) A schematic showing that alterations in gut microbiota can increase susceptibility to pathogens (adapted from Rupnik et al. 2009 *Nat Rev Microbiol.* 7:526-36; and Ferreyra et al. 2014 *Cell Host Microbe* 16:770-777). (B) Etiology of diarrhea (n=115; miscellaneous includes lactose/fructose intolerance, dysautonomia, pelvic floor dysfunction, and lymphocytic colitis).

Figure 2 shows that clinical features predict dysbiosis in a subset of patients with diarrhea. Beta-diversity (unweighted UniFrac) of (A) patients with diarrhea clustered based on PAM: Cluster H, n=78, and Cluster D, n=37 (B) patients with diarrhea and healthy controls. (C) Unweighted UniFrac distances between healthy-like and dysbiotic patients with diarrhea, and healthy controls (plotted are median with IQR and SD, Bonferroni-corrected $p < 0.0001$, t-test). (D) Alpha-diversity of patients with dysbiotic and healthy-like microbial communities (plotted averages with SEM; t-test; *** $p < 0.0005$, t-test). (E) Heatmap of significantly different microbial taxa between healthy-like and dysbiotic communities (OTU number is featured after genus; all Bonferroni-corrected $p < 0.02$, Wilcoxon rank-sum test). (F) ROC curve based on 5 clinical risk factors predictive of dysbiosis: antibiotic use (odds ratio; 95% confidence interval: recent antibiotics (5.21; 2.14-12.71; $p < 0.001$), immunosuppression (2.87; 1.27-6.48; $p = 0.012$), current hospitalization (6.17; 2.22-17.15; $p < 0.001$), recent hospitalization (4.87; 1.72-13.74; $p = 0.003$), and prior *C. difficile* infection (CDI) (9.26; 2.37-36.20, $p = 0.001$; AUC = 0.777; Table 3).

Figure 3 shows that partitioning around medoids (PAM) identifies two clusters of patients with diarrhea based on the unweighted UniFrac distance metric. (A) The gap statistic and (B) average silhouette width were used to determine the optimal cluster number.

5 Figure 4 shows that healthy-like microbial communities are similar to healthy controls, and dysbiotic microbial communities are similar to microbial communities in patients with *C. difficile* infection (CDI). Confusion matrix generated using Random Forests classifier based on OTUs to determine similarity of (A) healthy-like and dysbiotic microbial communities to communities from healthy controls, and (B) dysbiotic microbial
10 communities to communities from healthy controls and patients with CDI, overlaid numbers represent absolute numbers, with shading representative of frequency.

Figure 5 shows experimental designs for ex-GF mouse experiments assessing *C. difficile* susceptibility. (A) Assessing susceptibility of humanized mice to CDI. (B) Assessing ability of FMT to protect dysbiotic animals from CDI.

15 Figure 6 shows humanized mice clusters by donor (dysbiotic or healthy-like) and dysbiotic mice show decreased diversity. (A) Weighted UniFrac and (B) unweighted UniFrac beta-diversity metric showing microbial communities from ex-GF humanized mice pre- and 2 days post-*C. difficile* challenge. (C) Distances (weighted UniFrac) within dysbiotic and healthy-like mouse groups compared to distances between dysbiotic and
20 healthy-like mice (within group vs. between dysbiotic/healthy-like groups: Bonferroni-corrected $p < 0.0001$, t-test). (D) Alpha-diversity in humanized mice with dysbiotic and healthy-like microbial communities (plotted averages with SEM, *** $p < 0.0001$, t-test). (E) Distances (weighted UniFrac) within dysbiotic and healthy-like microbial communities 2 days post-*C. difficile* challenge compared to distances between the
25 microbial communities pre- and 2 days post-*C. difficile* challenge (dysbiotic, Bonferroni-corrected $p = 1$, healthy-like, Bonferroni-corrected $p = 1$, t-test).

Figure 7 shows that mice with dysbiotic microbial communities exhibit loss of colonization resistance to *C. difficile*. (A) *C. difficile* CFUs in stool of ex-GF mice colonized with healthy-like (n=11) or dysbiotic (n=10) microbial communities. Data
30 points represent individual animals with lines indicating average and SEM. Assay limit of detection (LOD) indicated by a dashed horizontal line at 2×10^4 (** $p < 0.005$, **** $p < 0.00005$, two-way ANOVA). (B) Representative H&E-stained proximal colon of mice colonized with dysbiotic or (C) healthy-like communities. (D) Beta-diversity (unweighted UniFrac) of healthy individuals and patients with diarrhea (n=115) and CDI

(n=95). (E) Unweighted UniFrac distance between dysbiotic individuals and healthy controls and patients with CDI (plotted are median with IQR and SD, Bonferroni-corrected $p < 0.0001$, t-test).

Figure 8 shows differences in whole community pathway expression and metabolites pre- and 2 days post-*C. difficile* challenge in healthy-like and dysbiotic communities. (A) Distance box plots based on Jaccard similarity of pathway presence between human donors and representative humanized mice (** $p < 0.001$, Wilcoxon rank-sum test). Significant differences in pathway expression (DEseq2 v.1.8.2, $p < 0.05$). (B) Pre-*C. difficile* challenge (4 weeks post-humanization) and (C) 2 days post-*C. difficile* challenge from ex-GF mice colonized with healthy-like (n=6) or dysbiotic (n=6) donor (D) AA, in stool with healthy-like (n=11) or dysbiotic (n=10) microbial communities (plotted averages with SEM, * $p < 0.05$, ** $p < 0.005$, ns – not significant, ND – not detected, Mann-Whitney.) (E) *C. difficile* growth kinetics in basal defined medium (BDM) with 0%, 0.1% or 0.01% DCA and AA concentrations at full, $\frac{1}{2}$ and $\frac{1}{4}$ of the standard AA concentration (plotted averages with SEM).

Figure 9 shows metatranscriptomics and metabolomics reveal secondary bile acid (BAs) and short chain fatty acids (SCFAs) as inhibitors and amino acids (AAs) as promoters of *C. difficile* colonization. (A) A subset of pathway expression based on whole community gene expression (RNAseq) pre- and 2 days post-*C. difficile* challenge from ex-GF mice colonized with healthy-like (n=10) or dysbiotic (n=11) communities. (B) Primary and secondary BA. (C) Ratio of cholic acid (CA) / deoxycholic acid (DCA). (D) SCFA and (E) proline in stool from humanized mice with healthy-like (n=11) or dysbiotic (n=10) communities (plotted mean with SEM, * $p < 0.05$, ** $p < 0.005$, *** $p < 0.0005$, **** $p < 0.00005$, ns – not significant, ND – not detected; Mann-Whitney). (F) *prdA* and *prdE* gene expression in humanized mice with healthy-like and dysbiotic communities (points represent total RNAseq reads with lines at median with IQR and SD). (G) *prdA* and *prdE* gene expression by taxonomic ID in dysbiotic and healthy-communities at day 2 post-*C. difficile* challenge (Log2 transformed absolute counts). (H) *C. difficile* growth kinetics in the presence or absence of proline in BDM without glucose (plotted averages with SEM). (I) *C. difficile* colonization levels in animals maintained on proline⁺ or proline⁻ diets. Data points represent individual animals with lines indicating average and SEM. Assay limit of detection (LOD) indicated by a dashed horizontal line at 2×10^4 (* $p < 0.05$).

Figure 10 shows functional changes based on metabolomics. (A) Volcano plot of compounds detected using UPLC-MS in stool samples collected from ex-GF mice colonized with healthy-like (n=11) or dysbiotic (n=10) communities. Compounds with a Log2 fold change >1 and p<0.05 (Kruskal-Wallis H-Tests) are shown. (B) Principal component analysis (PCA) based on log transformed differences in metabolite profiles in healthy-like and dysbiotic communities, ellipses represent 95% confidence intervals. (C) ¹H-NMR of stool samples quantitating AA content in stool collected from dysbiotic humanized animals collected pre/post-FMT (plotted averages with SEM).

Figure 11 shows colonization resistance is restored in dysbiotic mice post-FMT with significant increases in BAs, SCFAs and decrease in proline. (A) Weighted and (B) unweighted UniFrac beta diversity metric showing microbial communities pre- and post-FMT (n=6; within pre-FMT samples vs. distance between pre- and post-FMT samples, Bonferroni-corrected p<0.0001, t-test, based on weighted UniFrac). (C) Pre- and post-FMT alpha-diversity in dysbiotic mice (n=6, ***p<0.0005, t-test). (D) Representative H&E-stained proximal colon of ex-GF mice with dysbiotic communities, post-FMT, post-*C. difficile* challenge. (E) BA, (F) SCFA, and (G) proline in stool pre- and post-FMT (plotted averages with SEM; *p<0.05, **p<0.005, Mann-Whitney).

Figure 12 is a table showing humanization efficiency for mice at the family level.

Figure 13 is a table showing colon inflammation scores in dysbiotic and healthy-like mice post-*C. difficile* challenge.

Figure 14 is a table showing upregulated pathways in dysbiotic communities at 4 weeks post-humanization (pre-*C. difficile* challenge).

Figure 15 is a table showing upregulated pathways in healthy-like communities at 4 weeks post-humanization (pre-*C. difficile* challenge).

Figure 16 is a table showing upregulated pathways in healthy-like communities at day 2 post-*C. difficile* challenge.

Figure 17 is a table showing upregulated pathways in dysbiotic communities at day 2 post-*C. difficile* challenge.

Figure 18 is a table showing metabolites found in higher concentrations in healthy-like communities at 4-weeks post-humanization (pre-*C. difficile* challenge).

Figure 19 is a table showing metabolites found in higher concentrations in dysbiotic communities at 4 weeks post-humanization (pre-*C. difficile* challenge).

Figure 20 shows an experimental time line for probiotic delivery to mice of gut microbiota from human patients.

DETAILED DESCRIPTION

This document provides materials and methods related to preventing and/or treating *C. difficile* infection (CDI). In some cases, this document provides methods for predicting dysbiosis in patients with gastrointestinal disorders, to treat gastrointestinal disorders (*e.g.*, diarrhea that is not related to a pathogenic bacteria) and/or to prevent pathogenic infection (*e.g.*, by *C. difficile*) of the gut. For example, dysbiosis associated with susceptibility to CDI can be treated using a bacterial composition described herein.

The ability to determine a clinical risk factor profile can help identify patients with diarrhea and dysbiosis who may be at higher risk of CDI (*e.g.*, patients having irritable bowel disease, patients who are immunosuppressed, and/or hospitalized patients).

Biomarkers

A biological marker, or “biomarker,” as used herein refers to a measurable marker that can be used as an indicator of gut microbiota dysbiosis (*e.g.*, in a mammal with diarrhea). The amount or level of a biomarker can be altered (*e.g.*, increased or decreased) in gut microbiota dysbiosis relative to a healthy mammal (*e.g.*, mammal without diarrhea). For example, an altered amount or level of a biomarker described herein can be used to predict susceptibility to *C. difficile* infection in a mammal (*e.g.*, a mammal with diarrhea).

In some cases, a biomarker that can be used indicate gut microbiota dysbiosis (*e.g.*, to predict susceptibility to *C. difficile* infection) in a mammal can be one or more (*e.g.*, at least one, at least two, at least three, at least four, or more) bacteria. In some cases, bacteria can be decreased in gut microbiota dysbiosis. Examples of bacteria that can be decreased in gut microbiota dysbiosis include, without limitation, bacteria belonging to the genera *Roseburia*, *Faecalibacterium*, *Akkermansia*, *Bacteroides*, *Blautia*, and *Bacteroides*. In some embodiments, biomarkers that are decreased in gut microbiota dysbiosis include bacteria belonging to the genera *Roseburia*, *Faecalibacterium*, and *Akkermansia*. For example, biomarkers that are decreased in gut microbiota dysbiosis can include *Roseburia feacis*, *Faecalibacterium prausnitzii*, and *Akkermansia muciniphila*. In some cases, bacteria can be increased in gut microbiota dysbiosis. Examples of biomarkers that can be increased in gut microbiota dysbiosis include, without limitation, bacteria belonging to the genera *Escherichia*, *Shigella*, *Enterobacter*, *Enterococcus*, *Parasutterella*, and *Bacteroides*.

In some cases, a biomarker that can be used indicate gut microbiota dysbiosis (e.g., to predict susceptibility to *C. difficile* infection) in a mammal can be one or more (e.g., at least one, at least two, at least three, at least four, or more) free AAs. A free AA can be any appropriate amino acid. A free AA can be a naturally occurring AA. A free
5 AA can be an L- or a D- AA. A free AA can be increased in gut microbiota dysbiosis. Examples of free AAs include, without limitation, proline, alanine, glycine, histidine, isoleucine, leucine, methionine, phenylalanine, threonine, tryptophan, tyrosine, and valine. In some cases, an increased level of free proline can be used to predict susceptibility to *C. difficile* infection in a mammal.

10 In some cases, a biomarker that can be used indicate gut microbiota dysbiosis and/or to predict susceptibility to *C. difficile* infection in a mammal can be one or more (e.g., at least one, at least two, at least three, at least four, or more) SCFAs. A SCFA can be any appropriate SCFA. A free SCFA can be increased or decreased in gut microbiota dysbiosis. For example, a SCFA can be decreased in gut microbiota dysbiosis. Examples
15 of additional SCFAs include, without limitation, butyrate, propionate, acetate, valerate, and hexanoate.

In some cases, a biomarker that can be used to indicate gut microbiota dysbiosis and/or to predict susceptibility to *C. difficile* infection in a mammal can be one or more (e.g., at least one, at least two, at least three, at least four, or more) BAs (e.g., a primary
20 BA or a secondary BA). A BA can be increased or decreased in gut microbiota dysbiosis. Examples of primary BAs include, without limitation, taurocholic acid (TA or TCA), cholic acid (CA), and chenodeoxycholic acid (CDCA). Examples of secondary BAs include, without limitation, deoxycholic acid (DCA), lithocholic acid (LCA), ursodeoxycholic acid (UDCA), and taurodeoxycholic acid (TDCA). For example, a
25 decreased level of DCA and/or LCA can be used to predict susceptibility to *C. difficile* infection in a mammal. For example, an increased level of TCA can be used to predict susceptibility to *C. difficile* infection in a mammal. In some cases, a ratio of a primary BA (e.g., CA) to a secondary BA (e.g., CDA) can be used to indicate gut microbiota dysbiosis and/or to predict susceptibility to *C. difficile* infection in a mammal. For
30 example, an increased ratio of CA/CDA can be used to predict susceptibility to *C. difficile* infection in a mammal.

Compositions

Provided herein are bacterial compositions including bacteria that are decreased in gut microbiota dysbiosis. A bacterial composition can include bacteria derived (*e.g.*, obtained) from one or more healthy donors. A bacterial composition can include at least two (*e.g.*, two, three, four, five, or more) bacteria that are decreased in gut microbiota dysbiosis. For example, a bacterial composition provided herein can include at least two bacteria that are decreased in gut microbiota dysbiosis. Examples of bacteria that can be used as described herein include, without limitation, those belonging to the genera *Prevotella*, *Bacteroides*, *Clostridium*, *Faecalibacterium*, *Eubacterium*, *Ruminococcus*, *Peptococcus*, *Peptostreptococcus*, *Bifidobacterium*, *Escherichia*, *Lactobacillus*, *Akkermansia*, and *Roseburia*. In some cases, at least two bacteria that are decreased in gut microbiota dysbiosis are selected from the genera *Roseburia*, *Faecalibacterium*, *Bacteroides*, *Blautia*, and *Bacteroides*. In some embodiments, a composition described herein can include *Roseburia feacis* and *Faecalibacterium prausnitzii*. In some cases, at least two bacteria that are decreased in gut microbiota dysbiosis are selected from the genera *Roseburia*, *Faecalibacterium*, *Akkermansia*, *Bacteroides*, *Blautia*, and *Bacteroides*. In some embodiments, a composition described herein can include *Roseburia feacis*, *Faecalibacterium prausnitzii*, and *Akkermansia muciniphila*.

A composition containing at least two bacteria that are decreased in gut microbiota dysbiosis can contain one or more additional probiotic microorganisms. Examples of other probiotic microorganisms that can be included within a composition containing at least two bacteria that are decreased in gut microbiota dysbiosis include, without limitation, *Prevotella coprii*, *Bifidobacterium infantis*, *Lactobacillus rhamnosis* GG, *Lactobacillus plantarum*, *Bifidobacterium breve*, *Bifidobacterium longum*, *Lactobacillus acidophilus*, *Lactobacillus paracasei*, *Lactobacillus bulgaricus*, *Streptococcus thermophilus*, and *Faecalibacterium prausnitzii*.

Compositions provided herein can include any amount of bacteria described herein. In some cases, a composition provided herein can contain bacteria (*e.g.*, *Roseburia feacis*, *Faecalibacterium prausnitzii*, and optionally *Akkermansia muciniphila*) in an amount such that from about 0.001 to about 100 percent (*e.g.*, from about 1 percent to about 95 percent, from about 10 to about 95 percent, from about 25 to about 95 percent, from about 50 to about 95 percent, from about 20 to about 80 percent, from about 50 to about 95 percent, from about 60 to about 95 percent, from about 70 to about 95 percent, from about 80 to about 95 percent, from about 90 to about 95 percent, from about

95 to about 99 percent, from about 50 to about 100 percent, from about 60 to about 100 percent, from about 70 to about 100 percent, from about 80 to about 100 percent, from about 90 to about 100 percent, or from about 95 to about 100 percent), by weight, of the composition can be bacteria. In some cases, a composition provided herein can contain
5 from about 10^3 to about 10^8 bacteria.

In some cases, a composition provided herein can contain bacteria (*e.g.*, *Roseburia feacis*, *Faecalibacterium prausnitzii*, and optionally *Akkermansia muciniphila*) in the amounts and dosages as described elsewhere for probiotic bacteria (U.S. Patent Application Publication No. 2008/0241226; see, *e.g.*, paragraphs [0049-0103]). In
10 addition, a composition provided herein containing bacteria (*e.g.*, *Roseburia feacis*, *Faecalibacterium prausnitzii*, and *Akkermansia muciniphila*) can be administered as described elsewhere for probiotic bacteria (U.S. Patent Application Publication No. 2008/0241226; see, *e.g.*, paragraphs [0049-0103]).

Bacteria can be obtained from the digestive system of any appropriate mammal
15 (*e.g.*, a human). For example, bacteria that are decreased in gut microbiota dysbiosis (*e.g.*, *Roseburia feacis*, *Faecalibacterium prausnitzii*, and optionally *Akkermansia muciniphila*) can be isolated from small intestinal mucosa (*e.g.*, a small bowel biopsy or aspirate sample) of a human (*e.g.*, a healthy human patient). Bacterial strains (*e.g.*, *Roseburia feacis*, *Faecalibacterium prausnitzii*, and optionally *Akkermansia muciniphila*)
20 can be identified via 16S rRNA PCR using 16S rRNA primers. In some cases, bacteria can be commercially obtained (*e.g.*, from the American Type Culture Collection).

Any appropriate method can be used to obtain a culture of bacteria. For example, microbial culturing techniques can be used to obtain bacteria. In general, bacteria can be cultured in broth containing milk (*e.g.*, skim milk) to obtain a culture containing greater
25 than 1×10^8 bacteria per mL of broth. The bacteria can be removed from the broth via centrifugation. Once obtained, the bacteria can be formulated into a medicament or nutritional supplement composition for administration to a mammal (*e.g.*, a human), can be added to a food product for consumption, or can be frozen for later use.

In some cases, a preparation of bacteria, which can be stored frozen in 2X skim
30 milk, can be thawed and grown on CDC Anaerobe Laked Sheep Blood Agar with kanamycin and vancomycin (KV) (Becton, Dickson and Company, Sparks, MD, product number 221846) in an anaerobe jar with AnaeroPack System (product number 10-01, Mitsubishi Gas Chemical America, Inc., New York, NY). The culture can be incubated at 35-37°C for at least 48 hours.

A composition containing at least two bacteria that are decreased in gut microbiota dysbiosis can be in the form of a medicament or nutritional supplement. For example, compositions containing at least two bacteria that are decreased in gut microbiota dysbiosis can be in the form of a pill, tablet, powder, liquid, capsule, or enema. A
5 medicament or nutritional supplement can be prepared with pharmaceutically acceptable excipients such as binding agents, fillers, lubricants, disintegrants, or wetting agents. In some cases, medicaments or nutritional supplements (*e.g.*, tablets) can be coated. In some cases, a composition containing at least two bacteria that are decreased in gut microbiota dysbiosis can be formulated such that the bacteria are encapsulated for release within the
10 intestines of a mammal. Liquid preparations for administration can take the form of, for example, solutions, syrups, or suspension, or they can be presented as a dry product for constitution with saline or other suitable liquid vehicle before use. In some cases, a composition provided herein containing at least two bacteria that are decreased in gut microbiota dysbiosis (*e.g.*, *Roseburia feacis*, *Faecalibacterium prausnitzii*, and
15 optionally *Akkermansia muciniphila*) can be in a dosage form as described elsewhere (U.S. Patent Application Publication No. 2008/0241226; see, *e.g.*, paragraphs [0129-0135]). For example, a composition provided herein can be in the form of a food product formulated to contain at least two bacteria that are decreased in gut microbiota dysbiosis (*e.g.*, *Roseburia feacis*, *Faecalibacterium prausnitzii*, and optionally *Akkermansia*
20 *muciniphila*). Examples of such food products include, without limitation, milk (*e.g.*, acidified milk), yogurt, milk powder, tea, juice, beverages, candies, chocolates, chewable bars, cookies, wafers, crackers, cereals, treats, and combinations thereof.

A composition containing at least two bacteria that are decreased in gut microbiota dysbiosis can contain other ingredients such as buffers, radical scavengers, antioxidants,
25 reducing agents, or mixtures thereof. Examples of other additional ingredients that can be formulated into a single composition or a separate composition for delivery to a mammal (*e.g.*, a human) include, without limitation, those ingredients described elsewhere (U.S. Patent Application Publication No. 2008/0241226; see, *e.g.*, paragraphs [0104-0128]).

In some cases, a composition containing at least two bacteria that are decreased in
30 gut microbiota dysbiosis can contain a pharmaceutically acceptable carrier for administration to a mammal, including, without limitation, sterile aqueous or non-aqueous solutions, suspensions, and emulsions. Examples of non-aqueous solvents include, without limitation, propylene glycol, polyethylene glycol, vegetable oils, and organic esters. Aqueous carriers include, without limitation, water, alcohol, saline, and

buffered solutions. Pharmaceutically acceptable carriers also can include physiologically acceptable aqueous vehicles (*e.g.*, physiological saline) or other known carriers for oral administration.

Methods

5 Provided herein are methods for using the biomarkers described herein. The methods include determining the amount of at least one biomarker of gut microbiota dysbiosis. In some embodiments, this disclosure provides methods of predicting dysbiosis in a mammal with diarrhea. In some embodiments, this disclosure provides methods of predicting susceptibility to CDI in a mammal with diarrhea. In some
10 embodiments, this disclosure provides methods of treating and/or preventing CDI in a mammal with dysbiosis.

 Methods provided herein can include, for example, determining the amount of at least one biomarker (*e.g.*, determining the amount of 1 or more biomarkers, 2 or more biomarkers, 3 or more biomarkers, 4 or more biomarkers, 5 or more biomarkers, 6 or
15 more biomarkers, 7 or more biomarkers, or 8 or more biomarkers) of gut microbiota dysbiosis in a fecal (*i.e.*, stool) sample obtained from a mammal. In some cases, the methods can include identifying the mammal as having dysbiosis if the amount of the at least one biomarker of gut microbiota is altered relative to a mammal without diarrhea. In some cases, the methods can include identifying the mammal as susceptible to CDI if the
20 amount of the at least one biomarker of gut microbiota is altered relative to a mammal without diarrhea. A mammal (*e.g.*, a mammal with diarrhea) can have increased susceptibility to *C. difficile* infection if the level of the at least one amino acid is altered in a sample from the mammal (*e.g.*, a fecal sample) relative to a mammal without diarrhea. For example, a mammal can have increased susceptibility to *C. difficile* infection if the
25 level of proline in the sample is increased. A mammal (*e.g.*, a mammal with diarrhea) can have increased susceptibility to *C. difficile* infection if the mammal has at least one clinical risk factor. For example, a mammal can have increased susceptibility to *C. difficile* infection if the mammal has one or more of current/recent hospitalization(s), immune suppression, current/recent antibiotic use, and prior *C. difficile* infection(s). A
30 mammal (*e.g.*, a mammal with diarrhea) can have increased susceptibility to *C. difficile* infection if the level of the at least one SCFA or BA is altered in a sample from the mammal (*e.g.*, a fecal sample) relative to a mammal without diarrhea. For example, a mammal can have increased susceptibility to *C. difficile* infection if the level of CA,

DCA, LCA, and/or UDCA is decreased in the sample. For example, a mammal can have increased susceptibility to *C. difficile* infection if the ratio of CA/DCA is increased in the sample.

The alteration in the gut microbiota is altered relative to a mammal without diarrhea. In some embodiments, the alteration in gut microbiota can be a decrease in at least one of biomarkers described herein. For example, the alteration in gut microbiota can be a decrease in at least one of *Roseburia*, *Faecalibacterium*, *Akkermansia*, *Bacteroides*, or *Blautia*. In some embodiments, the alteration in gut microbiota is an increase in at least one of biomarkers described herein. For example, the alteration in gut microbiota can be an increase in at least one of *Escherichia*, *Shigella*, *Enterobacter*, *Enterococcus*, or *Parasutterella*. In some embodiments, the alteration in gut microbiota includes both a decrease in at least one of *Roseburia*, *Faecalibacterium*, *Akkermansia*, *Bacteroides*, or *Blautia* and an increase in at least one of *Escherichia*, *Shigella*, *Enterobacter*, *Enterococcus*, or *Parasutterella*.

Also provided herein are methods of using compositions including at least two bacteria that are decreased in gut microbiota dysbiosis (e.g., *Roseburia feacis*, *Faecalibacterium prausnitzii*, and optionally *Akkermansia muciniphila*). The methods include administering to a mammal a composition described herein. For example, compositions including at least two bacteria that are decreased in gut microbiota dysbiosis can be used to restore healthy gut microbiota (e.g., by probiotic or by FMT) to treat *C. difficile* infection in a mammal.

In some embodiments, this disclosure provides methods of treating CDI in a mammal (e.g., a mammal having dysbiosis). Treating CDI can include prophylactic treatment (i.e., delivered prior to the development of symptoms to prevent a disease from occurring) or therapeutic treatment (i.e., delivered after development of symptoms). For example, a method of preventing CDI in a mammal having dysbiosis can include administering by FMT a composition described herein (e.g., including *Roseburia feacis*, *Faecalibacterium prausnitzii*, and optionally *Akkermansia muciniphila*) that was derived from a healthy donor.

A composition as described herein can include at least two bacteria selected from the groups consisting of *Roseburia*, *Faecalibacterium*, *Akkermansia*, *Bacteroides*, *Blautia*, and *Bacteroides*. In some embodiments, the composition includes *Roseburia feacis*, *Faecalibacterium prausnitzii*, and optionally *Akkermansia muciniphila*.

A composition can be administered by any suitable means. In some embodiments, a composition can be administered orally (e.g., via a pill, tablet, or capsule). In other embodiments, a composition can be administered by FMT (e.g., via enema, colonoscope, nasogastric tube, or nasoduodenal tube).

- 5 In some embodiments, methods provided herein can also include identifying a mammal as being susceptible to *C. difficile* infection or as having said *C. difficile* infection prior to administering to the mammal a composition described herein. In some cases, a mammal (e.g., a mammal with diarrhea) can be identified as having increased susceptibility to *C. difficile* infection using the biomarkers and methods described herein.
- 10 For example, a mammal can be identified as having increased susceptibility to *C. difficile* infection if the level of at least one amino acid (e.g., proline) is altered (e.g., increased) in a sample from the mammal (e.g., a fecal sample) relative to a mammal without diarrhea. For example, a mammal can be identified as having increased susceptibility to *C. difficile* infection if the mammal has at least one clinical risk factor (e.g., one or more of
- 15 current/recent hospitalization(s), immune suppression, current/recent antibiotic use, and prior *C. difficile* infection(s)). For example, a mammal can be identified as having increased susceptibility to *C. difficile* infection if the level of at least one BA (e.g., CA, DCA, LCA, and/or UDCA) is altered (e.g., decreased) in a sample from the mammal (e.g., a fecal sample) relative to a mammal without diarrhea. For example, a mammal can
- 20 be identified as having increased susceptibility to *C. difficile* infection if the ratio of CA/DCA is increased in a sample from the mammal (e.g., a fecal sample) relative to a mammal without diarrhea.

Examples of mammals that can be treated as described herein include, without limitation, humans, monkeys, dogs, cats, cows, horses, pigs, and sheep. In some

25 embodiments, a mammal is a human. In some embodiments, the mammal also exhibits at least one clinical biomarker of dysbiosis. Non-limiting examples of clinical biomarkers of dysbiosis include current/recent hospitalization, immune suppression, recent/current antibiotic use, and prior *C. difficile* infection.

In some embodiments, methods of treating *C. difficile* infection in a mammal

30 described herein can be used in combination with another *C. difficile* treatment. Examples of other *C. difficile* infection treatments include, without limitation, antibiotics (e.g., metronidazole, vancomycin, and fidaxomicin), surgery (e.g., surgery to remove the diseased portion of the colon), and dietary modifications (e.g., low protein diets).

Any amount of a composition containing at least two bacteria can be administered to a mammal. The dosages of the compositions provided herein can depend on many factors including the desired results. Typically, the amount of bacteria contained within a single dose can be an amount that effectively exhibits improved gastrointestinal function within the mammal. For example, a composition containing at least two bacteria can be formulated in a dose such that a mammal receives from about 10^3 to about 10^9 bacteria.

The final pH of a composition containing at least two bacteria can be from about 3.5 to about 9.5 (*e.g.*, from about 4.0 to about 9.0; from about 4.5 to about 9.0; from about 4.5 to about 8.5; from about 5.0 to about 8.5; or from about 6.5 to about 8.0). To obtain such a pH, the pH of the composition can be adjusted using a pH-adjusting agent, for example. It will be appreciated that pH adjustment can be accomplished with any of a wide variety of acids should the composition have a pH that is too high (*e.g.*, greater than 10.0 before adjustment). Likewise, pH adjustment can be accomplished with any of a wide variety of bases should the composition have a pH that is too low (*e.g.*, less than 3.0 before adjustment).

The invention will be further described in the following examples, which do not limit the scope of the invention described in the claims.

EXAMPLES

Example 1: Clostridium difficile in microbial dysbiosis in patients with diarrhea

The gut microbiome of humans with diarrhea was studied by modeling these microbiomes in ex-germ-free (GF) mice, elucidated mechanisms underlying susceptibility to CDI. Specific risk factors in a subset of patients with diarrhea were identified, and it was demonstrated that alterations in their gut microbiota, when modeled in GF mice were associated with increased free amino acids, decreased short-chain fatty acids and an increased ratio of cholic acid to deoxycholic acid – all of which provide an optimal niche for pathogens such as *C. difficile*. Mice humanized with these dysbiotic communities were more susceptible to CDI, and community structure accommodated *C. difficile* expansion. Prophylactic FMT with a healthy microbial community restructured the metabolic landscape, restoring colonization resistance to *C. difficile*. Results showed that lack of colonization resistance can be an inherent phenotype of the microbiome, dictated by selective forces including those driven by host factors. This phenotype, defined with simple stool metabolic parameters, can be corrected by introducing a diverse microbial community. The ability to identify at-risk individuals using simple noninvasive metrics

and restore colonization resistance through FMT represents a novel approach to the prevention of diseases like CDI, especially among hospitalized and immunocompromised patients.

Results

To determine the effect of diarrhea on the gut microbiota, community composition was profiled using the 16S rRNA gene in 115 patients who presented with diarrhea (Table 1). All individuals tested negative for *C. difficile* and had a spectrum of underlying conditions (Fig. 1). Principal Coordinate analysis (PCoA) plots based on beta-diversity showed a wide distribution of microbial communities (Fig. 2A). Partitioning Around Medoids (PAM) clustering analysis with the gap statistic identified 2 distinct clusters as optimal (cluster H; and cluster D; Extended Data Fig. 7A, B) (Tibshirani *et al.* 2001, *J R Stat Soc: Ser B (Stat Methodol)* 63:411-423). Microbial communities from patients with diarrhea within cluster H grouped with the 118 healthy controls as compared to those within cluster D (Fig. 2B, C). Additionally, patients within cluster H were more likely to be misclassified as healthy controls compared to patients in cluster D based on Random Forests supervised learning algorithm using Operational Taxonomic Unit (OTU)-level abundances (Fig. 4A). Hence, patients within cluster H were referred to as healthy-like. Patients within cluster D were referred to as dysbiotic given the difference in their microbial composition from healthy controls.

Table 1. Demographic data of healthy controls, patients with diarrhea, and patients with *C. difficile* infection.

	Healthy (n=118)	Diarrhea (n=115)	<i>C. difficile</i> infection (n=85)	p-value
Sex, n (%)				
Male	58 (49)	39 (34)	35 (41)	0.06
Female	60 (51)	76 (66)	50 (59)	
Age (yr)				
Mean (SD)	49.7 (15.8)	47.4 (12.4)	49.3 (18.0)	0.49
Range	25-79	20-64	20-96	
BMI (SD)	28.1 (7.5)	28.3 (7.0)	27.2 (6.3)	0.55

The dysbiotic group was characterized by significantly decreased microbial richness and evenness (Fig. 2D), and significantly increased relative abundances of OTUs within *Enterococcus*, *Enterobacter*, and *Bacteroides*, and decreased *Faecalibacterium*, *Roseburia*, *Blautia* and *Bacteroides* (Fig. 2E, Table 2), when compared to the healthy-like group. Alteration in gut microbial community structure was not associated with a defined

etiology of diarrhea (Table 3). To identify drivers of dysbiosis, the clinical metadata was examined and 5 discrete clinical factors were identified that predicted dysbiosis in patients with diarrhea: antibiotic use within the previous 3 weeks, immunosuppression, current hospitalization, recent hospitalization – within the previous 4 weeks, and prior *C. difficile* infection (CDI); age, gender and body mass index were not significantly associated with dysbiosis (Table 3). Patients within the dysbiotic group exhibited a significantly greater number of clinical risk factors as compared to healthy-like individuals (dysbiotic: 1.97 (1.19); healthy-like: 0.64 (0.93) risk factors per person, mean (SD), $p < 10^{-8}$, Wilcoxon rank-sum test) and these risk factors were strong predictors of dysbiosis based on receiver operator characteristic (ROC) curve analysis (area under the curve (AUC) = 0.777; Fig. 2F).

Table 2. Differences in microbial taxa read numbers between healthy-like and dysbiotic microbial communities in patients with diarrhea.

Taxonomy	Healthy-like Mean Reads per Sample	Dysbiotic Mean Reads per Sample	Bonferroni corrected p-value
Bacteroidetes; Bacteroidia; Bacteroidales; Bacteroidaceae; Bacteroides	1376	42	$p < 0.0001$
Firmicutes; Clostridia; Clostridiales; Lachnospiraceae; Roseburia	1716	189	$p < 0.0001$
Firmicutes; Clostridia; Clostridiales; Ruminococcaceae; Faecalibacterium	1417	39	$p < 0.0001$
Bacteroidetes; Bacteroidia; Bacteroidales; Bacteroidaceae; Bacteroides	4113	2012	$p < 0.0001$
Firmicutes; Clostridia; Clostridiales; Lachnospiraceae; Blautia	1800	1187	$p < 0.0001$
Proteobacteria; Gammaproteobacteria; Enterobacteriales; Enterobacteriaceae; Enterobacter	115	5993	0.001
Bacteroidetes; Bacteroidia; Bacteroidales; Bacteroidaceae; Bacteroides	817	2373	0.004
Firmicutes; Bacilli; Lactobacillales; Enterococcaceae; Enterococcus	29	2401	0.016

Table 3. Risk factors that differentiate healthy-like and dysbiotic microbial communities in patients with diarrhea.

	Risk Factors in Individuals with Diarrhea				
	Healthy-like (n=78)	Dysbiotic (n=37)	Odds Ratio	Lower/Upper Confidence Intervals	p-value
Sex, n (%)					
Male	28 (36)	26 (30)	1.32	0.57 / 3.08	0.515
Female	50 (64)	11 (70)			
Age (yr)					
Mean (SD)	50.7 (12.4)	50.6 (12.8)	1	0.97 / 1.03	0.956
Range	24-68	23-67			
Body Mass Index (SD)	27.4 (6.5)	30.2 (7.8)	1.06	1.00 / 1.12	0.050
Recent Hospitalization, n (%) (within last 4 weeks)	7 (9)	12 (32)	4.87	1.72 / 13.74	0.003
Current Hospitalization, n (%)	7 (9)	14 (37)	6.17	2.22 / 17.15	< 0.001
Prior <i>C. difficile</i> infection, n (%)	3 (4)	10 (26)	9.26	2.37 / 36.20	0.001
Immune suppressed, n (%)	21 (27)	19 (50)	2.87	1.27 / 6.48	0.012
Recent antibiotics, n (%) (within last 3 weeks)	12 (15)	18 (47)	5.21	2.14 / 12.71	< 0.001
Etiology of Diarrhea	NA	NA	NA	NA	0.120

To determine the functional consequence of dysbiosis, susceptibility of microbial communities within these 2 distinct clusters to a pathogen, *C. difficile*, which is commonly associated with microbial dysbiosis was investigated. The microbial communities were modeled in ex-germ-free (GF) mice by humanizing these mice with stool from 2 dysbiotic donors (Dysbiotic A, Dysbiotic B) and 2 healthy-like donors (Healthy-like C, Healthy-like D; Fig. 5A) as previously shown to recapture microbial composition and function (Marcobal *et al.* 2013 *ISME J.* 7:1933-1943; Turnbaugh *et al.* 2009 *Sci Transl Med.* 1:6ra14). 16S rRNA gene sequencing of the fecal microbial community in ex-GF-humanized mice (4 weeks post-humanization) indicated that microbial communities clustered based on donor type, reproducing the human state (Fig. 6A, B). UniFrac distances within dysbiotic and healthy-like mouse groups were significantly shorter than distances between dysbiotic and healthy-like mice (Fig. 6C), and humanization efficiency was 86% at the family level (Fig. 12), similar to previous studies (Ridaura *et al.* 2013 *Sci* 341). Gut microbial communities in mice humanized from the dysbiotic donors were significantly less diverse (Fig. 7D). When mice were challenged with an overnight culture of *C. difficile* by oral gavage, the dysbiotic group had significantly higher stool *C. difficile* colony forming units (CFU) at Day 1, 2, and 6 post-challenge. The difference grew over time, differing on average by 13.9-, 262-, and >1000-fold, respectively (Fig. 7A). Additionally, significant inflammation on H&E stained sections of the proximal colon was observed in the dysbiotic group as compared to the healthy-like group (Fig. 7B, C, Table 4, Fig. 13).

Table 4. Mouse colon inflammation scoring rubric.

Measure of Inflammation	Score
Inflammation in the lamina propria	0 = none
	1 = focal, minimal
	2 = focal, marked
	3 = diffuse, marked
Maximum polymorphonuclear cells (neutrophils) in high power field	0 = none
	1 = 5-10
	2 = 10-20
	3 = 20-30
	4 = >30
Depth of inflammation	0 = lamina propria only
	1 = superficial submucosa
	2 = deep submucosa
	3 = transmural
Total	0 - 10

To investigate if susceptibility to *C. difficile* represented an inherent feature of the community, the gut microbial community structure in humanized mice pre- and 2 days post-*C. difficile* challenge in the dysbiotic and healthy-like humanized mice was compared. UniFrac distances within the microbial communities post-*C. difficile* challenge were not significantly different from the distances between the microbial communities pre- and post-*C. difficile* challenge (Fig. 6E) suggesting that susceptibility is an inherent feature of the community rather than a result of *C. difficile*-related perturbation. To examine whether this could be extrapolated to human subjects, the microbial communities of dysbiotic patients and a cohort of patients with CDI (Fig. 7D) was examined. Interestingly, it was found that microbial communities of patients within the dysbiotic group were significantly closer to communities in patients with CDI as compared to healthy controls (Fig. 7E) and more likely to be misclassified as CDI as opposed to healthy controls based on Random Forests supervised learning algorithm (Fig. 9B).

To determine the microbial community phenotype responsible for susceptibility to CDI, the functional capacity of the humanized mouse communities at the transcriptional and metabolic level was assessed. Whole community gene expression using RNAseq on stool from dysbiotic and healthy-like humanized mice was assessed. Pathway analysis using HUMAnN2 (Abubucker *et al.* 2012 *PLoS Comput Biol* 8:e1002358) followed by a Jaccard similarity calculation showed that microbial community function within dysbiotic

mice was significantly closer to their dysbiotic donor than to the healthy-like humanized mice or healthy-like donor and vice versa (Fig. 8A). Differential expression analysis indicated that there were significant differences in 306 pathways between the 2 groups of humanized mice pre-*C. difficile* challenge (Fig. 8B, Fig. 14, and Fig. 15). The healthy-like communities had increased expression of short chain fatty acid (SCFA) biosynthesis pathways including butyrate, propionate, and acetate generated from L-glutamate as a precursor, and secondary bile acid (BA) biosynthesis systems (Fig. 9A). A significant increase in the expression of carbohydrate utilization systems including arabinose, glucose, sucrose, and fucose was also observed in healthy-like communities (Fig. 15). To determine if there was a shift in community functionality following *C. difficile* challenge, global gene expression profiles 2 days post-*C. difficile* challenge were compared and differences in 281 pathways were found that included a majority of the same pathways seen prior to *C. difficile* challenge, suggesting gene expression, like composition, is a stable community feature conducive to pathogen invasion (Fig. 8C, Fig. 16, and Fig. 17).

The functional relevance of transcriptional differences was assessed using metabolomics in stool samples collected from humanized mice before *C. difficile* challenge. There were significant differences in 269 metabolites detected using UPLC-MS untargeted metabolomics, which included differential levels of BAs, SCFAs, and amino acids (AAs) (Fig. 10A, B, Fig. 18, and Fig. 19). A targeted UPLC-MS panel indicated that dysbiotic communities had significantly reduced secondary BAs, deoxycholic acid (DCA), lithocholic acid (LCA), taurodeoxycholic acid (TDCA), and ursodeoxycholic acid (UDCA), and significantly more primary BA taurocholic acid (TA) (Fig. 9B). Dysbiotic mice also displayed a >500-fold increase in the predominant primary/secondary BA (cholic acid (CA)/DCA ratio), indicating a bias toward primary BAs (Fig. 9C). A GC-MS targeted panel revealed significantly lower levels of SCFAs including propionate, acetate, butyrate, valerate, and hexanoate in the dysbiotic mice (Fig. 9D). ¹H-NMR of fecal pellet extracts showed higher free AAs in the dysbiotic community (Fig. 8D). The significance of AAs in supporting expansion of *C. difficile* in the dysbiotic community was evident by a concentration-dependent increase in *C. difficile* growth seen with increase in AA concentration in defined medium either lacking or containing low concentrations of DCA (Fig. 8E). Growth was completely inhibited at high concentrations of DCA irrespective of AA concentration, reflective of the metabolic milieu in the healthy-like community (Fig. 8E). In order to determine if specific AAs provided a selective advantage for *C. difficile*, we examined the role of proline, which

showed the greatest difference in concentration between the healthy-like and dysbiotic community (4.8 fold; Fig. 9E), and is known to support *C. difficile* growth via Strickland fermentation (Bouillaut *et al.* 2015 *Res Microbiol.* 166:375-383; Bouillaut *et al.* 2013 *J Bacteriol.* 195:844-854; Jackson *et al.* 2006 *J Bacteriol.* 188:8487-8495). Proline reductase expression as a marker for proline utilization in whole community RNAseq data was assessed. Humanized mice with a dysbiotic community had lower expression of proline reductase A (*prdA*) and E (*prdE*) compared to humanized mice with a healthy-like community (Fig. 9F), corresponding to the increased level of fecal proline seen in these mice (Fig. 9E). Expression of *prdA* and *prdE* in dysbiotic mice post-*C. difficile* challenge was attributed entirely to *C. difficile* supporting the role of proline in expansion of *C. difficile*. In contrast, in healthy-like mice, *prdA* and *prdE* expression was attributed primarily to *C. hylemonae*, *Dorea longicatena*, and *Lachnospiraceae bacterium 5_1_57FAA* (Fig. 9G). Further supporting the role of proline, *C. difficile* was unable to grow in the absence of proline (Fig. 9H). Using patient derived microbial communities, we validate previous studies that demonstrate the inhibitory effect of secondary BAs on *C. difficile* growth (Buffie *et al.* 2015 *Nature* 517:205-208; Sorg *et al.* 2010 *J Bacteriol.* 192:4983-4990; Sorg *et al.* 2008 *J Bacteriol.* 190: 2505-2512; Sorg *et al.* 2009 *J Bacteriol.* 191:1115-1117) and further suggest a role for AA availability, specifically proline, in facilitating *C. difficile* expansion by providing a favorable nutritional niche. To further evaluate the role of proline availability *in vivo*, GF mice were administered a custom diet either with or without proline prior to humanization with dysbiotic communities. Animals that received a proline deficient diet showed a 4.99 fold decrease in colonization at Day 1 post infection (Fig. 9I). This suggests proline availability is relevant for early emergence and establishing infection.

FMT was successful in treating recurrent CDI in 80-95% of patients and has been shown to increase SCFA and secondary BA concentrations in the gut (van Nood *et al.* 2013 *N Engl J Med* 368:407-415; Lawley *et al.* 2012 *PLoS Pathog.* 8; Weingarden *et al.* 2014 *Am J Physiol Gastrointest Liver Physiol.* 306:G310-319). It was predicted that the significant metabolic alterations in the dysbiotic community described above could be restored using a prophylactic transfer of a healthy microbial community to re-establish colonization resistance. To test this, a mouse-adapted, healthy human-derived FMT community was delivered to ex-GF mice 4 weeks after being humanized with dysbiotic microbial communities (Fig. 5B). 16S rRNA community analysis revealed a significant shift in the gut microbial communities of dysbiotic mice to resemble the donor microbial

community after FMT (Fig. 11A, B). There was also a significant increase in alpha-diversity following transplantation in dysbiotic mice (Fig. 11C).

There was no detectable *C. difficile* in stool on day 1, 2, or 6 following *C. difficile* challenge and no significant inflammation on H&E-stained sections from the proximal colon (Fig. 11D). Metabolically, a significant increase in stool secondary BAs (DCA, LCA and UDCA) and decrease in primary BA (TA) (Fig. 11E) was observed. Concentrations of the SCFAs butyrate, acetate, propionate, and valerate also significantly increased after FMT (Fig. 11F). Proline concentrations decreased significantly after FMT (Fig. 11G) and many free AAs showed a similar trend (Fig. 10C). These results suggested that preemptive FMT from a healthy individual can restore colonization resistance in mice with dysbiotic communities by restoring the metabolic milieu and eliminating open niches for *C. difficile*.

Methods

Human Study. All human studies were approved by the Mayo Clinic Institutional Review Board. Adults (>18 years old) who presented with diarrhea and tested negative for *Clostridium difficile* (n=115; IRB #12-007176), and those who tested positive for *C. difficile* via PCR (Sloan *et al.* 2008 *J Clin Microbiol* 46:1996-2001; n=95; IRB #12-000554) were voluntarily enrolled. Upon receiving consent from participants, frozen stool left over from clinical testing was obtained and stored at -80°C until DNA extraction. Participants were recruited at Mayo Clinic in Rochester, Minnesota. The healthy control group (n=118) was comprised of volunteers who provided stool samples to the Midwest Reference Range Biobank (Chen *et al.* 2016 *PeerJ* 4:e1514; IRB #13-003694).

Bacterial Strains and Growth Conditions. All strains for this study were maintained inside an anaerobic growth chamber with a gas mixture of 75% N₂/20% CO₂/5% H₂ (Coy Lab Products, Grass Lake, MI). Liquid and solid growth media was allowed to reduce in the anaerobic chamber for a minimum of 24 hours prior to use. For transfer out of the chamber, liquid stocks were sealed in sterile, gas-tight crimp cap glass vials. *C. difficile* strain 630 was maintained at 37°C on *Clostridium difficile* Moxalactam Norfloxacin (CDMN) blood agar plates (Aspinall *et al.* 1992 *J Clin Pathol.* 45:812-814), in Reinforced Clostridial Medium (RCM) broth (Difco DF1808173), or in Basal Defined Medium (BDM) (Karasawa *et al.* 1995 *Microbiology.* 141:371-375) broth. *C. difficile* amino acid (AA) utilization was assessed using modified BDM containing 1/2 or 1/4 of

the standard AA content. Proline utilization was assessed in modified BDM lacking glucose and proline. Bacterial growth rates were assessed using a BioTek Eon microplate spectrophotometer (BioTek, Winooski, VT).

Oral Gavage Preparation and Delivery. Fecal suspensions from human or mouse
5 samples were prepared by combining equal volumes of stool (human) with sterile pre-reduced phosphate buffered saline (PBS) or 6 pellets (mouse) with 600 µl of PBS in a 10 mL conical vial inside an anaerobic chamber. The vials were sealed, removed from the chamber, vortexed for 5 minutes at room temperature, allowed to settle at 4°C for up to 2 hours, and transferred into the gnotobiotic isolators. Mice were gavaged with 300 µl of
10 the fecal suspension as described previously (Reigstad *et al.* 2015 *FASEB J.* 29:1395-1403).

Mouse Husbandry. Mouse experiments were performed with germ-free (GF) Swiss Webster mice born and maintained in the Mayo Clinic Germ Free Facility as described previously (Reigstad *et al.* 2015 *FASEB J.* 29:1395-1403). Where appropriate,
15 animals were switched to a defined diet (OpenStandard Diet A11112201, Research Diets, New Brunswick, NJ) with and a variation deficient in proline (Research Diets, New Brunswick, NJ). All mouse experiments complied with Institutional Animal Care and Use Committee guidelines (IACUC protocol #A32015).

Mouse Experiments. Human community *C. difficile* susceptibility was assessed
20 using sex matched, GF mice. Experiment sample sizes were chosen based on similar prior studies (Turnbaugh *et al.* 2009 *Sci Transl Med.* 1:6ra14; Backhed *et al.* 2007 *Proc Natl Acad Sci U S A* 104:979-984; Ridaura *et al.* 2013 *Science* 341:1241214) and logistical constraints within gnotobiotic isolators. Littermates were used when possible to minimize contamination risks associated with multiple GF transfers, however formal
25 randomization was not employed. GF animal technicians performed mouse allocation and investigators were blinded to selection. Mice were humanized using fecal suspensions prepared from 2 patients in the human “dysbiotic” group: dysbiotic donor A (2 risk factors – prior *C. difficile* infection (CDI) and immune suppressed) and dysbiotic donor B (3 risk factors - recent antibiotics, recent hospitalization, immune suppressed);
30 and 2 patients in the human “healthy-like” group: healthy-like donor C (no risk factors) and healthy-like donor D (no risk factors). A total of 21 4-week old mice were humanized with either dysbiotic A stool (n=4), dysbiotic B stool (n=6), healthy-like C stool (n=5) or healthy-like D stool (n=6) (Fig. 5A). Mice humanized from the same

human sample were co-housed in covered cages (separated by sex), and mice humanized with like communities (dysbiotic or healthy-like) were co-housed in the same isolator.

Human-derived communities were allowed 4 weeks to adapt to the mouse gut; then, the mice were challenged by oral gavage with 300 μ l of overnight liquid culture growth of *C. difficile* strain 630. Fecal pellets were collected pre- and at day 1, day 2, and day 6 post-challenge for *C. difficile* colony counts, 16S rRNA community analysis, and metabolomics (Fig. 5A). Mice were euthanized on day 7 and proximal colon tissue samples were collected at necropsy. Colon contents were removed and the tissue was rinsed with Krebs Mannitol (115mM NaCl, 2mM KH₂PO₄, 2.4 mM MgCl₂*6H₂O, 25 mM NaHCO₃, 8 mM KCl, 1.3 mM CaCl₂, 250 mM Mannitol). A 5 mm by 5 mm section of proximal colon tissue was stored in 10% formalin for paraffin embedding and hematoxylin and eosin (H&E) staining.

The ability of dietary intervention to restore colonization resistance was assessed using custom diets as described above. GF animals were switched to the custom chow (proline⁺ n=5, proline⁻ n=5) and humanized with dysbiotic stool. After a 4 week adaptation period, animals were challenged with *C. difficile* and pellets collected at Day 1 post infection for *C. difficile* colony counts.

The ability of prophylactic FMT to confer resistance to susceptible communities was also assessed in the GF Mouse model (Fig. 5B). Fecal suspensions were generated by suspending frozen mouse pellets collected 4 weeks after humanization from mice humanized with dysbiotic A or dysbiotic B stool from the *C. difficile* susceptibility experiment described above. A total of 6 4-week old mice received fecal suspensions via oral gavage from dysbiotic A (n=3) or dysbiotic B (n=3) and were housed as described above.

Four weeks after colonization, mice were given 2 FMTs 4 days apart. FMTs were prepared by combining 6 freshly collected mouse pellets from mice previously humanized with stool from a healthy human donor mixed with pre-reduced 1X PBS. 300 μ l of the suspension was administered to each mouse via oral gavage. One week after the FMTs, the mice were challenged with *C. difficile* as described above. Fecal pellets were collected from the mice pre-FMT, post-FMT, and on day 1, day 2, and day 6 post-*C. difficile* challenge for *C. difficile* colony counts, 16S community analysis, and metabolomics. Mice were euthanized on day 7 post-*C. difficile* challenge and colon tissue samples were collected at necropsy as described above.

C. difficile stool quantification. One pellet was used to quantify *C. difficile* stool burden at day 1, 2, and 6 post-*C. difficile* challenge. A 1 μ L aliquot of each fecal pellet was serially diluted in duplicate, spotted onto pre-reduced CDMN agar media and incubated anaerobically at 37°C for 24 hours. Identifiable *C. difficile* colonies were counted and CFU/mL of stool calculated. 2-way ANOVA in SAS 9.3 was used to compare *C. difficile* concentrations across treatment groups and days.

Colon pathology and analyses. Formalin-preserved paraffin-embedded colon tissue was submitted for sectioning, slide preparation, and H&E staining (Mayo Clinic, Phoenix, Arizona). A pathologist who was blinded to mouse IDs and treatment groups reviewed slides and colon inflammation was graded on number of polymorphonuclear cells (PMN) per high power field (HPF) (score of 0-4), presence of inflammatory cells in the lamina propria (score of 0-3), and tissue layer depth of inflammatory cells (score of 0-3) (Table 2, Table 3). To compare inflammation scores between the dysbiotic and healthy-like groups, a linear mixed effects model (LME) was fit to the data using R-3.1.2 with a random intercept for the donor type to account for within-donor correlation.

16S Extraction, sequencing, and analysis. DNA was extracted from human stool samples (0.25 g stool per extraction) and mouse pellets (1 pellet per extraction) using a MoBio PowerSoil Kit (MoBio Laboratories, Carlsbad, CA, USA). The V4 region (515F, 806R) of the 16S rRNA gene was amplified and sequenced using an Illumina MiSeq (Illumina, San Diego, CA) at the Mayo Clinic Medical Genome Facility (Mayo Clinic, Rochester, MN). Demultiplexing and quality filtering was performed in QIIME 1.9.1. Operational taxonomic unit (OTU) clustering at 97% sequence similarity and taxonomic assignment was performed with UCLUST, RDP classifier, and Greengenes (DeSantis et al. 2006). OTUs were picked closed-reference and de novo. A total of 10 human subjects (8 healthy, 2 diarrhea) were excluded from 16S rRNA analyses due to low reads or failing to pass quality thresholds during sequencing. Human samples were rarefied at 8,000 reads. Mouse samples from the first experiment testing *C. difficile* susceptibility were rarefied at 15,000 reads. Mouse samples from the second experiment testing prophylactic FMT were rarefied at 15,000 reads.

Data analyses were performed in QIIME 1.9.1, R-3.1.2, and SAS 9.3. Partitioning around medoids (PAM) clustering performed in R-3.1.2 was used to define clusters in human patient samples. Optimal cluster number was determined by gap statistic and confirmed by ASW (average silhouette width) statistic based on unweighted UniFrac distances (Tibshirani et al. 2001 *J Roy Stat Soc B* 63:411-423; Rousseeuw et al. 1987 *J*

Comput Appl Math 20:53-65). A univariable logistic regression model was used to calculate the odds ratio and the significance of individual clinical risk factors. ROC curve was constructed using 0.632+ bootstrap method based (Efron *et al.* 1997 *J Am Stat Assoc* 92:548-560) on a multivariable logistic regression model. Cluster analysis, logistic regression, and ROC analysis were performed in R-3.1.2. Shannon diversity indices (assessing microbial abundance and evenness) were calculated in QIIME and compared using t-tests in Microsoft Excel. Relative abundances of microbial taxa were compared between groups using Kruskal-Wallis (group_significance.py in QIIME), LefSe (Segata *et al.* 2011 *Genome Biol* 12:R60-R60; which incorporates the Wilcoxon rank-sum test), and the Boruta algorithm (Kursa *et al.* 2010 *J Stat Softw* 36:1-13). Random Forests (supervised_learning.py) and distance analyses (make_distance_boxplots.py) were also run in QIIME to classify and determine similarities between groups.

RNA isolation. Fecal pellets collected for RNA extraction were transferred into tubes containing 600µl of pre-chilled (-20°C) RNeasy-later-ice (Life Technologies, Carlsbad, CA) and incubated at -20°C for 24 hours. Samples were then centrifuged at 14,000 g at 4°C in an Eppendorf 5810R centrifuge (Eppendorf, Germany) for 5 minutes, the RNeasy-later-ice containing supernatant removed, and 500 µl of Buffer A (200mM NaCl, 20mM EDTA), 210 µl of 20% SDS, 500µl of acidified phenol:chloroform (125:24:1, pH 4.5) and sterile glass beads (MoBio 13118-50, Carlsbad, CA) were added to each tube. The samples were homogenized by bead beating using a MP Bio Fast Prep 24 (MP Biomedicals, Santa Ana, CA) using 6.0 m/s pulses for 60 seconds, and then centrifuged at 14,000 g at 4°C for 5 minutes. The aqueous phase was removed to a clean tube and extracted a second time with 500 µl of phenol:chloroform (125:25:1, pH 4.5). The samples were centrifuged at 14,000 g at 4°C for 5 minutes, the aqueous phase removed into a clean 1.5 mL microcentrifuge tube and combined with 60µl of 3M sodium acetate and 600 µl of -20°C 100% ethanol. Samples were mixed by inversion and allowed to incubate on dry ice for 10 minutes, wet ice for 10 minutes, and centrifuged at 14,000 g at 4°C for 5 minutes. The supernatant was removed and the nucleic acid containing pellet washed with -20°C 100% ethanol and centrifuged at 14,000 g at 4°C for 5 minutes. The ethanol wash was removed, the pellet allowed to air dry for 10 minutes, and resuspended in 100 µL of nuclease free water. After complete resuspension, 350 µL of Buffer RLT + 10µl/mL BME was added and the sample processed with a RNeasy Mini Kit (Qiagen, Valencia, CA) and contaminating DNA was removed using 2 on-column DNase treatment steps. Samples were eluted in 50 µL of nuclease free water. Total RNA yield

and quality were assessed using RNA Screen Tape (Agilent, Santa Clara, CA) and an Agilent 2200 TapeStation (Agilent, Santa Clara, CA). Contaminating ribosomal RNA (rRNA) was removed using a RiboZero rRNA Removal Kit (Epicentre, Madison, WI). Depletion was confirmed using RNA Screen Tape and 2200 Tape Station before

5 submitting samples for library preparation.

RNAseq. mRNA enriched samples were submitted to the Mayo Clinic Next Generation Sequencing Core for Library Preparation and sequencing. Library Preparation was completed using the NEB directional Library Preparation Kit (New England Biolabs, Ipswich, MA) and the samples were sequenced with an Illumina HiSeq 10 2500 Rapid Run with paired 101bp reads (Illumina, San Diego, CA). The resulting sequence data was stripped of adapters and quality filtered using Trimmomatic v. 0.32 (Bolger *et al.* 2014 *Bioinformatics* 30:2114-2120) with parameters “ILLUMINACLIP:Adapters.fasta:2:30:10 LEADING:3 TRAILING:3 MAXINFO:75:0.1 MINLEN:75”. Gene and pathway expression profiles with taxonomic identifiers when 15 appropriate were obtained using HUMAnN2 v. 0.5.0 (Abubucker *et al.* 2012 *PLoS Comput Biol* 8:e1002358) and Jaccard Similarity analysis. Differential expression analysis was performed using DESeq2 v. 1.8.2 (Love *et al.* 2014 *Genome Biol* 15:550), with a p-value cutoff of $p < 0.05$.

Untargeted Metabolomics. Metabolomics samples were extracted by bead beating 20 with acid-washed 0.1 μm Zirconia beads in acidified water (0.01% formic acid) and acetonitrile, centrifuged at 9,000 rcf, filtered (0.22 μm) and resuspended in 5% formic acid / 5% acetonitrile in water. Samples were maintained at 4°C while extracting and stored at -80°C. The samples were analyzed by reverse-phase chromatography on a Dionex Ultimate 3000 HPLC (Dionex, Sunnyvale, CA) using a 150 μm ID nanospray 25 column that was packed with 3 μm 2A C18 beads (ProntoSIL, MAC-MOD, Chadds Ford, PA) to ~150 mm. Injection volumes were 2 μL and samples were maintained at 7°C while in the autosampler awaiting injection. The mobile phase buffer A was 0.2% FA, 5% DMSO in water. The mobile phase buffer B was 0.2% FA, 5% DMSO in acetonitrile. A constant flow rate of 0.4 mL/minute was delivered throughout the following 35 minute 30 gradient (percentages indicate buffer B concentration): 0-3 minutes, 3%; 3-21 minutes, 3-95%; 24-25 minutes, 95-3%; 25-35 minutes, 3%; 50-51 minutes, 97-3%; 51-55 minutes, 3%. A coupled Thermo Orbitrap Velos mass spectrometer (Thermo Fisher, Waltham, MA) was used to collect MS data in positive ion mode (MS1 parameters: mass range: 95-1000 m/z , 60,000 R; MS2 parameters: Top 5, data-dependent mode, no charge-

state exclusion, exclusion duration 15 seconds). Peak data were processed by first applying non-linear alignment using XCMS (Smith *et al.* 2006 *Anal Chem* 78:779-787) and log2 normalization. PCoA analyses were performed on these aligned and normalized data and a volcano plot was constructed by using log2 peak fold-change and p-values

5 calculated with Kruskal-Wallis H-tests.

Stool SCFA Quantification. Stool samples (~1.8-20 mg) were extracted for SCFAs by mixing frozen feces with acidified water (pH 2.3 with HCl) containing 6 µg/mL of an internal standard, sodium butyrate-(¹³C)₄, in a ratio of 50 µL water per mg fecal mass. Samples were vortexed for 10 minutes, sonicated for 10 minutes, and
10 vortexed for an additional 10 minutes, and then centrifuged at 17,200 g for 10 minutes at 4°C. Supernatant from extracted samples were stored at -80°C prior to analysis by GC-MS.

The samples were analyzed using a Trace GC 1310 coupled to a Thermo ISQ-LT (Thermo Fisher, Waltham, MA) scanning from m/z 30–300 at a rate of 5 scans/second in
15 electron impact mode. Samples were injected at a 5:1 split ratio, and the inlet was held at 250°C and transfer line was held at 230°C. Separation was achieved on a 30m TG-WAXMS column (Thermo Scientific, 0.25 mm ID, 0.25 µm film thickness) using a temperature program of 100°C for 1 minute, ramped at 20°C per minute to 240°C and held at 240°C for 2 minutes. Helium carrier flow was held at 1.2 mL per minute.

20 Amounts of acetate, propionate, butyrate, isobutyrate, isovalerate, valerate, caproate, and heptanoate in stool samples were determined. A mix of all analytes across a range of concentrations, also containing the labeled internal standards present in the extracts, was examined during fecal extract analysis to create a calibration curve and absolute quantitation. Analyte peak areas were normalized to the internal standard peak areas
25 using the following equation: normalized analyte response = analyte peak area * (internal standard concentration / internal standard peak area).

Stool BA Quantification. LC-MS was performed on a Waters Acquity UPLC coupled to a Waters Xevo TQ-S triple quadrupole mass spectrometer (Waters, Milford, MA). Chromatographic separations were carried out on a Waters HSS T3 stationary
30 phase (1 x 100 mm, 1.8 µM). Mobile phases were methanol (B) and water with 0.1% formic acid and 2 mM ammonium hydroxide (A). The analytical gradient was as follows: time = 0 minute, 0.1% B; time = 0.5 minute, 0.1% B; time = 2 minutes, 30% B; time = 15 minutes, 97% B; time = 16 minutes, 97% B; time 16.5 minutes, 0.1% B; time 21 minutes,

0.1% B. Flow rate was 210 μ L/min and injection volume was 5 μ L. Samples were held at 4°C in the autosampler, and the column was operated at 70°C.

The MS was operated in selected reaction monitoring (SRM) mode, where a parent ion is selected by the first quadrupole, fragmented in the collision cell, then a fragment ion selected for by the third quadrupole. Product ions, collision energies, and cone voltages were optimized for each analyte by direct injection of individual synthetic standards. Inter-channel delay was set to 3 ms. The MS was operated in both negative and positive ionization modes with the capillary voltage set to 2.1 and 3.2 kV respectively. Source temperature was 150°C and desolvation temperature 500°C.

Desolvation gas flow was 1000 L/hour, cone gas flow was 150 L/h, and collision gas flow was 0.2 mL/min. Nebuliser pressure was set to 7 Bar. Argon was used as the collision gas, otherwise nitrogen was used.

Fecal samples were extracted as described previously (Humbert *et al.* 2012 *J Chromatogr B Analyt Technol Biomed Life Sci* 899:135-145) with minor modifications.

In short, 70 μ L of 0.1 M NaOH containing internal standards at 4 μ g/mL was added for every 2 mg of feces (the range of sample weights was 2-3 mg). Samples were vortexed to mix, sonicated 10 minutes, then incubated at 60°C for 1 hour. Samples were diluted 3-fold into water, then sonicated for 10 minutes, then vortexed for 10 minutes, then frozen at -80°C overnight. After thawing, samples were centrifuged for 20 minutes at 4°C at 16,000 x g, then the supernatant analyzed by LC-MS. A 9-point calibration curve was prepared in similar fashion.

Peak integration was performed using Waters TargetLynx software (Waters, Milford, MA). Absolute concentration calculations were performed in Excel, and based on a 5-point minimum calibration curve. For quantitation, a signal to noise greater than 10 was required. For detection, a signal to noise greater than 3 was required.

Stool AA Quantification. H^1 -NMR analysis was performed on aqueous stool extracts to quantitate free AA concentrations. Pellets mass was determined before resuspending in 1 mL of molecular grade water, and subjected to 3 rounds of freeze-thaw cycles using dry ice. Glass beads (MoBio 13118-50, Carlsbad, CA) were added to the tubes and the samples bead beaten using a MP Bio Fast Prep 24 (MP Biomedicals, Santa Ana, CA) for 60 seconds with 6.0 m/second pulses. Large particulate matter and the glass beads were pelleted by centrifugation at 14,000 g for 10 minutes at 4°C. The resulting supernatant was removed and stored at -80°C prior to analysis.

Stool extract samples were thawed at room temperature for 10–15 minutes. Then 300 µl of 0.1 M phosphate buffer (K₂HPO₄/KH₂PO₄, pH 7.4) and 50 µl of 1 mM TSP-*d*₄ solution (Sigma 269913, St. Louis, MO) in D₂O (Sigma 613444, St. Louis, MO) are added. Samples are shaken by vortex for 20 seconds and spun down at 13,300 rpm for 5 min. Supernatants are transferred to 5 mm NMR tubes stored at 4°C prior to NMR measurements. The NMR analysis was performed on a Bruker AVANCE III 600 MHz instrument (Bruker, Billerica, MA) equipped with BBI probe head and SampleJet autosampler. ¹H-NMR spectra were recorded using 1D NOESY pulse sequence with presaturation (noesygppr1d) under following conditions: 90 degree pulse for excitation, acquisition time 3.89 seconds, relaxation delay 5 seconds. All spectra were acquired with 256 scans at room temperature (298K), with 64k data points and 8417 Hz (14 ppm) spectral width. The recorded ¹H-NMR spectra were phase corrected using Bruker TopSpin 3.5 (Bruker, Billerica, MA). Then the spectra were processed using Chenomx NMR Suite 8.1 (Chenomx, Edmonton, AB). The compounds were identified by comparing spectra to database Chenomx 600 MHz Version 10 and using available literature data (Saric *et al.* 2008 *PLoS Negl Trop Dis.* 2:e254; Wu *et al.* 2010 *Analyst.* 135:1023-1030; Zhao *et al.* 2013 *J Proteome Res.* 12:2987-2999). Quantification was based on internal standard peak integration (TSP-*d*₄). For statistical analysis the NMR spectral region from 0.6 to 9 ppm was divided in 0.04 ppm wide bins (solvent region 4.6-5.2 ppm was excluded). The bins were normalized using total peak area normalization, and standardized peak area (TSP-*d*₄) normalization.

These results demonstrate that a subset of patients with diarrhea have gut microbial communities distinct from healthy controls. Dysbiotic gut microbial communities were characterized by decreased microbial richness and evenness, increased relative abundances of OTUs within *Enterococcus*, *Enterobacter*, and *Bacteroides*, and decreased *Faecalibacterium*, *Roseburia*, *Blautia* and *Bacteroides*.

These results also demonstrated that clinical biomarkers (*e.g.*, current/recent hospitalization, immune suppression, recent antibiotics, and prior CDI) can, independent of underlying disease state, predict dysbiosis.

These results showed that humanized mice colonized with dysbiotic microbiota exhibit increased susceptibility to colonization and inflammation following CDI, and that fecal transplant from healthy human donor can decrease susceptibility to CDI in humanized mice with dysbiotic microbiota.

Example 2: Study on Individuals with Diarrhea

Using the 5 clinical risk factors identified in Example 1, the records of 20,687 patients (Table 4) who presented with diarrhea and were tested for *Clostridium difficile* at Mayo Clinic, Rochester, MN between 2011 – 2016 were examined. All patients were over 18 years of age (IRB 16-003622). Patients who tested negative and then subsequently tested positive were marked as “converters.” Patients who tested negative but never tested positive were marked as “non-converters.” A single “test negative” date was preserved for each patient and no patients were duplicated in this analysis. Based on the “test negative” date, all 5 risk factors were evaluated for each patient including: prior *C. difficile* infection, recent hospitalization (within the previous 4 weeks), current hospitalization, antibiotic use (within the previous 3 weeks), and immunosuppression.

Table 4: Demographic information on converters and non-converters

	Converter (n=662)	Non-Converter (n=22,141)
Sex, n (%)		
Male	311 (47)	9,873 (45)
Female	351 (53)	12,268 (55)
Age (yr)		
Mean (SD)	60.0 (15.2)	59.9 (17.7)
Range	18-95	18-106
BMI (SD)	29.8 (7.3)	29.1 (7.3)

Using univariate logistic regression analysis, each risk factor significantly predicted *C. difficile* susceptibility, or “conversion” to a *C. difficile* positive state from a *C. difficile* negative state (Table 5).

Table 5. Univariate Logistic Regression

Risk Factor	p-value
Prior <i>C. difficile</i> infection	<2e-16
Current Hospitalization	<2e-16
Recent Hospitalization (within previous 4 weeks)	<2e-16
Antibiotics (within previous 3 weeks)	<2e-16
Immunosuppression	<2e-16

Relative risk was calculated for each risk factor (Table 6) and for the number of risk factors each converter exhibited (Table 7). Individuals with 2 or more risk factors were between 1.22-6.8 times more likely to convert to a *C. difficile* positive state.

Table 6: Relative risk of converting by risk factor.

Risk Factor	Relative Risk
Antibiotics	3.38
Immunosuppression	2.50
Recent Hospitalization	2.95
Current Hospitalization	3.20
Prior CDI	5.17

Table 7. Risk of converting based on number of risk factors.

Number of risk factors	Relative Risk	Odds Ratio
0	0.33	1
1	0.43	1.16
2	1.22	2.86
3	1.81	3.83
4	3.33	6.50
5	6.8	16.06

5 *Example 3: Treating Mice at Risk of C. difficile Infection With Probiotic Cocktail*

Germ free mice were given to probiotic delivery of gut microbiota from patients who had diarrhea with either healthy-like or dysbiotic microbiota as shown in Figure 20.

The probiotic cocktail included 3 microbial biomarkers associated with healthy-like humans: *Roseburia feacis*, *Faecalibacterium prausnitzii*, *Akkermansia muciniphila*.

10

Table 8. Probiotic Cocktail.

Bacterial Genera	Test-Statistic	p-value	Bonferroni p-value	Dysbiotic Mean	Healthy-like Mean	Feature Importance Score	Boruta Algorithm
<i>Roseburia</i>	33.14	< 0.0001	< 0.0001	523.80	1845.95	8	Confirmed
<i>Faecalibacterium</i>	32.05	< 0.0001	< 0.0001	510.43	1383.51	6	Confirmed
<i>Akkermansia</i>	2.54	0.11	1.00	1263.02	2102.48	1421	Confirmed
<i>Bacteroides</i>	27.08	< 0.0001	< 0.0001	387.24	1442.80	2	Confirmed
<i>Blautia</i>	16.13	< 0.0001	0.001	1209.83	1950.36	4	Confirmed
<i>Bacteroides</i>	14.27	< 0.0001	0.003	2614.15	4165.36	9	Confirmed

OTHER EMBODIMENTS

It is to be understood that while the disclosure has been described in conjunction with the detailed description thereof, the foregoing description is intended to illustrate and not limit the scope of the disclosure, which is defined by the scope of the appended
5 claims. Other aspects, advantages, and modifications are within the scope of the following claims.

WHAT IS CLAIMED IS:

1. A method for predicting dysbiosis in a mammal with diarrhea, the method comprising:
determining an amount of at least one biomarker of gut microbiota dysbiosis in a fecal sample obtained from the mammal; and
identifying the mammal as having dysbiosis if the amount of the at least one biomarker of gut microbiota is altered relative to a mammal without diarrhea.
2. The method of claim 1, wherein the alteration in gut microbiota is a decrease in at least one of *Roseburia*, *Faecalibacterium*, *Akkermansia*, *Bacteroides*, or *Blautia*.
3. The method of claim 1, wherein the alteration in gut microbiota is an increase in at least one of *Escherichia*, *Shigella*, *Enterobacter*, *Enterococcus*, or *Parasutterella*.
4. The method of claim 1, wherein the alteration in gut microbiota is a decrease in at least one of *Roseburia*, *Faecalibacterium*, *Akkermansia*, *Bacteroides*, or *Blautia* and an increase in at least one of *Escherichia*, *Shigella*, *Enterobacter*, *Enterococcus*, or *Parasutterella*.
5. A method for predicting susceptibility to *C. difficile* infection in a mammal with diarrhea, the method comprising:
determining an amount of at least one biomarker of gut microbiota dysbiosis in a fecal sample obtained from the mammal; and
identifying the mammal as having increased susceptibility to *C. difficile* infection if the amount of the at least one biomarker of gut microbiota is altered relative to a mammal without diarrhea.
6. The method of claim 5, wherein the alteration in gut microbiota is a decrease in at least one of *Roseburia*, *Faecalibacterium*, *Akkermansia*, *Bacteroides*, or *Blautia*.
7. The method of claim 5, wherein the alteration in gut microbiota is an increase in at least one of *Escherichia*, *Shigella*, *Enterobacter*, *Enterococcus*, or *Parasutterella*.

8. The method of claim 5, wherein the alteration in gut microbiota is a decrease in at least one of *Roseburia*, *Faecalibacterium*, *Akkermansia*, *Bacteroides*, or *Blautia* and an increase in at least one of *Escherichia*, *Shigella*, *Enterobacter*, *Enterococcus*, or *Parasutterella*.

9. A method for treating *C. difficile* infection in a mammal, the method comprising:
administering to the mammal a composition comprising at least three bacteria that are decreased in gut microbiota dysbiosis;

wherein the at least three bacteria that are decreased in gut microbiota dysbiosis are selected from the group consisting of *Roseburia*, *Faecalibacterium*, *Akkermansia*, *Bacteroides*, *Blautia*, and *Bacteroides*.

10. The method of claim 9, wherein the at least three bacteria that are decreased in gut microbiota dysbiosis comprise *Roseburia feacis*, *Faecalibacterium prausnitzii*, and *Akkermansia muciniphila*.

11. The method of claim 9, wherein the method comprises identifying said mammal as having said *C. difficile* infection prior to said administration.

12. The method of any of claims 1, 5, or 9, wherein said mammal is a human.

13. The method of claim 12, wherein said human exhibits at least one clinical biomarker of dysbiosis.

14. The method of claim 13, wherein the at least one clinical biomarker selected from the group consisting of current/recent hospitalization, immune suppression, current/recent antibiotic use, and prior *C. difficile* infection.

15. A composition comprising at least three bacteria that are decreased in gut microbiota dysbiosis selected from the group consisting of *Roseburia*, *Faecalibacterium*, *Akkermansia*, *Bacteroides*, *Blautia*, and *Bacteroides*.

16. The composition of claim 15, wherein the at least three bacteria that are decreased in gut microbiota dysbiosis comprise *Roseburia feacis*, *Faecalibacterium prausnitzii*, and *Akkermansia muciniphila*.
17. The composition of claim 15, wherein the composition is a pill, tablet, capsule, or enema.
18. The composition of claim 15, wherein the composition is configured to deliver said at least three bacteria to the intestines of said mammal.
19. A method for predicting susceptibility to *C. difficile* infection in a mammal with diarrhea, the method comprising:
- determining a level of at least one free amino acid in a fecal sample obtained from the mammal; and
 - identifying the mammal as having increased susceptibility to *C. difficile* infection if the level of the at least one amino acid is altered relative to a mammal without diarrhea.
20. The method of claim 19, wherein the alteration in the free amino acid level is an increase in the at least one amino acid.
21. The method of claim 20, wherein the at least one amino acid is selected from the group consisting of proline, alanine, glycine, histidine, isoleucine, leucine, methionine, phenylalanine, threonine, tryptophan, tyrosine, and valine.
22. The method of claim 21, wherein the at least one amino acid is proline.
23. A method for predicting susceptibility to *C. difficile* infection in a mammal with diarrhea, the method comprising:
- determining a clinical risk factor profile; and
 - identifying the mammal as having increased susceptibility to *C. difficile* infection if the mammal has at least one clinical risk factor.

24. The method of claim 23, wherein the clinical risk factor is selected from the group consisting of current/recent hospitalization, immune suppression, current/recent antibiotic use, and prior *C. difficile* infection.

25. A method for predicting susceptibility to *C. difficile* infection in a mammal with diarrhea, the method comprising:

determining a level of at least one short chain fatty acid (SCFA) in a fecal sample obtained from the mammal; and

identifying the mammal as having increased susceptibility to *C. difficile* infection if the level of the at least one SCFA is altered relative to a mammal without diarrhea.

26. The method of claim 25, wherein the alteration in the SCFA level is a decrease in the at least one SCFA.

27. A method for predicting susceptibility to *C. difficile* infection in a mammal with diarrhea, the method comprising:

determining a level of at least one bile acid (BA) in a fecal sample obtained from the mammal; and

identifying the mammal as having increased susceptibility to *C. difficile* infection if the level of the at least one BA is altered relative to a mammal without diarrhea.

28. The method of claim 27, wherein the BA is selected from the group consisting of cholic acid (CA), deoxycholic acid (DCA), lithocholic acid (LCA), and ursodeoxycholic acid (UDCA).

29. The method of claim 27, wherein the determining a level of at least one BA comprises determining a level of cholic acid (CA), and determining a level of deoxycholic acid (DCA).

30. The method of claim 29, further comprising determining a ratio of CA/DCA.

31. The method of claim 30, wherein the alteration in the BA level is an increase in the ratio of CA/DCA.

32. A method for preventing *C. difficile* infection in a mammal, the method comprising:
administering to the mammal a composition comprising at least three bacteria that are decreased in gut microbiota dysbiosis;

wherein the at least two bacteria that are decreased in gut microbiota dysbiosis are selected from the group consisting of *Roseburia*, *Faecalibacterium*, *Akkermansia*, *Bacteroides*, *Blautia*, and *Bacteroides*.

33. The method of claim 32, wherein the at least two bacteria that are decreased in gut microbiota dysbiosis comprise *Roseburia feacis* and *Faecalibacterium prausnitzii*.

34. The composition of claim 32, wherein the composition is administered by fecal microbiota transplant (FMT).

35. The composition of claim 32, wherein the FMT is administered by enema, colonoscope, nasogastric tube, or nasoduodenal tube.

36. The method of claim 32, wherein the method comprises identifying said mammal as having increased susceptibility to *C. difficile* infection prior to said administration.

37. The method of claim 34, wherein the mammal is identified as having increased susceptibility to *C. difficile* infection using the method of any of claims 5, 19, 23, 25, or 27.

38. The method of claim 32, wherein said mammal is a human.

FIG. 1

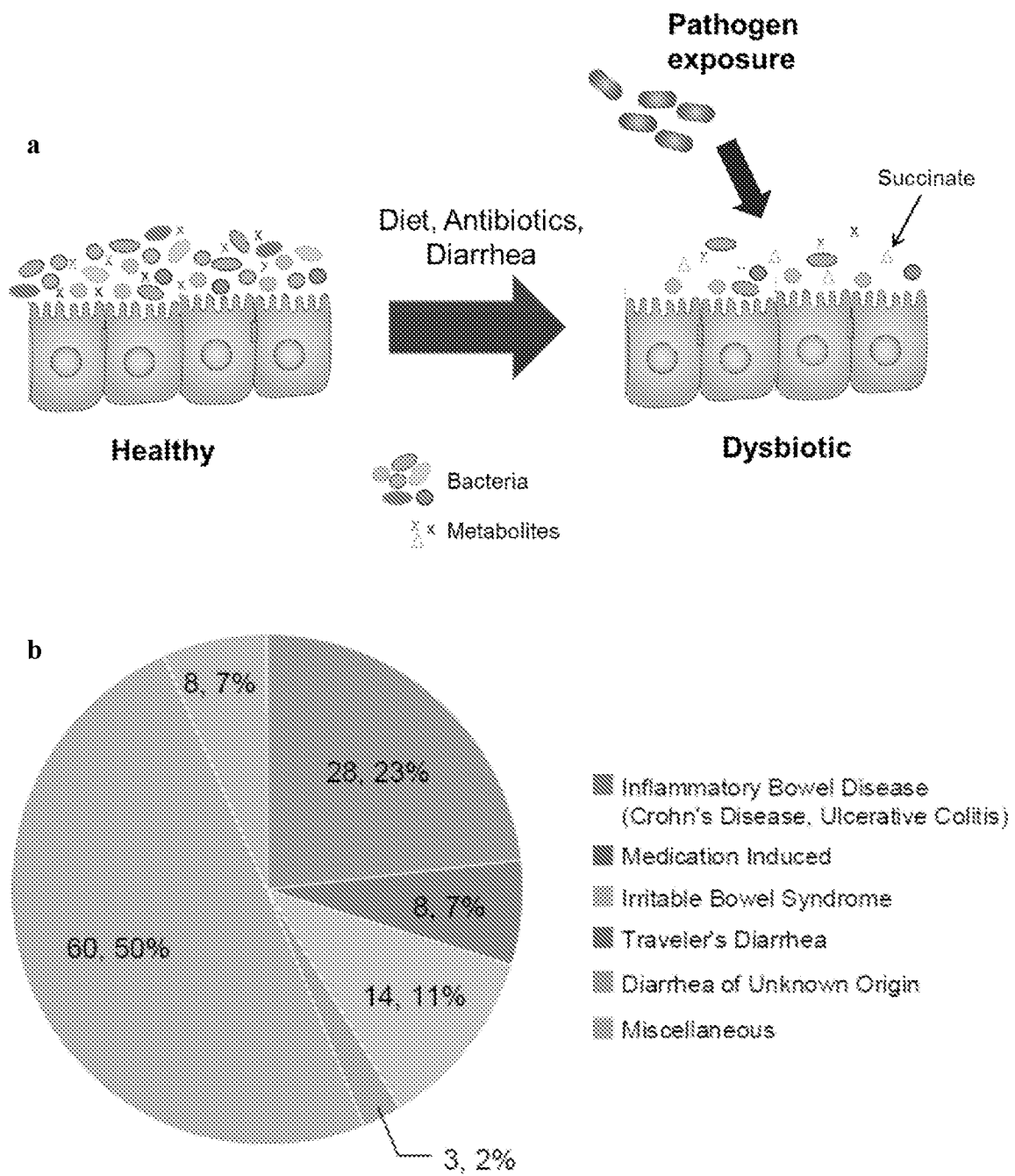


FIG. 2

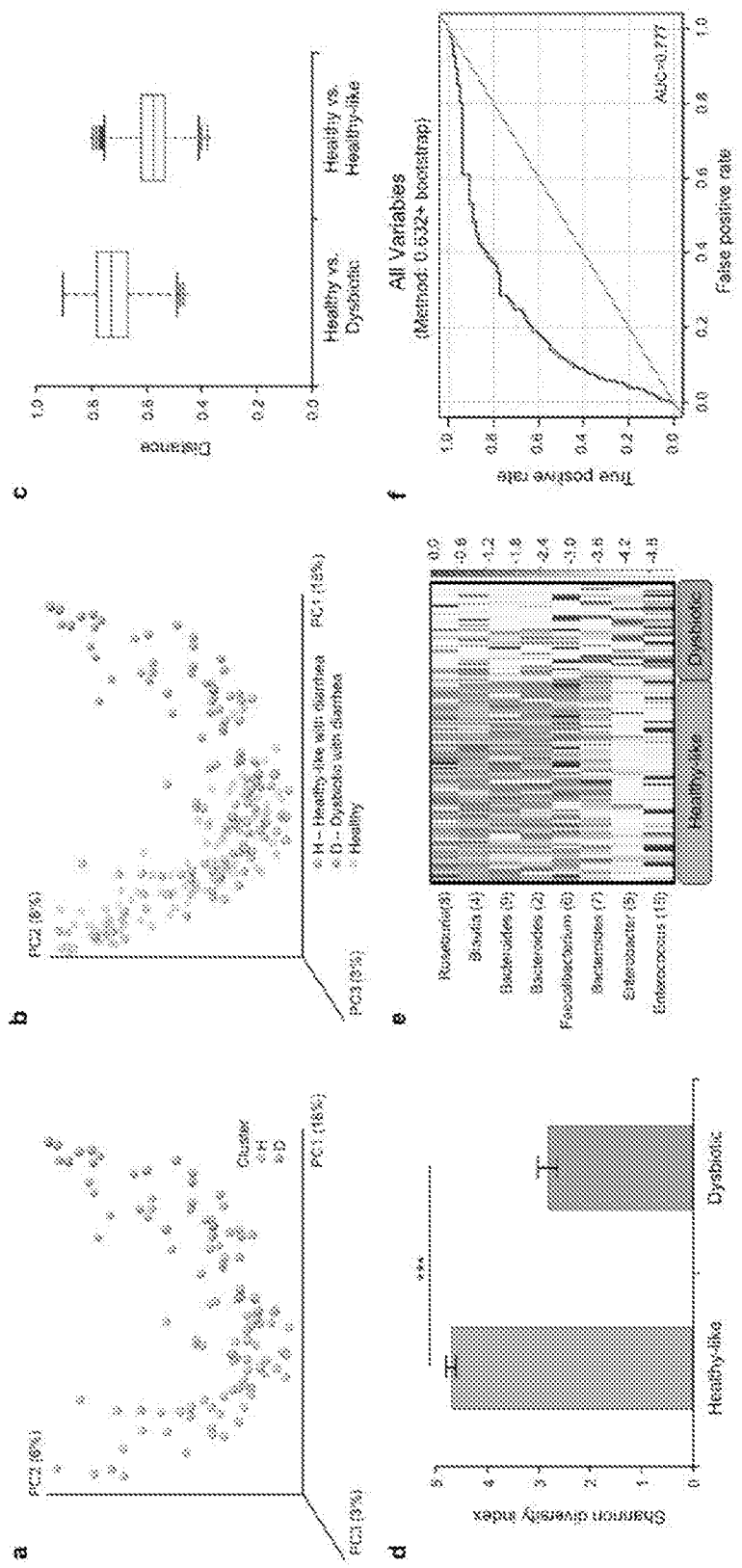


FIG. 3

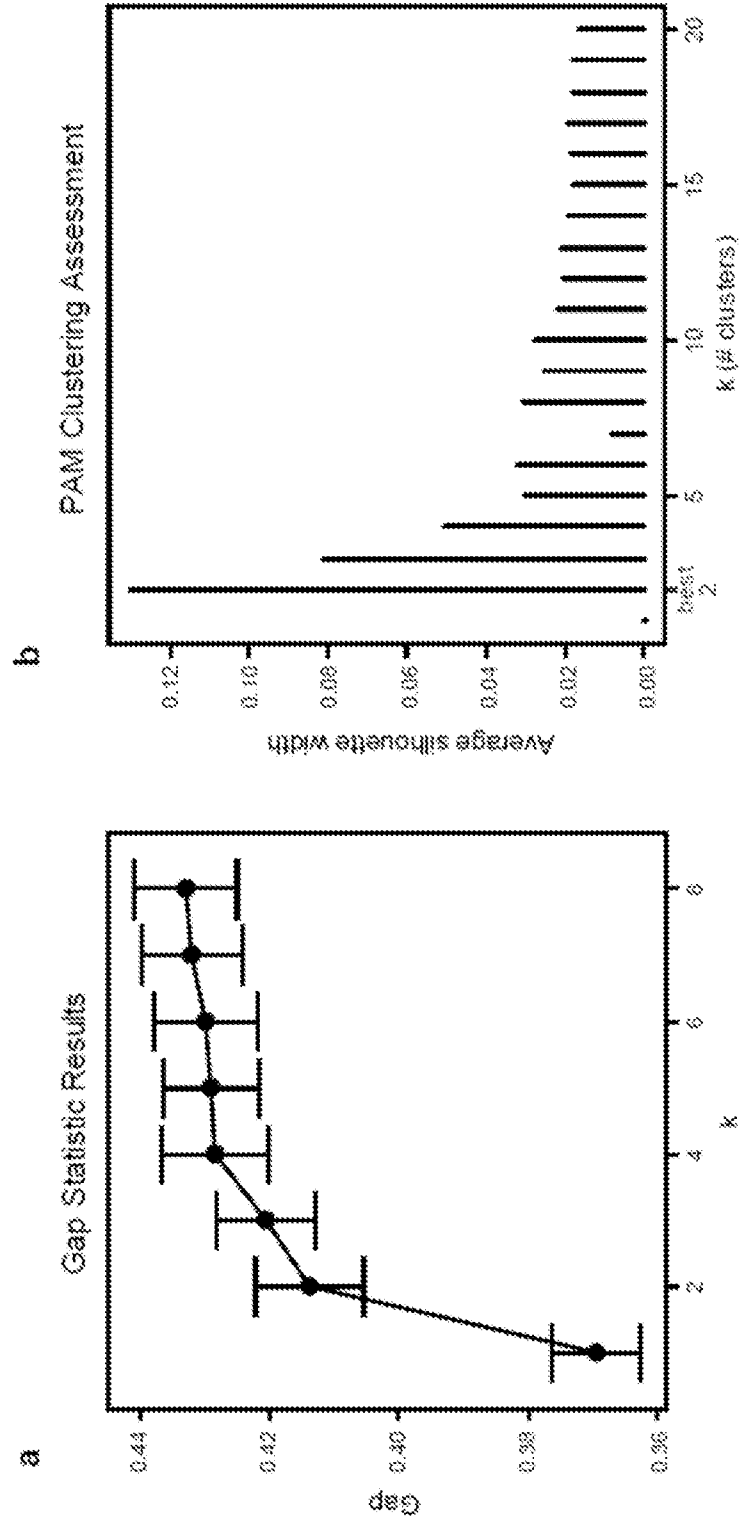


FIG. 4

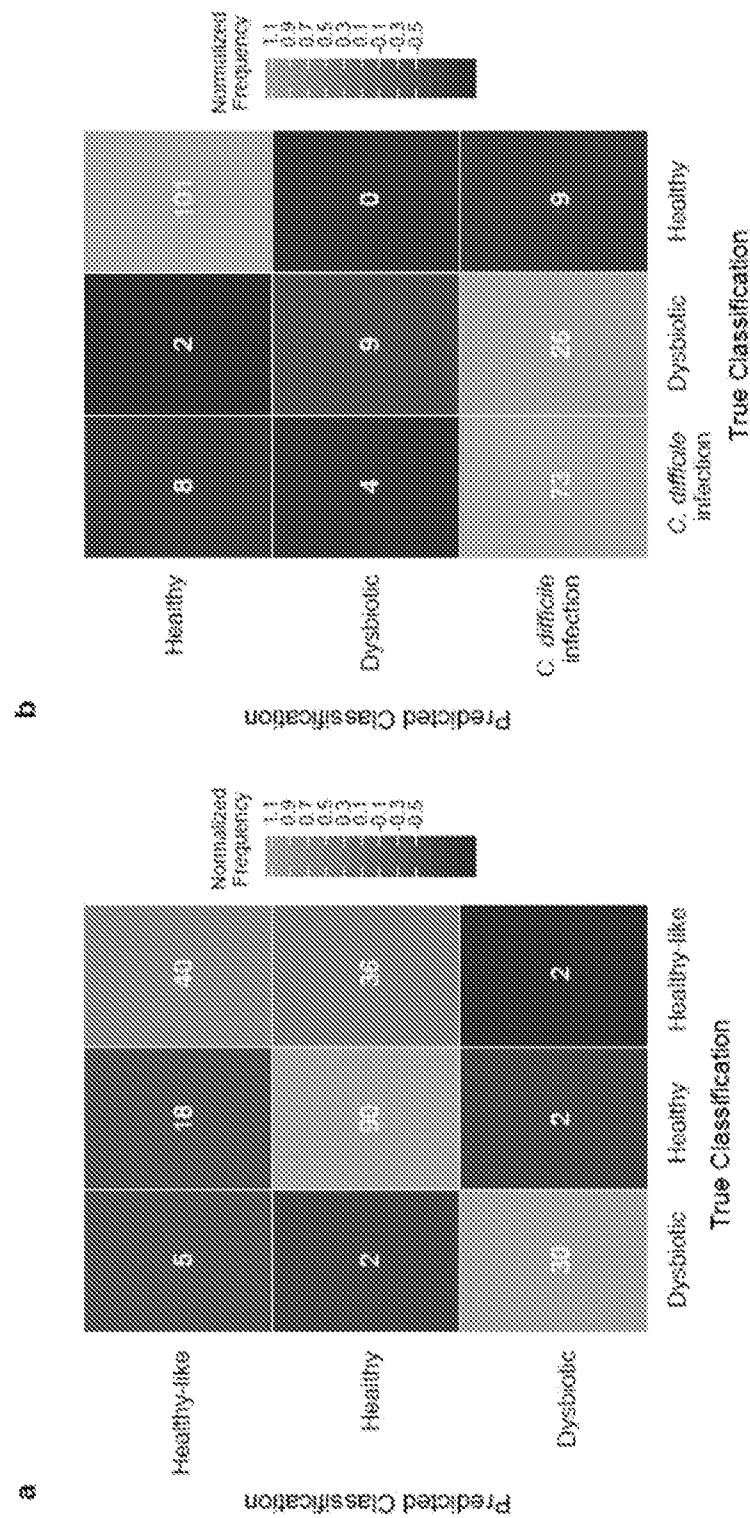


FIG. 5

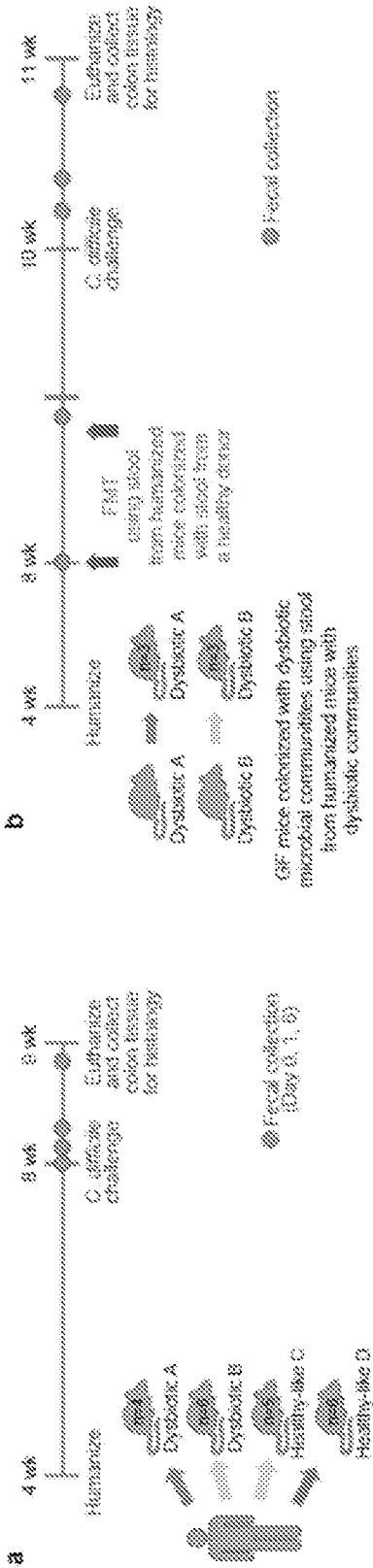


FIG. 6

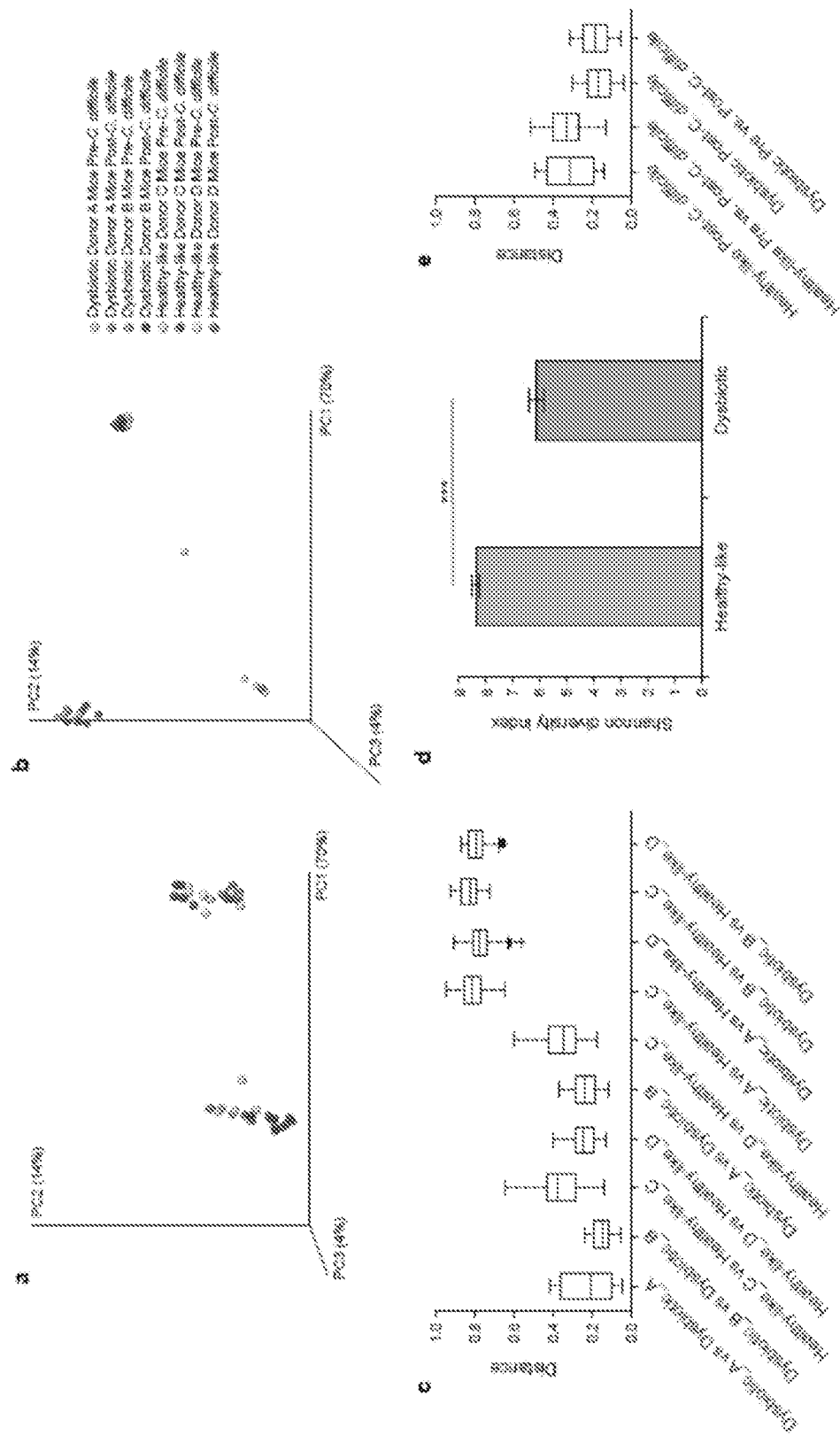


FIG. 7

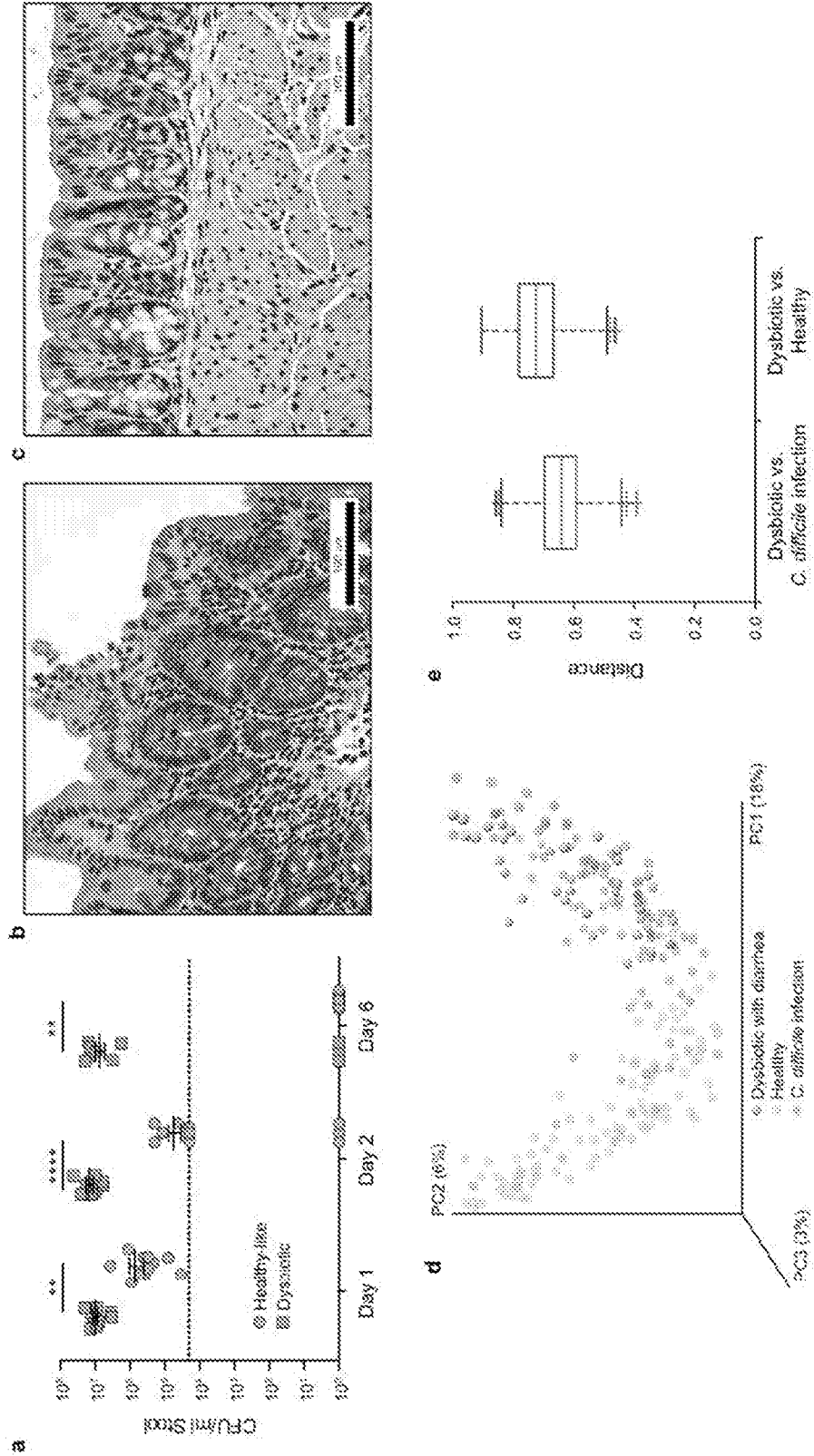


FIG. 8

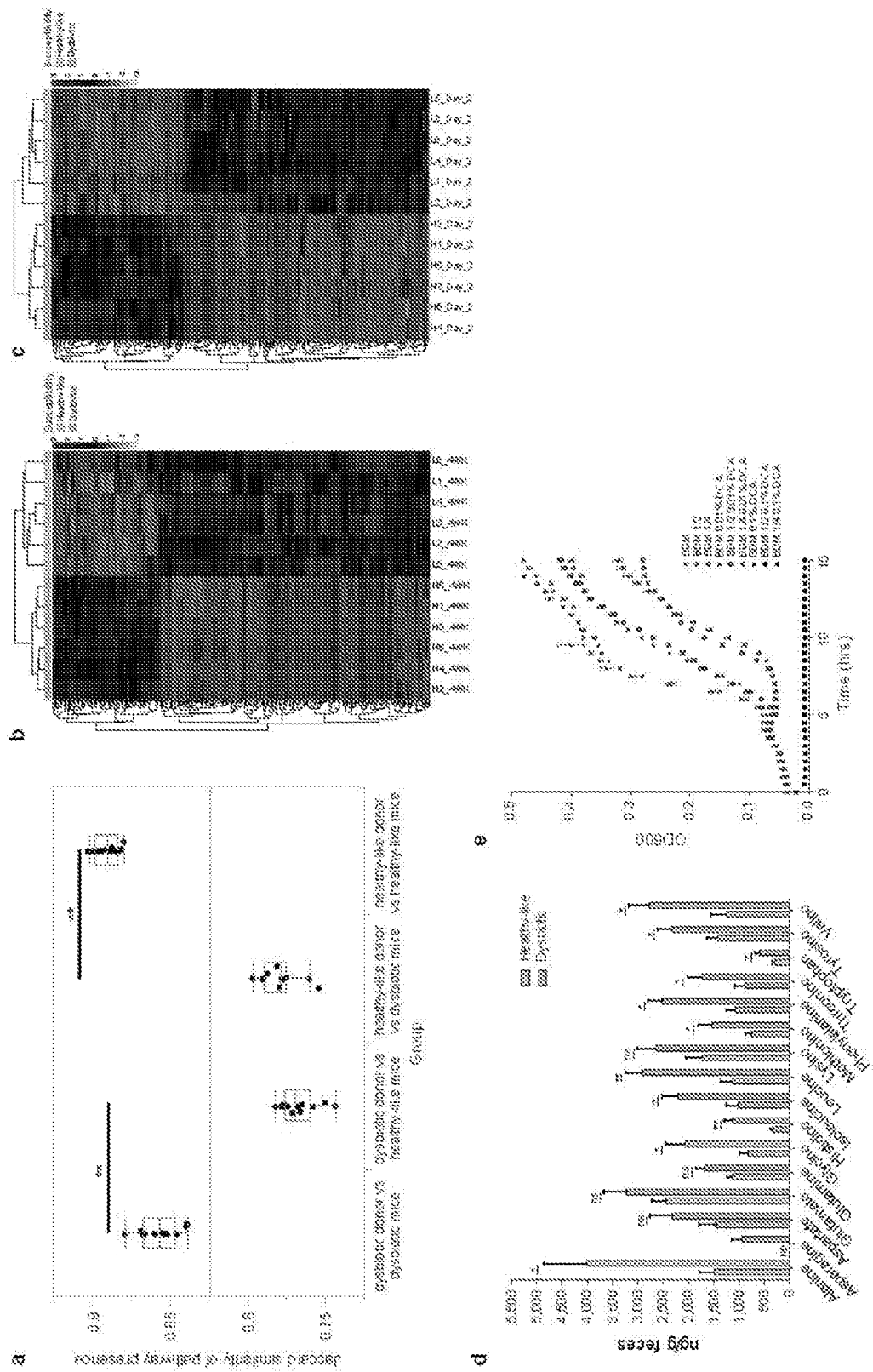


FIG. 9

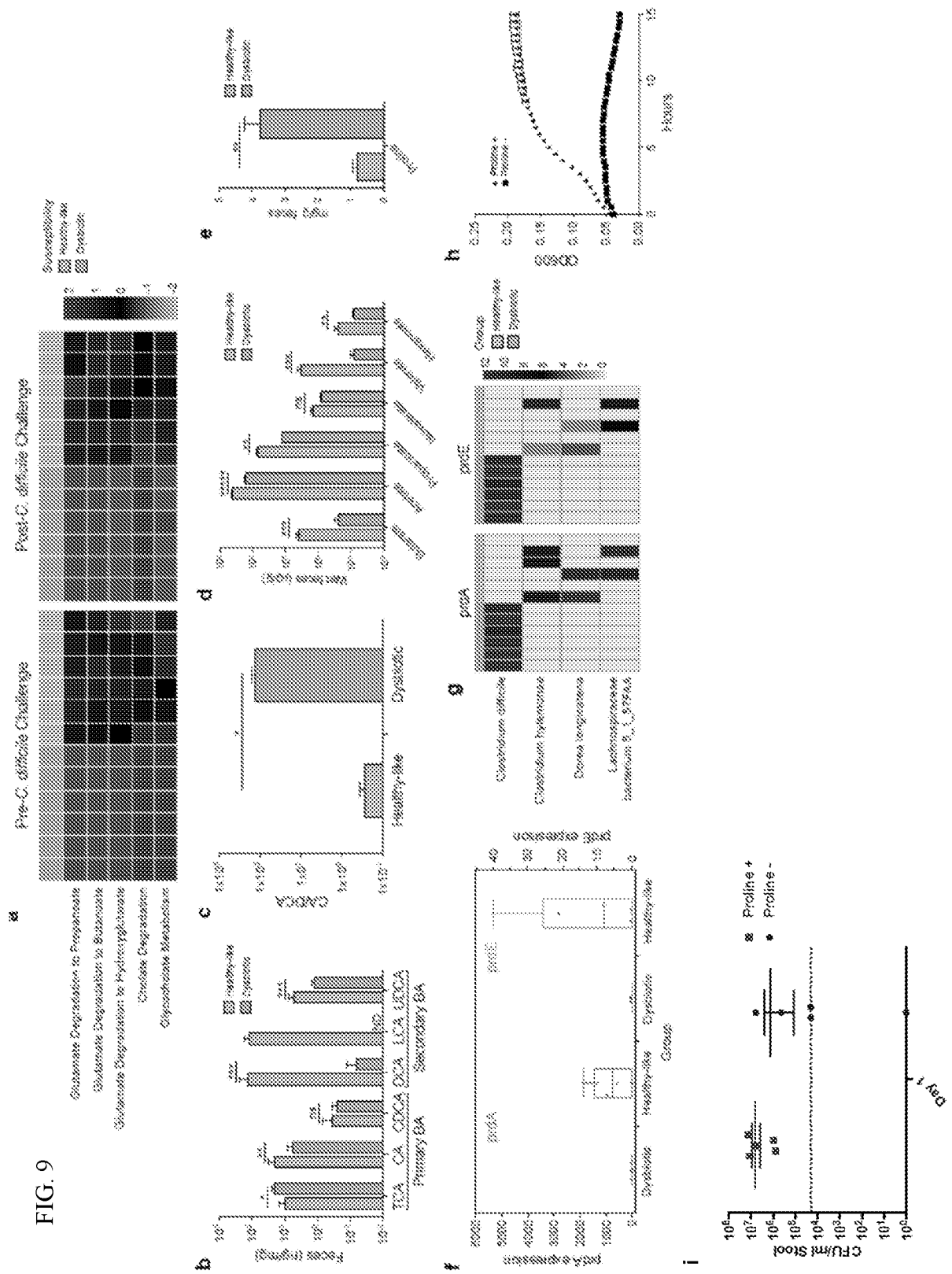


FIG. 10

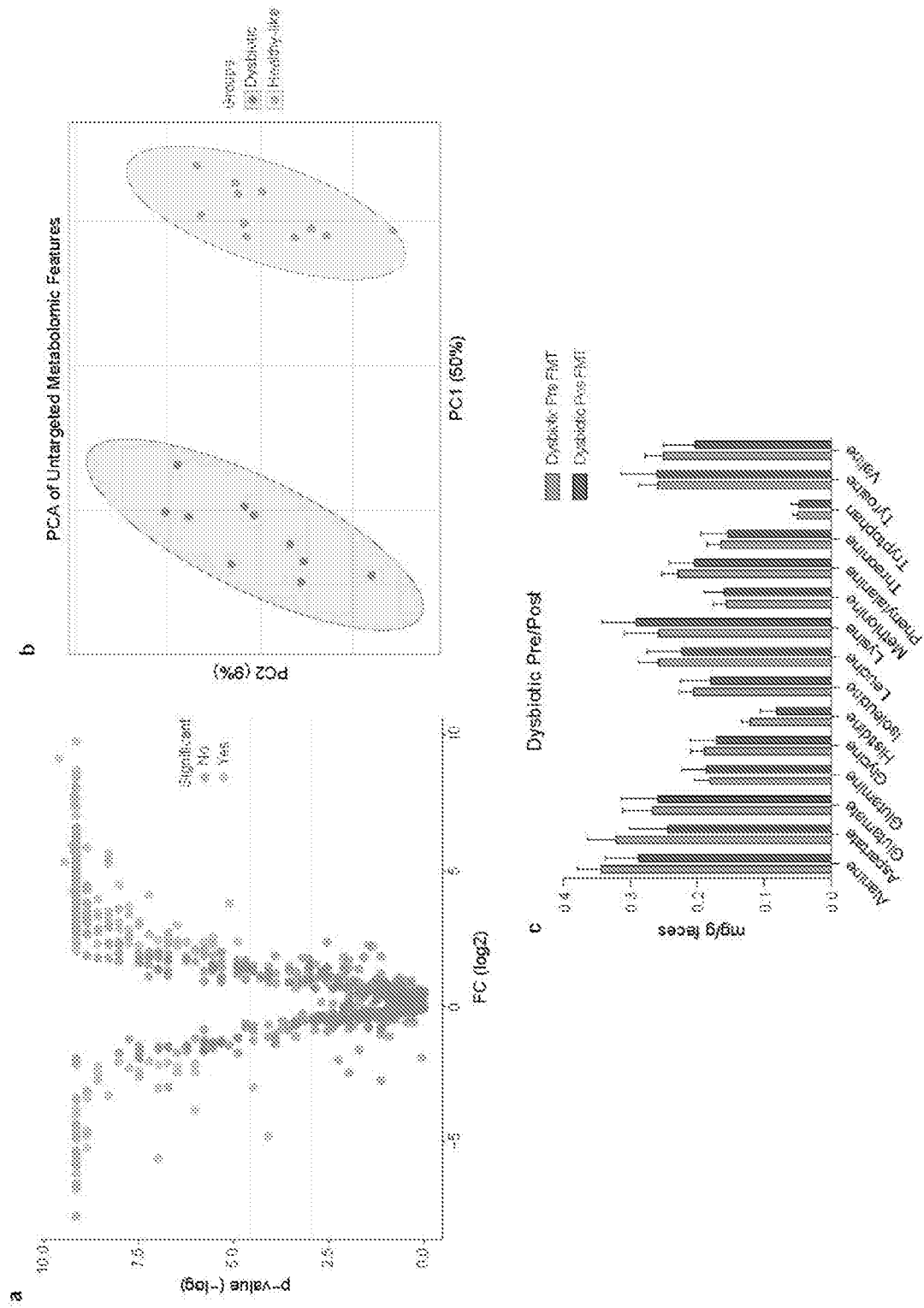


FIG. 11

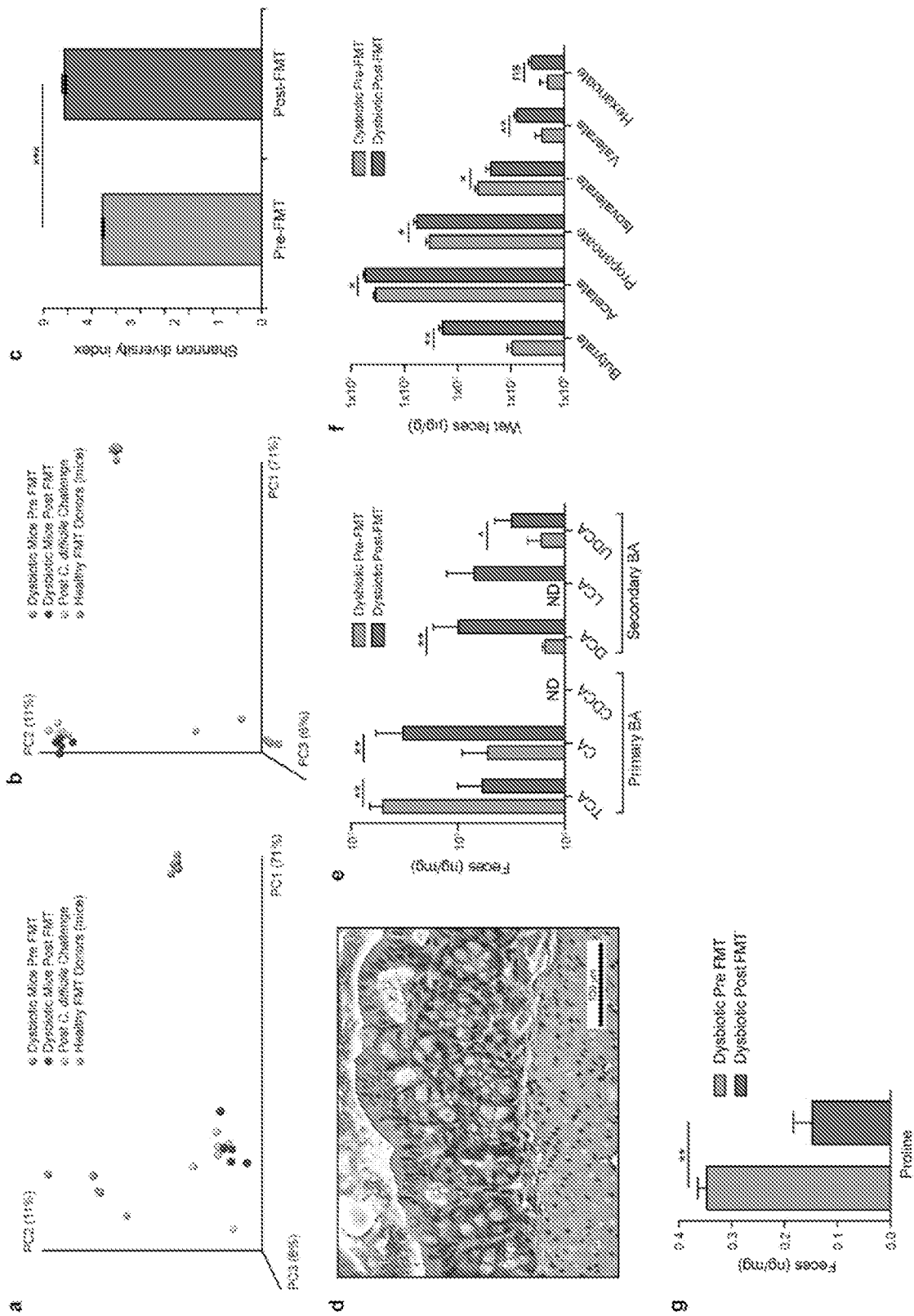


FIG. 12

Taxa Present in Humans	Transferred to Mice at a Family Level?
Bacteria; Proteobacteria; Betaproteobacteria; Neisseriales; Neisseriaceae	N
Bacteria; Proteobacteria; Gammaproteobacteria; Enterobacteriales; Enterobacteriaceae	Y
Bacteria; Firmicutes; Clostridia; Clostridiales; Veillonellaceae	Y
Bacteria; Fusobacteria; Fusobacteriia; Fusobacteriales; Fusobacteriaceae	N
Bacteria; Proteobacteria; Betaproteobacteria; Burkholderiales;	Y
Bacteria; Firmicutes; Bacilli; Lactobacillales; Lactobacillaceae	Y
Bacteria; Proteobacteria; Deltaproteobacteria; Desulfovibrionales; Desulfovibrionaceae	Y
Bacteria; Proteobacteria; Epsilonproteobacteria; Campylobacteriales; Campylobacteraceae	N
Bacteria; Bacteroidetes; Bacteroidia; Bacteroidales; S24-7	Y
Bacteria; Bacteroidetes; Bacteroidia; Bacteroidales; Bacteroidaceae	Y
Bacteria; Bacteroidetes; Bacteroidia; Bacteroidales; Prevotellaceae	Y
Bacteria; Firmicutes; Bacilli; Lactobacillales; Streptococcaceae	Y
Bacteria; Actinobacteria; Actinobacteria; Actinomycetales; Micrococcaceae	Y
Bacteria; Bacteroidetes; Bacteroidia; Bacteroidales; [Barnesiellaceae]	Y
Bacteria; Firmicutes; Clostridia; Clostridiales	Y
Bacteria; Firmicutes; Clostridia; Clostridiales; Lachnospiraceae	Y
Bacteria; Firmicutes; Clostridia; Clostridiales; Ruminococcaceae	Y
Bacteria; Proteobacteria; Betaproteobacteria	Y
Bacteria; Proteobacteria; Gammaproteobacteria; Aeromonadales; Aeromonadaceae	Y
Bacteria; Verrucomicrobia; Verrucomicrobiae; Verrucomicrobiales; Verrucomicrobiaceae	Y
Bacteria; Actinobacteria; Actinobacteria; Bifidobacteriales; Bifidobacteriaceae	Y
Bacteria; Actinobacteria; Coriobacteriia; Coriobacteriales; Coriobacteriaceae	Y
Bacteria; Firmicutes; Bacilli; Lactobacillales; Enterococcaceae	Y
Bacteria; Firmicutes; Bacilli; Lactobacillales; Carnobacteriaceae	Y
Bacteria; Bacteroidetes; Bacteroidia; Bacteroidales; Porphyromonadaceae	Y
Bacteria; Actinobacteria; Actinobacteria; Actinomycetales; Corynebacteriaceae	Y
Bacteria; Firmicutes; Bacilli; Bacillales; Planococcaceae	N
Bacteria; Firmicutes; Erysipelotrichi; Erysipelotrichales; Erysipelotrichaceae	Y
Bacteria; Proteobacteria; Gammaproteobacteria; Pseudomonadales; Moraxellaceae	Y

FIG. 13

Mouse ID	Risk	Donor ID	Inflammation in the Lamina Propria	Maximum PMN/HPF	Depth of Inflammation	TOTAL
1A	dysbiotic	A	3	4	3	10
1B	dysbiotic	A	2	1	2	5
1C	dysbiotic	A	1	1	3	5
1D	dysbiotic	A	2	3	2	7
2A	dysbiotic	B	2	4	2	8
2B	dysbiotic	B	3	3	2	8
2C	dysbiotic	B	3	4	2	9
2D	dysbiotic	B	3	4	2	9
2E	dysbiotic	B	3	4	3	10
2F	dysbiotic	B	3	4	2	9
3A	healthy-like	C	0	0	0	0
3B	healthy-like	C	1	2	2	5
3C	healthy-like	C	1	1	0	2
3D	healthy-like	C	1	1	0	2
3E	healthy-like	C	1	1	0	2
4A	healthy-like	D	0	0	0	0
4B	healthy-like	D	0	0	0	0
4C	healthy-like	D	0	0	0	0
4D	healthy-like	D	0	0	0	0
4E	healthy-like	D	0	0	0	0
4F	healthy-like	D	0	0	0	0

FIG. 14

Pathway	baseMean	log2FoldChange	padj
PWY_7254_TCA_cycle_VII_acetate_producers	9736.88	6.73	5.69E-38
PWY_922_mevalonate_pathway_I	89.23	3.74	2.32E-09
PWY_5910_superpathway_of_geranylgeranyldiphosphate_biosynthesis_I_via_mevalonate	121.10	3.63	1.32E-09
PWY_7391_isoprene_biosynthesis_II_engineered	57.77	3.62	1.09E-05
PWY_5109_2_methylbutanoate_biosynthesis	241.55	3.06	2.61E-16
PWY_5173_superpathway_of_acetyl_CoA_biosynthesis	2757.97	2.99	1.66E-07
PWY_7117_C4_photosynthetic_carbon_assimilation_cycle_PEPCK_type	5508.76	2.95	5.82E-16
PWY_5677_succinate_fermentation_to_butanoate	45.46	2.91	1.82E-06
LACTOSECAT_PWY_lactose_and_galactose_degradation_I	5229.57	2.86	7.53E-32
PWY_1861_formaldehyde_assimilation_II_RuMP_Cycle	1772.47	2.80	2.41E-09
PWY_5791_1_4_dihydroxy_2_naphthoate_biosynthesis_II_plants	372.80	2.76	2.04E-04
PWY_5837_1_4_dihydroxy_2_naphthoate_biosynthesis_I	372.80	2.76	2.04E-04
P163_PWY_L_lysine_fermentation_to_acetate_and_butanoate	4640.04	2.72	3.09E-21
PWY_241_C4_photosynthetic_carbon_assimilation_cycle_NADP_ME_type	3928.84	2.70	7.86E-17
PWY_5863_superpathway_of_phylloquinol_biosynthesis	390.46	2.65	3.21E-04
PWY_6549_L_glutamine_biosynthesis_III	5509.91	2.51	6.92E-36
PWY_7456_mannan_degradation	5576.37	2.47	1.90E-12
PWY_5754_4_hydroxybenzoate_biosynthesis_I_eukaryotes	1276.29	2.38	1.52E-09
PWY_6572_chondroitin_sulfate_degradation_I_bacterial	24.32	2.36	5.63E-08
PWY_7288_fatty_acid_beta_oxidation_peroxisome_yeast	407.27	2.27	1.91E-10
PWY_5676_acetyl_CoA_fermentation_to_butanoate_II	6362.87	2.24	3.52E-70
HEXITOLDEGSUPER_PWY_superpathway_of_hexitol_degradation_bacteria	513.82	2.21	3.90E-06
PWY_6478_GDP_D_glycero_alpha_D_manno_heptose_biosynthesis	31.70	2.19	1.16E-07
P562_PWY_myoinositol_degradation_I	690.83	2.18	2.31E-09
PWY_4041_gamma_glutamyl_cycle	486.87	2.14	5.93E-06
PWY66_391_fatty_acid_beta_oxidation_VI_peroxisome	715.88	2.09	2.30E-10
PWY_7220_adenosine_deoxyribonucleotides_de_novo_biosynthesis_II	12237.44	2.06	2.02E-22
PWY_7222_guanosine_deoxyribonucleotides_de_novo_biosynthesis_II	12237.44	2.06	2.02E-22
GLUCARDEG_PWY_D_glucarate_degradation_I	311.09	2.05	1.06E-12
PWY_6588_pyruvate_fermentation_to_acetone	3075.60	2.00	3.42E-12
RUMP_PWY_formaldehyde_oxidation_I	769.95	1.97	1.58E-06
PWY_4984_urea_cycle	3246.49	1.97	4.56E-15
P461_PWY_hexitol_fermentation_to_lactate_formate_ethanol_and_acetate	439.90	1.93	1.02E-03
PWY_621_sucrose_degradation_III_sucrose_invertase	1296.11	1.91	6.97E-05
P124_PWY_Bifidobacterium_shunt	12605.25	1.84	1.15E-14
P122_PWY_heterolactic_fermentation	11318.71	1.84	1.09E-13
PWY_5138_unsaturated_even_numbered_fatty_acid_beta_oxidation	667.02	1.84	1.92E-08
PWY_7413_dTDP_6_deoxy_alpha_D_allose_biosynthesis	15.33	1.82	1.33E-02
ASPASN_PWY_superpathway_of_L_aspartate_and_L_asparagine_biosynthesis	16386.35	1.75	2.44E-14
P108_PWY_pyruvate_fermentation_to_propanoate_I	19222.52	1.75	3.15E-25
PWY_7234_inosine_5_phosphate_biosynthesis_III	1096.41	1.72	7.33E-06
PWY_5861_superpathway_of_demethylmenaquinol_8_biosynthesis	407.81	1.71	1.33E-02
PWY_5897_superpathway_of_menaquinol_11_biosynthesis	530.87	1.71	1.08E-02
PWY_5898_superpathway_of_menaquinol_12_biosynthesis	530.87	1.71	1.08E-02
PWY_5899_superpathway_of_menaquinol_13_biosynthesis	530.87	1.71	1.08E-02
COBALSYN_PWY_adenosylcobalamin_salvage_from_cobinamide_I	1525.05	1.70	7.15E-22
P42_PWY_incomplete_reductive_TCA_cycle	15645.05	1.67	4.58E-13
PWY_5840_superpathway_of_menaquinol_7_biosynthesis	559.27	1.62	1.47E-02
CITRULBIO_PWY_L_citrulline_biosynthesis	3764.76	1.61	1.47E-20

FIG. 14 (cont.)

Pathway	baseMean	log2FoldChange	padj
PWY_6305 putrescine biosynthesis IV	2640.56	1.60	4.30E-24
FERMENTATION PWY mixed acid fermentation	7531.52	1.59	1.35E-09
PWY_6883 pyruvate fermentation to butanol II	1175.63	1.59	1.35E-09
PWY_5690 TCA cycle II plants and fungi	12806.45	1.56	4.06E-12
PWY_6901 superpathway of glucose and xylose degradation	24465.06	1.56	1.13E-22
TCA TCA cycle I prokaryotic	17101.59	1.55	6.37E-21
PWY_5913 TCA cycle VI obligate autotrophs	4733.90	1.55	2.19E-07
PWY_5838 superpathway of menaquinol 8 biosynthesis I	522.35	1.54	2.00E-02
GALACTARDEG PWY D galactarate degradation I	534.41	1.45	1.90E-05
GLUCARGALACTSUPER PWY superpathway of D glucarate and D galactarate degradation	534.41	1.45	1.90E-05
PWY_6269 adenosylcobalamin salvage from cobinamide II	1013.38	1.42	1.17E-13
P125 PWY superpathway of R R butanediol biosynthesis	471.95	1.41	3.03E-03
PWY_7431 aromatic biogenic amine degradation bacteria	742.45	1.40	3.30E-02
PWY_6595 superpathway of guanosine nucleotides degradation plants	3715.65	1.40	3.37E-04
PENTOSE P PWY pentose phosphate pathway	22328.25	1.37	2.68E-10
THISYNARA PWY superpathway of thiamin diphosphate biosynthesis III eukaryotes	2940.14	1.34	1.74E-04
PWY_2221 Entner Doudoroff pathway III semi phosphorylative	215.54	1.33	4.20E-04
PWY_6612 superpathway of tetrahydrofolate biosynthesis	749.32	1.31	8.35E-04
PWY0_1479 tRNA processing	5211.65	1.31	3.82E-15
PWY_6396 superpathway of 2 3 butanediol biosynthesis	729.96	1.29	1.74E-04
PWY_7384 anaerobic energy metabolism invertebrates mitochondrial	5342.10	1.28	1.81E-12
FOLSYN PWY superpathway of tetrahydrofolate biosynthesis and salvage	1073.69	1.27	8.62E-04
PWY_6125 superpathway of guanosine nucleotides de novo biosynthesis II	10383.98	1.25	1.84E-16
GLUCONEO PWY gluconeogenesis I	44782.81	1.24	2.72E-31
PWY_6969 TCA cycle V 2 oxoglutarate ferredoxin oxidoreductase	20147.65	1.22	9.23E-32
CENTFERM PWY pyruvate fermentation to butanoate	2509.33	1.20	2.11E-06
PRPP PWY superpathway of histidine purine and pyrimidine biosynthesis	3217.58	1.20	2.63E-06
PWY_5509 adenosylcobalamin biosynthesis from cobyrinate a c diamide I	883.92	1.17	2.32E-09
PWY_6692 Fe II oxidation	8929.64	1.15	1.82E-04
PWY_6471 peptidoglycan biosynthesis IV Enterococcus faecium	1507.54	1.11	5.56E-05
PWY4LZ_257 superpathway of fermentation Chlamydomonas reinhardtii	18337.72	1.11	3.11E-09
PWY_6590 superpathway of Clostridium acetobutylicum acidogenic fermentation	3000.89	1.09	8.01E-06
PWY_7279 aerobic respiration II cytochrome c yeast	8242.64	1.09	1.41E-04
PWY_7228 superpathway of guanosine nucleotides de novo biosynthesis I	10779.53	1.07	1.25E-17
PWY_7237 myo chiro and scillo inositol degradation	8853.64	1.04	1.15E-05
PWY_7282 4 amino 2 methyl 5 phosphomethylpyrimidine biosynthesis yeast	4376.34	1.03	2.53E-04
PWY0_1298 superpathway of pyrimidine deoxyribonucleosides degradation	3361.11	1.02	7.74E-07
PWY_7209 superpathway of pyrimidine ribonucleosides degradation	1636.61	1.00	1.53E-07

FIG. 15

Pathway	baseMean	log2FoldChange	padj
PWY_6891_thiazole_biosynthesis_II_Bacillus	1038.04	12.90	3.86E-30
PWY_6895_superpathway_of_thiamin_diphosphate_biosynthesis_II	2298.58	12.48	7.68E-67
PWY_6731_starch_degradation_III	530.72	12.07	1.76E-25
PWY_7315_dTDP_N_acetylthomosamine_biosynthesis	417.04	11.80	3.81E-24
PWY_5088_L_glutamate_degradation_VIII_to_propanoate	1268.20	11.39	9.67E-68
PWY_6318_L_phenylalanine_degradation_IV_mammalian_via_side_chain	1505.51	11.36	5.23E-73
GLUDEG_II_PWY_L_glutamate_degradation_VII_to_butanoate	562.52	10.94	6.15E-42
METH_ACETATE_PWY_methanogenesis_from_acetate	2036.93	10.36	3.24E-125
PWY_1622_formaldehyde_assimilation_I_serine_pathway	124.61	10.19	3.42E-16
PWY_4702_phytate_degradation_I	116.01	10.08	1.15E-15
PWY_6165_chorismate_biosynthesis_II_archaea	97.88	9.93	2.13E-15
PWY_6803_phosphatidylcholine_acyl_editing	3352.12	9.89	4.66E-114
P162_PWY_L_glutamate_degradation_V_via_hydroxyglutarate	1800.47	9.78	4.52E-153
PWY0_1261_anhydromuropeptides_recycling	389.09	9.71	2.24E-43
GLYOXYLATE_BYPASS_glyoxylate_cycle	579.41	9.70	5.72E-17
PWY_5508_adenosylcobalamin_biosynthesis_from_cobyrinate_a_c_diamide_II	102.84	9.45	5.20E-12
7ALPHADEHYDROX_PWY_cholate_degradation_bacteria_anaerobic	66.30	9.28	1.93E-12
PWY_7295_L_arabinose_degradation_IV	53.34	8.99	1.70E-11
CODH_PWY_reductive_acetyl_coenzyme_A_pathway	54.51	8.89	6.98E-11
PWY_181_photorespiration	240.78	8.80	7.87E-42
TYRFUMCAT_PWY_L_tyrosine_degradation_I	96.91	8.75	2.25E-14
NAGLIPASYN_PWY_lipid_IVA_biosynthesis	129.27	8.65	6.11E-18
PWY_622_starch_biosynthesis	51.22	8.53	2.22E-09
TCA_GLYOX_BYPASS_superpathway_of_glyoxylate_bypass_and_TCA	484.42	8.47	4.17E-13
PWY_6728_methylaspartate_cycle	34.49	8.47	5.27E-10
PWY_561_superpathway_of_glyoxylate_cycle_and_fatty_acid_degradation	610.91	8.29	2.71E-12
P105_PWY_TCA_cycle_IV_2_oxoglutarate_decarboxylase	900.53	8.22	7.24E-21
PWY_6863_pyruvate_fermentation_to_hexanol	25.72	8.22	1.43E-09
GLYCOLYSIS_TCA_GLYOX_BYPASS_superpathway_of_glycolysis_pyruvate_dehydrogenase_TCA_and_glyoxylate_bypass	847.34	8.08	7.38E-11
PWY_5273_p_cumate_degradation	25.91	7.98	1.79E-08
PWY_6518_glycocholate_metabolism_bacteria	526.44	7.97	2.96E-45
PWY490_3_nitrate_reduction_VI_assimilatory	349.72	7.93	1.41E-40
PWY_6708_ubiquinol_8_biosynthesis_prokaryotic	24.64	7.89	3.21E-08
ALL_CHORISMATE_PWY_superpathway_of_chorismate_metabolism	21.99	7.84	3.12E-08
PWY0_1277_3_phenylpropanoate_and_3_3_hydroxyphenyl_propanoate_degradation	22.00	7.71	9.34E-08
PWY_7165_L_ascorbate_biosynthesis_VI_engineered_pathway	20.39	7.67	9.36E-08
PWY_5055_nicotinate_degradation_III	16.10	7.66	3.56E-08
PWY_6415_L_ascorbate_biosynthesis_V	30.38	7.45	1.52E-06
PWY30_1109_superpathway_of_4_hydroxybenzoate_biosynthesis_yeast	18.28	7.45	3.86E-07
UBISYN_PWY_superpathway_of_ubiquinol_8_biosynthesis_prokaryotic	15.71	7.39	3.52E-07
PWY_7007_methyl_ketone_biosynthesis	2240.10	7.38	2.04E-98
PWY_6596_adenosine_nucleotides_degradation_I	48.96	7.36	1.06E-12

FIG. 15 (cont.)

Pathway	baseMean	log2FoldChange	padj
DHGLUCONATE_PYW_CAT_PWY_glucose_degradation_oxidative_	14.54	7.31	5.27E-07
P261_PWY_coenzyme_M_biosynthesis_I	12.03	7.17	7.44E-07
KDO_NAGLIPASYN_PWY_superpathway_of_Kdo_2_lipid_A_biosynthesis	13.44	7.09	2.07E-06
PWY_2723_trehalose_degradation_V	21.13	7.04	7.54E-06
PWY_5507_adenosylcobalamin_biosynthesis_I_early_cobalt_insertion_	10.91	7.00	1.99E-06
URSIN_PWY_ureide_biosynthesis	9.68	6.97	1.63E-06
HCAMHPDEG_PWY_3_phenylpropanoate_and_3_3_hydroxyphenyl_propanoate_degradation_to_2_oxopent_4_enoate	13.04	6.92	5.61E-06
PWY_6690_cinnamate_and_3_hydroxycinnamate_degradation_to_2_oxopent_4_enoate	13.04	6.92	5.61E-06
PWY_5044_purine_nucleotides_degradation_I_plants_	93.08	6.89	6.11E-18
PWY_5181_toluene_degradation_III_aerobic_via_p_cresol_	13.57	6.82	1.08E-05
PWY_5420_catechol_degradation_II_meta_cleavage_pathway_	9.02	6.69	9.42E-06
PWY_7317_superpathway_of_dTDP_glucose_derived_O_antigen_building_blocks_biosynthesis	8.82	6.63	1.25E-05
PWY_6906_chitin_derivatives_degradation	153.00	6.55	3.02E-37
P165_PWY_superpathway_of_purines_degradation_in_plants	6.76	6.53	1.13E-05
PWY_7371_1_4_dihydroxy_6_naphthoate_biosynthesis_II	6.75	6.53	1.19E-05
PWY_5415_catechol_degradation_I_meta_cleavage_pathway_	17.14	6.46	1.66E-07
PWY_6060_malonate_degradation_II_biotin_dependent_	6.49	6.46	1.66E-05
PWY_5742_L_arginine_degradation_IX_arginine_pyruvate_transaminase_pathway_	5.94	6.39	1.94E-05
ECASYN_PWY_enterobacterial_common_antigen_biosynthesis	8.45	6.38	4.69E-05
PWY_5265_peptidoglycan_biosynthesis_II_staphylococci_	7.37	6.35	4.32E-05
PWY_6565_superpathway_of_polyamine_biosynthesis_III	82.63	6.28	1.43E-31
PWY_5532_adenosine_nucleotides_degradation_IV	13.14	6.26	8.03E-08
PWY_6769_rhamnogalacturonan_type_I_degradation_I_fungi_	5.50	6.20	5.10E-05
PWY_5178_toluene_degradation_IV_aerobic_via_catechol_	6.33	6.16	8.69E-05
PWY_5419_catechol_degradation_to_2_oxopent_4_enoate_II	5.79	6.15	7.71E-05
PWY_7374_1_4_dihydroxy_6_naphthoate_biosynthesis_I	4.85	6.12	6.12E-05
PWY_6953_dTDP_3_acetamido_3_6_dideoxy_alpha_D_galactose_biosynthesis	30.20	6.09	3.69E-14
PWY_6981_chitin_biosynthesis	7.16	6.06	1.63E-04
PWY0_1241_ADG_L_glycero_beta_D_manno_heptose_biosynthesis	53.82	5.95	1.93E-27
P23_PWY_reductive_TCA_cycle_I	890.92	5.94	7.56E-40
GLYCOL_GLYOXDEG_PWY_superpathway_of_glycol_metabolism_and_degradation	346.54	5.90	8.60E-46
REDCTCYC_TCA_cycle_VIII_helicobacter_	838.70	5.90	9.72E-30
PWY_6107_chlorosalicylate_degradation	7.23	5.89	3.41E-04
LPSSYN_PWY_superpathway_of_lipopolysaccharide_biosynthesis	8.22	5.80	5.43E-04
PWY_5747_2_methylcitrate_cycle_II	13.78	5.78	3.86E-05
PWY_5417_catechol_degradation_III_ortho_cleavage_pathway_	7.70	5.76	5.98E-04
PWY_5431_aromatic_compounds_degradation_via_beta_ketoadipate	7.70	5.76	5.98E-04
PWY_7373_superpathway_of_demethylmenaquinol_6_biosynthesis_II	3.63	5.76	2.26E-04
PWY0_1338_polymyxin_resistance	10.16	5.67	1.67E-05
PWY_7414_dTDP_alpha_D_mycaminose_biosynthesis	4.37	5.66	4.72E-04

FIG. 15 (cont.)

Pathway	baseMean	log2FoldChange	padj
PWY_6562_norspermidine_biosynthesis	54.18	5.66	1.74E-23
PWY_6823_molybdenum_cofactor_biosynthesis	83.08	5.64	4.99E-21
PWY_5183_superpathway_of_aerobic_toluene_degradation	5.58	5.58	8.67E-04
PWY5F9_12_biphenyl_degradation	11.85	5.55	1.48E-03
UDPNACETYLGALSYN_PWY_UDP_N_acetyl_D_glucosamine_biosynthesis_II	70.14	5.55	1.05E-21
PWY0_42_2_methylcitrate_cycle_I	14.87	5.51	6.59E-06
PWY_6215_4_chlorobenzoate_degradation	8.36	5.47	1.57E-03
PWY_5531_chlorophyllide_a_biosynthesis_II_anaerobic_	5.31	5.41	1.43E-03
PWY_7159_chlorophyllide_a_biosynthesis_III_aerobic_light_independent_	5.31	5.41	1.43E-03
CATECHOL_ORTHO_CLEAVAGE_PWY_catechol_degradation_to_beta_ketoadipate	5.53	5.40	1.54E-03
PWY_5514_UDP_N_acetyl_D_galactosamine_biosynthesis_II	105.48	5.38	1.74E-26
PWY_7318_dTDP_3_acetamido_3_6_dideoxy_alpha_D_glucose_biosynthesis	34.99	5.36	6.63E-12
NPGLUCAT_PWY_Entner_Doudoroff_pathway_II_non_phosphorylative_	10.19	5.35	6.32E-08
PWY_7316_dTDP_N_acetylviosamine_biosynthesis	435.21	5.35	4.30E-77
CHLOROPHYLL_SYN_chlorophyllide_a_biosynthesis_I_aerobic_light_dependent_	4.79	5.31	1.83E-03
PWY_5430_meta_cleavage_pathway_of_aromatic_compounds	2.93	5.27	1.38E-03
DENITRIFICATION_PWY_nitrate_reduction_I_denitrification_	3.17	5.21	1.83E-03
PWY_6182_superpathway_of_salicylate_degradation	6.59	5.20	3.03E-03
PWY_5529_superpathway_of_bacteriochlorophyll_a_biosynthesis	3.62	5.08	3.11E-03
PWY_6886_1_butanol_autotrophic_biosynthesis	2.24	5.00	2.64E-03
PWY_5005_biotin_biosynthesis_II	37.37	4.95	7.02E-09
PWY_5855_ubiquinol_7_biosynthesis_prokaryotic_	25.24	4.89	2.05E-06
PWY_5857_ubiquinol_10_biosynthesis_prokaryotic_	25.24	4.89	2.05E-06
GLYCOCAT_PWY_glycogen_degradation_I_bacterial_	43.47	4.89	1.64E-17
3_HYDROXYPHENYLACETATE_DEGRADATION_PWY_4_hydroxyphenylacetate_degradation	20.60	4.84	9.24E-08
ARGDEG_IV_PWY_L_arginine_degradation_VIII_arginine_oxidase_pathway_	1.67	4.78	4.11E-03
P281_PWY_3_phenylpropanoate_degradation	2.56	4.69	7.52E-03
PWY_5656_mannosylglycerate_biosynthesis_I	2.56	4.68	7.90E-03
PWY_1361_benzoyl_CoA_degradation_I_aerobic_	2.73	4.63	8.99E-03
PWY_6467_Kdo_transfer_to_lipid_IVA_III_Chlamydia_	3.78	4.52	1.28E-02
PWY_7204_pyridoxal_5_phosphate_salvage_II_plants	54.71	4.49	1.30E-10
PWY_5870_ubiquinol_8_biosynthesis_eukaryotic_	2.30	4.47	1.22E-02
PWY_4202_arsenate_detoxification_I_glutaredoxin_	1.35	4.45	9.34E-03
PWY_7528_L_methionine_salvage_cycle_I_bacteria_and_plants_	2.04	4.26	1.86E-02
P164_PWY_purine_nucleobases_degradation_I_anaerobic_	9907.48	4.21	1.09E-18
LYSINE_DEG1_PWY_L_lysine_degradation_XI_mammalian_	1.37	4.19	1.87E-02
PWY_7270_L_methionine_salvage_cycle_II_plants_	1.84	4.16	2.23E-02
PWY_7527_L_methionine_salvage_cycle_III	1.84	4.16	2.23E-02
PWY_5179_toluene_degradation_V_aerobic_via_toluene_cis_diol_	1.73	4.11	2.41E-02
PWY3O_19_ubiquinol_6_biosynthesis_from_4_hydroxybenzoate_eukaryotic_	2.55	4.09	2.71E-02
THREOCAT_PWY_superpathway_of_L_threonine_metabolism	14.20	4.07	5.70E-07
PWY_3941_beta_alanine_biosynthesis_II	3.74	3.99	1.31E-02
PWY_7118_chitin_degradation_to_ethanol	24.96	3.98	3.74E-11

FIG. 15 (cont.)

Pathway	baseMean	log2FoldChange	padj
LYSINE AMINOAD PWY_L lysine biosynthesis_IV	15.62	3.90	1.60E-08
4_HYDROXYMANDELATE_DEGRADATION PWY_4_hydroxymandelate_degradation	4.35	3.89	3.42E-03
PWY_6263_superpathway_of_menaquinol_8_biosynthesis_II	14.70	3.87	2.75E-09
PWY0_321_phenylacetate_degradation_I_aerobic_	2.02	3.83	4.14E-02
AST_PWY_L_arginine_degradation_II_AST_pathway_	1.93	3.81	4.28E-02
PWY_822_fructan_biosynthesis	2.19	3.61	1.60E-02
PWY_5860_superpathway_of_demethylmenaquinol_6_biosynthesis_I	46.06	3.53	3.52E-06
PWY_5392_reductive_TCA_cycle_II	146.95	3.49	6.31E-11
PWY_5850_superpathway_of_menaquinol_6_biosynthesis_I	66.66	3.47	1.68E-06
PWY_4221_pantothenate_and_coenzyme_A_biosynthesis_II_plants_	10.68	3.36	1.07E-03
PWY_5743_3_hydroxypropanoate_cycle	5.65	3.35	4.91E-04
PWY_6992_1_5_anhydrofructose_degradation	374.80	3.29	3.86E-07
PWY_5367_petroselinic_acid_biosynthesis	1217.18	3.23	2.04E-18
PWY_5856_ubiquinol_9_biosynthesis_prokaryotic_	8.22	3.15	2.43E-03
PWY_7218_photosynthetic_3_hydroxybutanoate_biosynthesis_engineered_	1.46	3.11	4.22E-02
PWY_5724_superpathway_of_atrazine_degradation	1.51	3.10	4.98E-02
PWY_7090_UDP_2_3_diacetamido_2_3_dideoxy_alpha_D_mannuronate_biosynthesis	18.52	2.86	9.84E-06
PWY_6284_superpathway_of_unsaturated_fatty_acids_biosynthesis_E_coli_	2977.95	2.85	7.94E-19
PWY_6383_mono_trans_poly_cis_decaprenyl_phosphate_biosynthesis	41.80	2.61	1.94E-14
CRNFORCAT_PWY_creatinine_degradation_I	865.41	2.58	1.19E-32
FUCCAT_PWY_fucose_degradation	691.26	2.54	2.28E-10
PWY_7377_cob_II_yninate_a_c_diamide_biosynthesis_I_early_cobalt_insertion_	17.61	2.52	3.35E-06
PWY_6185_4_methylcatechol_degradation_ortho_cleavage_	74.40	2.43	3.59E-09
PWY66_201_nicotine_degradation_IV	8.29	2.34	8.49E-04
PWY1F_823_leucopelargonidin_and_leucocyanidin_biosynthesis	2.72	2.20	4.17E-02
PWY_7332_superpathway_of_UDP_N_acetylglucosamine_derived_O_antigen_building_blocks_biosynthesis	9.41	2.19	1.36E-04
PWY_6749_CMP_legionaminic_acid_biosynthesis_I	97.74	2.19	4.55E-08
PWY_6837_fatty_acid_beta_oxidation_V_unsaturated_odd_number_di_isomerase_dependent_	24.56	2.12	1.10E-06
FUC_RHAMCAT_PWY_superpathway_of_fucose_and_rhamnose_degradation	969.52	2.09	2.03E-10
PWY_6113_superpathway_of_mycolate_biosynthesis	7185.05	2.08	1.03E-17
PWY_7357_thiamin_formation_from_pyriothiamine_and_oxythiamine_yeast_	2749.77	2.07	3.58E-09
PWY_6531_mannitol_cycle	108.87	2.01	9.46E-05
PWY_6138_CMP_N_acetylneuraminic_acid_biosynthesis_I_eukaryotes_	91.47	2.00	4.66E-05
PWY_6897_thiamin_salvage_II	3067.01	1.98	4.75E-15
PWY_7268_NAD_NADP_NADH_NADPH_cytosolic_interconversion_yeast_	42.13	1.95	9.32E-05
PWY_6470_peptidoglycan_biosynthesis_V_beta_lactam_resistance_	159.46	1.94	2.05E-04
PWY_5101_L_isoleucine_biosynthesis_II	5278.64	1.88	1.26E-11
PWY_7345_superpathway_of_anaerobic_sucrose_degradation	44.24	1.77	1.15E-03
PWY_3801_sucrose_degradation_II_sucrose_synthase_	47.35	1.77	1.06E-03
PWY_7385_1_3_propanediol_biosynthesis_engineered_	345.51	1.77	4.40E-13
FASYN_INITIAL_PWY_superpathway_of_fatty_acid_biosynthesis_initiation_E_coli_	18360.00	1.71	1.93E-12

FIG. 15 (cont.)

Pathway	baseMean	log2FoldChange	padj
PROTocatechuate_ORTHO_CLEAVAGE_PWY_protocatechuate_degradation_II_ortho_cleavage_pathway_	56.90	1.68	7.02E-09
P241_PWY_coenzyme_B_biosynthesis	73.31	1.62	3.74E-11
KETOGLUCONMET_PWY_ketogluconate_metabolism	444.30	1.62	7.20E-10
GLUCUROCAT_PWY_superpathway_of_beta_D_glucuronide_and_D_glucuronate_degradation	8514.09	1.60	1.55E-18
ARGDEG_PWY_superpathway_of_L_arginine_putrescine_and_4_aminobutanoate_degradation	32.25	1.60	1.91E-02
ORNARGDEG_PWY_superpathway_of_L_arginine_and_L_ornithine_degradation	32.25	1.60	1.91E-02
PWY66_399_gluconeogenesis_III	6850.44	1.58	3.54E-11
RHAMCAT_PWY_L_rhamnose_degradation_I	2993.39	1.57	1.56E-07
PWY_6147_6_hydroxymethyl_dihydropterin_diphosphate_biosynthesis_I	1635.25	1.51	1.14E-17
PWY_7242_D_fructuronate_degradation	10182.99	1.49	3.10E-19
PWY_7654_8E_10E_dodeca_8_10_dienol_biosynthesis	15.90	1.48	2.04E-04
PHOSLIPSYN_PWY_superpathway_of_phospholipid_biosynthesis_I_bacteria_	2486.54	1.47	1.03E-11
PWY_7539_6_hydroxymethyl_dihydropterin_diphosphate_biosynthesis_III_Chlamydia_	1516.63	1.47	6.13E-17
PWY4FS_7_phosphatidylglycerol_biosynthesis_I_plastidic	1691.28	1.44	1.43E-09
PWY4FS_8_phosphatidylglycerol_biosynthesis_II_non_plastidic	1691.28	1.44	1.43E-09
POLYAMSYN_PWY_superpathway_of_polyamine_biosynthesis_I	218.06	1.44	8.16E-11
PWY_2201_folate_transformations_I	489.38	1.43	3.63E-06
ARG_POLYAMINE_SYN_superpathway_of_arginine_and_polyamine_biosynthesis	422.81	1.42	1.03E-11
PWY_7388_octanoyl_[acyl_carrier_protein]_biosynthesis_mitochondria_yeast_	13263.13	1.38	6.08E-08
HISTSYN_PWY_L_histidine_biosynthesis	3964.55	1.32	2.07E-17
PWY_6700_queuosine_biosynthesis	3616.11	1.31	4.59E-09
PWY_6309_L_tryptophan_degradation_XI_mammalian_via_kynurenine_	54.39	1.29	9.21E-04
PWY_5103_L_isoleucine_biosynthesis_III	10988.46	1.28	3.57E-12
SALVADEHYPOX_PWY_adenosine_nucleotides_degradation_II	5138.19	1.28	9.58E-11
PROPFERM_PWY_L_alanine_fermentation_to_propanoate_and_acetate	2006.85	1.26	1.29E-04
GALACTUROCAT_PWY_D_galacturonate_degradation_I	9698.30	1.24	5.61E-06
PWY_6168_flavin_biosynthesis_III_fungi_	3997.50	1.22	4.17E-06
ILEUSYN_PWY_L_isoleucine_biosynthesis_I_from_threonine_	13093.62	1.21	7.15E-10
VALSYN_PWY_L_valine_biosynthesis	13093.62	1.21	7.15E-10
PWY_7383_anaerobic_energy_metabolism_invertebrates_cytosol_	2681.54	1.21	5.72E-10
PWY_5104_L_isoleucine_biosynthesis_IV	11287.74	1.21	3.13E-11
PWY66_398_TCA_cycle_III_animals_	1000.25	1.19	2.25E-07
BRANCHED_CHAIN_AA_SYN_PWY_superpathway_of_branched_amino_acid_biosynthesis	11576.23	1.18	1.73E-10
PWY_6123_inosine_5_phosphate_biosynthesis_I	8650.58	1.17	6.99E-09
PWY_6124_inosine_5_phosphate_biosynthesis_II	9676.46	1.16	7.49E-10
PWY_6285_superpathway_of_fatty_acids_biosynthesis_E_coli_	1868.75	1.15	1.23E-23
PWY_7269_NAD_NADP_NADH_NADPH_mitochondrial_interconversion_yeast_	75.41	1.15	8.20E-04

FIG. 15 (cont.)

Pathway	baseMean	log2FoldChange	padj
PWY_6285_superpathway_of_fatty_acids_biosynthesis_E_coli	1868.75	1.15	1.23E-23
PWY_7269_NAD_NADP_NADH_NADPH_mitochondrial_interconversion_yeast	75.41	1.15	8.20E-04
PWY_6145_superpathway_of_sialic_acids_and_CMP_sialic_acids_biosynthesis	74.02	1.13	1.80E-02
PWY_6507_4_deoxy_L_threo_hex_4_enopyranuronate_degradation	7859.65	1.12	1.33E-11
PWY_3841_folate_transformations_II	11791.23	1.11	5.74E-10
PWY_5100_pyruvate_fermentation_to_acetate_and_lactate_II	22467.73	1.10	2.26E-05
THISYN_PWY_superpathway_of_thiamin_diphosphate_biosynthesis_I	4744.86	1.10	1.52E-08
PWY_5971_palmitate_biosynthesis_II_bacteria_and_plants	10989.24	1.09	3.35E-08
GLUTORN_PWY_L_ornithine_biosynthesis	4804.61	1.09	6.52E-11
PWY0_862_5Z_dodec_5_enoate_biosynthesis	9657.46	1.06	8.87E-06
PWY66_422_D_galactose_degradation_V_Leloir_pathway	10880.58	1.06	2.56E-03
PWY_7111_pyruvate_fermentation_to_isobutanol_engineered	16173.41	1.06	5.57E-08
PWY_5189_tetrapyrrole_biosynthesis_II_from_glycine	1530.21	1.05	3.61E-05
PWY_6353_purine_nucleotides_degradation_II_aerobic	6694.64	1.03	2.72E-07
RIBOSYN2_PWY_flavin_biosynthesis_I_bacteria_and_plants	3577.60	1.03	4.68E-05
PWY_6608_guanosine_nucleotides_degradation_III	7539.12	1.02	4.79E-05
PYRIDNUCSAL_PWY_NAD_salvage_pathway_I	916.14	1.02	5.70E-04
PWY_5156_superpathway_of_fatty_acid_biosynthesis_II_plant	531.21	1.01	1.67E-03

FIG. 16

Pathway	baseMean	log2FoldChange	padj
PWY_5088_L glutamate degradation_VIII_to_propanoate	1768.79	12.59	1.5E-59
PWY_6318_L phenylalanine degradation_IV_mammalian_via_side_chain	1690.15	12.24	9.9E-69
GLUDEG_II_PWY_L glutamate degradation_VII_to_butanoate	854.51	11.77	6.0E-51
PWY_6895_superpathway_of_thiamin_diphosphate_biosynthesis_II	1549.17	11.31	8.1E-79
PWY_7315_dTDP_N_acetylthomosamine_biosynthesis	575.21	11.27	1.8E-45
PWY_6731_starch_degradation_III	554.47	11.20	1.7E-44
GLYCOLYSIS_TCA_GLYOX_BYPASS_superpathway_of_glycolysis_pyruvate_dehydrogenase_TCA_and_glyoxylate_bypass	994.30	11.15	7.0E-46
PWY_6891_thiazole_biosynthesis_II_Bacillus	602.23	11.02	1.0E-39
GLYOXYLATE_BYPASS_glyoxylate_cycle	680.84	10.89	3.1E-36
TCA_GLYOX_BYPASS_superpathway_of_glyoxylate_bypass_and_TCA	594.14	10.76	2.1E-35
PWY_561_superpathway_of_glyoxylate_cycle_and_fatty_acid_degradation	713.19	10.70	5.2E-41
P162_PWY_L glutamate degradation_V_via_hydroxyglutarate	2197.56	9.82	6.2E-171
PWY490_3_nitrate_reduction_VI_assimilatory	506.18	9.61	1.9E-85
PWY_4702_phytate_degradation_I	124.55	9.30	4.6E-27
PWY_6165_chorismate_biosynthesis_II_archaea	99.93	9.11	3.2E-26
P105_PWY_TCA_cycle_IV_2_oxoglutarate_decarboxylase	988.15	9.11	3.1E-39
PWY_5508_adenosylcobalamin_biosynthesis_from_cobyrinate_a_c_diamide_II	81.08	8.52	2.0E-20
TYRFUMCAT_PWY_L_tyrosine_degradation_I	114.29	8.51	4.5E-25
PWY0_1277_3_phenylpropanoate_and_3_3_hydroxyphenyl_propanoate_degradation	100.45	8.30	1.6E-17
CODH_PWY_reductive_acetyl_coenzyme_A_pathway	70.65	8.20	5.2E-18
PWY_7295_L_arabinose_degradation_IV	52.29	8.14	6.6E-19
7ALPHADEHYDROX_PWY_cholate_degradation_bacteria_anaerobic	84.16	8.05	2.3E-21
PWY_6728_methylaspartate_cycle	38.67	7.80	4.1E-17
PWY0_42_2_methylcitrate_cycle_I	52.84	7.72	3.4E-15
HCAMHPDEG_PWY_3_phenylpropanoate_and_3_3_hydroxyphenyl_propanoate_degradation_to_2_oxopent_4_enoate	59.10	7.69	1.2E-14
PWY_6690_cinnamate_and_3_hydroxycinnamate_degradation_to_2_oxopent_4_enoate	59.10	7.69	1.2E-14
NAGLIPASYN_PWY_lipid_IVA_biosynthesis	120.78	7.54	1.8E-29
PWY_6803_phosphatidylcholine_acyl_editing	2309.22	7.47	6.1E-83
PWY_5747_2_methylcitrate_cycle_II	47.25	7.39	2.8E-13
PWY_5417_catechol_degradation_III_ortho_cleavage_pathway	28.29	7.37	1.2E-14
PWY_5431_aromatic_compounds_degradation_via_beta_ketoadipate	28.29	7.37	1.2E-14
PWY_6906_chitin_derivatives_degradation	249.34	7.23	5.8E-88
PWY_6182_superpathway_of_salicylate_degradation	24.68	7.14	2.2E-13
ALL_CHORISMATE_PWY_superpathway_of_chorismate_metabolism	28.47	7.13	6.6E-13
PWY_6641_superpathway_of_sulfolactate_degradation	53.38	7.04	3.9E-17
PWY_5055_nicotinate_degradation_III	18.94	7.02	1.9E-13
CATECHOL_ORTHO_CLEAVAGE_PWY_catechol_degradation_to_beta_ketoadipate	20.14	6.94	1.2E-12
PWY_5178_toluene_degradation_IV_aerobic_via_catechol	19.29	6.90	1.6E-12

FIG. 16 (cont.)

Pathway	baseMean	log2FoldChange	padj
P261_PWY_coenzyme_M_biosynthesis_I	18.08	6.89	1.1E-12
PWY_5181_toluene_degradation_III_aerobic_via_p_cresol	20.58	6.75	2.2E-11
PWY_6107_chlorosalicylate_degradation	25.36	6.73	7.8E-11
PWY_6863_pyruvate_fermentation_to_hexanol	19.50	6.71	2.6E-11
P23_PWY_reductive_TCA_cycle_I	678.91	6.54	1.4E-106
PWY_5109_2_methylbutanoate_biosynthesis	29.98	6.54	6.7E-17
URSIN_PWY_ureide_biosynthesis	13.05	6.45	1.1E-10
PWY_7165_L_ascorbate_biosynthesis_VI_engineered_pathway	17.33	6.42	6.0E-10
DHGLUCONATE_PYR_CAT_PWY_glucose_degradation_oxidative	12.64	6.39	1.8E-10
PWY5F9_12_biphenyl_degradation	32.59	6.39	5.3E-09
PWY_6708_ubiquinol_8_biosynthesis_prokaryotic	16.51	6.33	1.4E-09
PWY_7371_1_4_dihydroxy_6_naphthoate_biosynthesis_II	11.13	6.32	2.4E-10
UBISYN_PWY_superpathway_of_ubiquinol_8_biosynthesis_prokaryotic	15.84	6.31	1.4E-09
PWY_6060_malonate_degradation_II_biotin_dependent	10.26	6.24	4.5E-10
PWY_6215_4_chlorobenzoate_degradation	12.94	6.13	4.5E-09
KDO_NAGLIPASYN_PWY_superpathway_of_Kdo_2_lipid_A_biosynthesis	11.23	6.12	2.8E-09
PWY30_1109_superpathway_of_4_hydroxybenzoate_biosynthesis_yeast	30.55	6.11	3.5E-14
PWY_5183_superpathway_of_aerobic_toluene_degradation	9.20	6.06	2.5E-09
PWY_6953_dTDP_3_acetamido_3_6_dideoxy_alpha_D_galactose_biosynthesis	22.13	6.04	2.6E-13
PWY_7316_dTDP_N_acetylvirosamine_biosynthesis	591.48	6.02	3.2E-69
PWY_6565_superpathway_of_polyamine_biosynthesis_III	95.67	5.92	8.1E-47
PWY_5005_biotin_biosynthesis_II	185.39	5.91	3.5E-16
ECASYN_PWY_enterobacterial_common_antigen_biosynthesis	11.71	5.90	3.5E-08
PWY_5532_adenosine_nucleotides_degradation_IV	8.60	5.85	2.0E-08
PWY_6415_L_ascorbate_biosynthesis_V	24.06	5.85	2.3E-07
P165_PWY_superpathway_of_purines_degradation_in_plants	6.99	5.80	1.4E-08
PWY_7374_1_4_dihydroxy_6_naphthoate_biosynthesis_I	6.98	5.75	2.5E-08
P281_PWY_3_phenylpropanoate_degradation	9.11	5.74	7.8E-08
PWY_5743_3_hydroxypropanoate_cycle	6.52	5.64	6.4E-08
AST_PWY_L_arginine_degradation_II_AST_pathway	6.45	5.61	8.5E-08
PWY_7118_chitin_degradation_to_ethanol	29.26	5.57	1.2E-20
4_HYDROXYMANDELATE_DEGRADATION_PWY_4_hydroxymandelate_degradation	6.29	5.55	1.4E-07
PWY_5507_adenosylcobalamin_biosynthesis_I_early_cobalt_insertion	9.12	5.52	3.0E-10
DENITRIFICATION_PWY_nitrate_reduction_I_denitrification	6.92	5.50	2.9E-07
PWY_6769_rhamnogalacturonan_type_I_degradation_I_fungi	5.67	5.49	1.7E-07
PWY_7318_dTDP_3_acetamido_3_6_dideoxy_alpha_D_glucose_biosynthesis	29.41	5.46	5.2E-12
PWY_6981_chitin_biosynthesis	9.15	5.42	1.1E-06
PWY_6562_norspermidine_biosynthesis	64.05	5.34	6.2E-35
PWY_7007_methyl_ketone_biosynthesis	2139.12	5.26	3.3E-34
PWY_622_starch_biosynthesis	41.39	5.25	1.2E-06
PWY_5430_meta_cleavage_pathway_of_aromatic_compounds	4.42	5.23	9.0E-07
PWY_7317_superpathway_of_dTDP_glucose_derived_O_antigen_building_blocks_biosynthesis	5.45	5.16	2.6E-06

FIG. 16 (cont.)

Pathway	baseMean	log2FoldChange	padj
PWY_7373_superpathway_of_demethylmenaquinol_6_biosynthesis_II	4.09	5.16	1.4E-06
PWY_6596_adenosine_nucleotides_degradation_I	56.89	5.16	1.5E-10
PWY_5265_peptidoglycan_biosynthesis_II_staphylococci	6.15	5.05	7.5E-06
PWY_2723_trehalose_degradation_V	16.54	5.05	2.0E-05
PWY_5044_purine_nucleotides_degradation_I_plants	103.28	5.02	6.8E-12
REDCITCYC_TCA_cycle_VIII_helicobacter	1014.89	4.85	4.1E-16
GLYCOCAT_PWY_glycogen_degradation_I_bacterial	47.79	4.84	3.0E-22
PWY_5179_toluene_degradation_V_aerobic_via_toluene_cis_diol	4.52	4.83	2.0E-05
PWY_6518_glycocholate_metabolism_bacteria	352.61	4.75	7.6E-07
PWY_6531_mannitol_cycle	63.89	4.63	1.1E-36
PWY_5855_ubiquinol_7_biosynthesis_prokaryotic	16.07	4.53	1.2E-06
PWY_5857_ubiquinol_10_biosynthesis_prokaryotic	16.07	4.53	1.2E-06
PWY_6749_CMP_legionamine_biosynthesis_I	92.42	4.53	4.4E-36
PWY_5420_catechol_degradation_II_meta_cleavage_pathway	7.07	4.50	5.5E-07
LPSSYN_PWY_superpathway_of_lipopolysaccharide_biosynthesis	7.44	4.43	2.4E-04
UDPNACETYLGALSYN_PWY_UDP_N_acetyl_D_glucosamine_biosynthesis_II	123.13	4.39	1.3E-16
PWY_5514_UDP_N_acetyl_D_galactosamine_biosynthesis_II	184.59	4.36	8.6E-17
GLUDEG_I_PWY_GABA_shunt	426.68	4.34	1.1E-56
PWY_5419_catechol_degradation_to_2_oxopent_4_enoate_II	4.13	4.32	1.3E-05
PWY_5180_toluene_degradation_I_aerobic_via_o_cresol	117.25	4.29	1.3E-04
PWY_5182_toluene_degradation_II_aerobic_via_4_methylcatechol	117.25	4.29	1.3E-04
PWY_7384_anaerobic_energy_metabolism_invertebrates_mitochondrial	1837.62	4.21	8.1E-14
THREOCAT_PWY_superpathway_of_L_threonine_metabolism	19.57	4.05	1.6E-07
PWY30_19_ubiquinol_6_biosynthesis_from_4_hydroxybenzoate_eukaryotic	3.91	4.00	1.1E-03
PWY_5392_reductive_TCA_cycle_II	88.48	3.90	1.5E-49
PWY_6138_CMP_N_acetylneuraminate_biosynthesis_I_eukaryotes	60.48	3.82	9.1E-32
PWY_4321_L_glutamate_degradation_IV	76.29	3.80	2.6E-19
3_HYDROXYPHENYLACETATE_DEGRADATION_PWY_4_hydroxyphenylacetate_degradation	32.89	3.80	1.6E-08
PWY_6823_molybdenum_cofactor_biosynthesis	60.16	3.78	1.8E-21
P3_PWY_gallate_degradation_III_anaerobic	118.85	3.73	2.2E-04
PWY_5856_ubiquinol_9_biosynthesis_prokaryotic	9.25	3.70	3.3E-05
CRNFORCAT_PWY_creatinine_degradation_I	769.59	3.70	9.7E-12
PWY_822_fructan_biosynthesis	2.46	3.54	1.1E-03
PWY_7204_pyridoxal_5_phosphate_salvage_II_plants	46.04	3.53	6.9E-18
PWY_7389_superpathway_of_anaerobic_energy_metabolism_invertebrates	1404.17	3.49	3.3E-12
PWY_4202_arsenate_detoxification_I_glutaredoxin	2.16	3.40	1.5E-03
NPGLUCAT_PWY_Entner_Doudoroff_pathway_II_non_phosphorylative	11.89	3.33	1.0E-04
PWY_7414_dTDP_alpha_D_mycaminose_biosynthesis	1.46	3.32	7.8E-03
METH_ACETATE_PWY_methanogenesis_from_acetate	2240.01	3.29	2.2E-13
PWY0_1241_AD_P_L_glycero_beta_D_manno_heptose_biosynthesis	48.55	3.22	3.5E-21
PWY0_1261_anhydromuropeptides_recycling	272.39	3.11	2.0E-04

FIG. 16 (cont.)

Pathway	baseMean	log2FoldChange	padj
PWY_7090_UDP_2_3_diacetamido_2_3_dideoxy_alpha_D_mannuronate_biosynthesis	10.64	2.94	1.6E-06
PWY_5870_ubiquinol_8_biosynthesis_eukaryotic	4.95	2.91	2.4E-02
LYSINE_DEG1_PWY_L_lysine_degradation_XI_mammalian	1.12	2.85	2.6E-02
PWY66_399_gluconeogenesis_III	5270.58	2.83	1.2E-28
PWY_6383_mono_trans_poly_cis_decaprenyl_phosphate_biosynthesis	48.63	2.81	2.1E-37
KETOGLUCONMET_PWY_ketogluconate_metabolism	503.84	2.79	1.2E-41
PWY_6957_mandelate_degradation_to_acetyl_CoA	1.05	2.78	3.0E-02
PWY_6145_superpathway_of_sialic_acids_and_CMP_sialic_acids_biosynthesis	39.29	2.74	5.3E-08
PWY_5531_chlorophyllide_a_biosynthesis_II_anaerobic	11.22	2.73	1.1E-03
PWY_7159_chlorophyllide_a_biosynthesis_III_aerobic_light_independent	11.22	2.73	1.1E-03
PWY_6263_superpathway_of_menaquinol_8_biosynthesis_II	23.23	2.71	2.2E-14
CHLOROPHYLL_SYN_chlorophyllide_a_biosynthesis_I_aerobic_light_dependent	10.21	2.60	1.7E-03
PWY_6992_1_5_anhydrofructose_degradation	542.18	2.60	3.2E-05
PWY_7383_anaerobic_energy_metabolism_invertebrates_cytosol	2043.62	2.55	2.1E-30
PWY_6886_1_butanol_autotrophic_biosynthesis	0.77	2.55	4.9E-02
PWY_5306_superpathway_of_thiosulfate_metabolism_Desulfovibrio_sulfodismutans	1.80	2.51	4.6E-02
PWY_6876_isopropanol_biosynthesis	1482.98	2.49	2.5E-18
PWY_3941_beta_alanine_biosynthesis_II	2.90	2.41	2.6E-03
PWY_4221_pantothenate_and_coenzyme_A_biosynthesis_II_plants	8.38	2.40	2.2E-05
PWY_7357_thiamin_formation_from_pyrithiamine_and_oxythiamine_yeast	2137.76	2.27	2.9E-11
ARGDEG_PWY_superpathway_of_L_arginine_putrescine_and_4_aminobutanoate_degradation	27.59	2.22	2.5E-10
ORNARGDEG_PWY_superpathway_of_L_arginine_and_L_ornithine_degradation	27.59	2.22	2.5E-10
GLYCOL_GLYOXDEG_PWY_superpathway_of_glycol_metabolism_and_degradation	447.62	2.19	3.8E-04
ARGDEG_IV_PWY_L_arginine_degradation_VIII_arginine_oxidase_pathway	1.22	2.18	3.8E-02
PWY_7345_superpathway_of_anaerobic_sucrose_degradation	29.42	2.16	6.6E-09
PWY_3801_sucrose_degradation_II_sucrose_synthase	31.40	2.15	6.5E-09
PWY_6897_thiamin_salvage_II	2510.63	2.13	6.8E-17
PROPFERM_PWY_L_alanine_fermentation_to_propanoate_and_acetate	1582.34	2.09	1.7E-05
SALVADEHYPOX_PWY_adenosine_nucleotides_degradation_II	4779.67	2.06	7.3E-28
PWY_1622_formaldehyde_assimilation_I_serine_pathway	161.14	1.88	1.0E-04
P164_PWY_purine_nucleobases_degradation_I_anaerobic	10311.89	1.88	1.6E-21
PWY_5022_4_aminobutanoate_degradation_V	529.56	1.84	2.5E-03
PWY_6700_queuosine_biosynthesis	2851.02	1.83	1.6E-20
PWY_7377_cob_II_yninate_a_c_diamide_biosynthesis_I_early_cobalt_insertion	25.05	1.82	1.9E-11
PWY66_201_nicotine_degradation_IV	7.51	1.75	6.7E-03
GALACTARDEG_PWY_D_galactarate_degradation_I	174.18	1.73	6.6E-19
GLUCARGALACTSUPER_PWY_superpathway_of_D_glucarate_and_D_galactarate_degradation	174.18	1.73	6.6E-19

FIG. 16 (cont.)

Pathway	baseMean	log2FoldChange	padj
PWY_181_photorespiration	369.11	1.52	1.3E-02
PWY_7242_D_fructuronate_degradation	11749.36	1.47	2.4E-22
PWY_7268_NAD_NADP_NADH_NADPH_cytosolic_interconversion_yeast_	26.28	1.39	6.7E-03
PWY_6608_guanosine_nucleotides_degradation_III	7143.86	1.37	5.5E-13
THISYN_PWY_superpathway_of_thiamin_diphosphate_biosynthesis_I	3868.29	1.35	2.7E-17
PWY_2201_folate_transformations_I	430.07	1.35	7.1E-20
GLUTORN_PWY_L_ornithine_biosynthesis	3495.23	1.28	5.2E-36
FUCCAT_PWY_fucose_degradation	1067.02	1.28	1.4E-06
PWY_5529_superpathway_of_bacteriochlorophyll_a_biosynthesis	6.44	1.23	5.0E-02
PWY_6892_thiazole_biosynthesis_I_E_coli_	3637.23	1.22	7.9E-07
PWY_5367_petroselinic_acid_biosynthesis	1171.62	1.12	1.6E-04
FASYN_INITIAL_PWY_superpathway_of_fatty_acid_biosynthesis_initiation_E_coli_	14420.51	1.12	2.8E-13
PWY_3841_folate_transformations_II	10412.30	1.11	2.2E-16
PWY_6124_inosine_5_phosphate_biosynthesis_II	9637.12	1.08	2.1E-44
TRPSYN_PWY_L_tryptophan_biosynthesis	67.83	1.07	1.9E-02
PWY_6629_superpathway_of_L_tryptophan_biosynthesis	144.69	1.06	1.7E-02
PWY_7269_NAD_NADP_NADH_NADPH_mitochondrial_interconversion_yeast_	43.70	1.05	9.4E-04
FUC_RHAMCAT_PWY_superpathway_of_fucose_and_rhamnose_degradation	1547.70	1.04	2.1E-05
PWY_6123_inosine_5_phosphate_biosynthesis_I	8169.52	1.03	5.9E-87
PWY_6284_superpathway_of_unsaturated_fatty_acids_biosynthesis_E_coli_	2956.01	1.02	8.2E-06

FIG. 17

Pathway	baseMean	log2FoldChange	padj
PWY 922 mevalonate pathway I	61.65	4.36	4.23E-10
PWY 5910 superpathway of geranylgeranyldiphosphate biosynthesis I via mevalonate	85.58	4.24	3.46E-09
PWY 7391 isoprene biosynthesis II engineered	40.16	4.00	5.39E-05
PWY 7433 mucin core 1 and core 2 O glycosylation	5.96	3.97	4.77E-05
PWY 6857 retinol biosynthesis	27.23	3.72	8.76E-15
PWY 7420 monoacylglycerol metabolism yeast	5.59	3.70	1.39E-05
PWY 6351 D myo inositol 1 4 5 trisphosphate biosynthesis	2.42	3.48	9.29E-04
PWY 5677 succinate fermentation to butanoate	79.27	3.36	1.25E-04
PWY 5173 superpathway of acetyl CoA biosynthesis	2312.82	3.28	3.21E-23
PWY 6367 D myo inositol 5 phosphate metabolism	0.93	3.21	9.09E-03
LACTOSECAT PWY lactose and galactose degradation I	6926.21	3.19	6.41E-72
PWY 6342 noradrenaline and adrenaline degradation	2.31	3.16	1.27E-02
PWY 5754 4 hydroxybenzoate biosynthesis I eukaryotes	1211.73	3.03	3.20E-10
PWY 5384 sucrose degradation IV sucrose phosphorylase	788.10	3.00	4.39E-22
PWY 4041 gamma glutamyl cycle	512.49	2.96	6.02E-15
PWY 5791 1 4 dihydroxy 2 naphthoate biosynthesis II plants	395.20	2.95	2.60E-05
PWY 5837 1 4 dihydroxy 2 naphthoate biosynthesis I	395.20	2.95	2.60E-05
PWY 7117 C4 photosynthetic carbon assimilation cycle PEPCK type	3204.80	2.92	8.68E-20
PWY 6362 1D myo inositol hexakisphosphate biosynthesis II mammalian	1.63	2.86	1.13E-02
PWY 5863 superpathway of phyloquinol biosynthesis	419.41	2.85	3.86E-05
PWY 241 C4 photosynthetic carbon assimilation cycle NADP ME type	2552.59	2.85	1.24E-20
PWY 7277 sphingolipid biosynthesis mammals	0.80	2.80	2.77E-02
PWY 621 sucrose degradation III sucrose invertase	2688.21	2.78	3.79E-17
PWY 6352 3 phosphoinositide biosynthesis	1.58	2.73	1.93E-02
PWY 5381 pyridine nucleotide cycling plants	35.75	2.64	6.88E-05
PWY 6554 1D myo inositol hexakisphosphate biosynthesis V from Ins 1 3 4 P3	6.52	2.62	5.67E-05
PWY 6185 4 methylcatechol degradation ortho cleavage	433.71	2.60	3.11E-15
PWY 7511 protein ubiquitylation	1.17	2.55	2.45E-02
PWY 7434 terminal O glycans residues modification	9.17	2.47	3.92E-04
PWY 6555 superpathway of 1D myo inositol hexakisphosphate biosynthesis plants	8.14	2.44	3.92E-05
PWY 7039 phosphatidate metabolism as a signaling molecule	2.29	2.42	8.91E-03
PWY 7616 methanol oxidation to carbon dioxide	63.26	2.39	3.46E-09
PWY 6549 L glutamine biosynthesis III	3649.20	2.37	8.42E-37
PWY 7220 adenosine deoxyribonucleotides de novo biosynthesis II	10317.58	2.36	2.35E-32
PWY 7222 guanosine deoxyribonucleotides de novo biosynthesis II	10317.58	2.36	2.35E-32
PWY 1861 formaldehyde assimilation II RuMP Cycle	839.82	2.35	8.21E-06
PWY 6478 GDP D glycerol alpha D manno heptose biosynthesis	20.99	2.19	1.95E-08
PWY 6883 pyruvate fermentation to butanol II	1279.01	2.18	3.23E-30
P124 PWY Bifidobacterium shunt	9880.71	2.18	6.45E-12
P122 PWY heterolactic fermentation	8359.17	2.16	4.87E-12
RUMP PWY formaldehyde oxidation I	504.38	2.11	1.73E-05
PWY 6572 chondroitin sulfate degradation I bacterial	24.21	2.08	2.07E-05
PWY 6470 peptidoglycan biosynthesis V beta lactam resistance	478.42	2.08	1.05E-20
PWY30 355 stearate biosynthesis III fungi	927.64	2.08	1.17E-12
PWY0 41 allantoin degradation IV anaerobic	40.66	1.93	1.62E-04
PWY 5861 superpathway of demethylmenaquinol 8 biosynthesis	403.04	1.93	2.53E-03
PWY 5897 superpathway of menaquinol 11 biosynthesis	547.22	1.93	2.28E-03
PWY 5898 superpathway of menaquinol 12 biosynthesis	547.22	1.93	2.28E-03
PWY 5899 superpathway of menaquinol 13 biosynthesis	547.22	1.93	2.28E-03

FIG. 17 (cont.)

Pathway	baseMean	log2FoldChange	padj
HEXITOLDEGSUPER PWY superpathway of hexitol degradation bacteria	248.55	1.92	6.44E-03
PWY 7234 inosine 5 phosphate biosynthesis III	1194.50	1.91	6.12E-11
PWY_7328_superpathway_of_UDP_glucose_derived_O_antigen_building_blocks_biosynthesis	1020.84	1.86	1.89E-14
PWY 5840 superpathway of menaquinol 7 biosynthesis	577.44	1.84	3.14E-03
PWY 5692 allantoin degradation to glyoxylate II	37.20	1.82	2.99E-05
URDEGR PWY superpathway of allantoin degradation in plants	37.20	1.82	2.99E-05
PWY 5705 allantoin degradation to glyoxylate III	58.30	1.82	1.73E-05
PWY 5838 superpathway of menaquinol 8 biosynthesis I	531.80	1.81	3.51E-03
PWY 7456 mannan degradation	3776.46	1.76	2.15E-05
PWY 5994 palmitate biosynthesis I animals and fungi	1060.29	1.75	1.26E-10
PWY 2221 Entner Doudoroff pathway III semi phosphorylative	283.16	1.70	3.44E-04
P562 PWY myo inositol degradation I	518.22	1.69	9.87E-11
PWY 6612 superpathway of tetrahydrofolate biosynthesis	730.83	1.69	4.81E-10
PWY 7409 phospholipid remodeling phosphatidylethanolamine yeast	11.16	1.64	8.19E-03
FOLSYN PWY superpathway of tetrahydrofolate biosynthesis and salvage	1035.16	1.62	6.95E-10
PWY 5083 NAD NADH phosphorylation and dephosphorylation	1335.17	1.56	5.30E-03
PWY 6471 peptidoglycan biosynthesis IV Enterococcus faecium	1489.89	1.55	1.37E-09
PWY4LZ_257 superpathway of fermentation Chlamydomonas reinhardtii	16582.56	1.55	1.11E-69
PWY 6595 superpathway of guanosine nucleotides degradation plants	3127.18	1.54	8.14E-08
PWY 7237 myo chiro and scillo inositol degradation	10898.90	1.42	3.62E-13
PWY 6396 superpathway of 2 3 butanediol biosynthesis	711.01	1.42	3.65E-06
PWY 6125 superpathway of guanosine nucleotides de novo biosynthesis II	8847.81	1.39	6.21E-51
PWY 6901 superpathway of glucose and xylose degradation	17459.14	1.38	8.79E-40
PWY0_845 superpathway of pyridoxal 5 phosphate biosynthesis and salvage	2848.83	1.37	1.53E-12
METHGLYUT PWY superpathway of methylglyoxal degradation	797.82	1.33	3.36E-08
PWY 7224 purine deoxyribonucleosides salvage	16.48	1.32	2.72E-03
PWY 6630 superpathway of L tyrosine biosynthesis	3199.17	1.31	2.38E-12
PWY 5941 glycogen degradation II eukaryotic	3845.08	1.28	5.79E-04
P125 PWY superpathway of R R butanediol biosynthesis	373.52	1.28	9.37E-05
PWY 6126 superpathway of adenosine nucleotides de novo biosynthesis II	10307.84	1.27	5.07E-28
ASPASN PWY superpathway of L aspartate and L asparagine biosynthesis	10274.14	1.25	8.56E-15
PWY 6269 adenosylcobalamin salvage from cobinamide II	847.25	1.25	4.76E-12
PWY_5464_superpathway_of_cytosolic_glycolysis_plants_pyruvate_dehydrogenase_and_TC_A_cycle	2234.58	1.16	3.65E-06
PWY 7046 4 coumarate degradation anaerobic	438.32	1.12	1.77E-02
PWY0_1479 tRNA processing	4056.12	1.11	6.81E-12
PWY66_367 ketogenesis	18.06	1.11	1.20E-02
PWY 3481 superpathway of L phenylalanine and L tyrosine biosynthesis	59.79	1.11	1.41E-04
PWY0_166_superpathway_of_pyrimidine_deoxyribonucleotides_de_novo_biosynthesis_E_coili	2853.48	1.10	2.09E-17
PWY 7197 pyrimidine deoxyribonucleotide phosphorylation	2054.02	1.10	3.95E-08
PRPP PWY superpathway of histidine purine and pyrimidine biosynthesis	3044.52	1.09	5.26E-07
GLUCONEO PWY gluconeogenesis I	38276.59	1.08	6.01E-38
HEMESYN2 PWY heme biosynthesis II anaerobic	194.92	1.08	3.46E-03
PWY 821 superpathway of sulfur amino acid biosynthesis Saccharomyces cerevisiae	636.26	1.08	9.45E-11
PWY 7228 superpathway of guanosine nucleotides de novo biosynthesis I	9516.92	1.08	1.82E-12
PWY 7337 10 cis heptadecenoyl CoA degradation yeast	28.75	1.05	1.91E-03
PWY 7338 10 trans heptadecenoyl CoA degradation reductase dependent yeast	28.75	1.05	1.91E-03
PENTOSE P PWY pentose phosphate pathway	15216.66	1.03	3.50E-13
PWY 7184 pyrimidine deoxyribonucleotides de novo biosynthesis I	3815.99	1.03	1.75E-22
PWY 6519 8 amino 7 oxononanoate biosynthesis I	1207.04	1.02	1.02E-02
PWY 7198 pyrimidine deoxyribonucleotides de novo biosynthesis IV	2367.86	1.01	2.86E-09

FIG. 18

Candidate Name	candidate_kegg	Log2Fold Change	pvalue
1,2-Dioleoyl PC		7.73	6.76E-03
1,2-Dioleoyl phosphatidyl ethanolamine		7.72	6.11E-03
Sphinganine-phosphate	C01120	6.75	5.41E-03
Vitamin D2 3-glucuronide	C03033	6.68	1.57E-03
L-Oleandrosyl-oleandolide	C11992	6.56	4.25E-05
Butirosin B	C17586	6.50	1.46E-03
Ouabain	C01443	6.15	6.07E-04
S-(2-Methylpropionyl)-dihydrolipoamide-E	C15977	5.85	5.44E-03
Astaxanthin	C08580	5.83	8.19E-06
6,8a-Seco-6,8a-deoxy-5-oxoavermectin "1b" aglycone	C11961	5.69	2.77E-03
Estrone	C00468	5.62	2.06E-02
N-Desmethyltamoxifen	C16546	5.57	4.96E-03
Mesobilirubinogen	C05790	5.45	3.25E-05
2-Octaprenyl-3-methyl-6-methoxy-1,4-benzoquinone	C05814	5.35	3.93E-03
6,8a-Seco-6,8a-deoxy-5-oxoavermectin "1a" aglycone	C11977	5.31	1.24E-04
3 α ,12 α -Dihydroxy-5 β -chol-6-en-24-oic Acid	C11637	5.21	6.57E-03
Ergocornine	C09162	4.89	4.11E-04
Tetrahydrocorticosterone	C05476	4.81	4.57E-04
Butyryl-CoA	C00136	4.80	7.77E-03
25-hydroxyvitamin D3 / 25-hydroxycholecalciferol / calcidiol	C01561	4.75	6.16E-03
Cucurbitacin A	C08793	4.74	5.66E-03
13(Z)-Docosenoic Acid	C08316	4.61	9.21E-03
Adrenic Acid	C16527	4.60	7.89E-03
LPA(0:0/18:0)	C00416	4.39	3.80E-03
D-Urobilinogen	C05791	4.34	1.79E-04
5,10-Methylenetetrahydromethanopterin	C04377	4.01	1.21E-02
NeuAcalpha2-3Galbeta1-4GlcNAcbeta1-3(Galalpha1-3Galbeta1-4GlcNAcbeta1-6)Galbeta1-4GlcNAcbeta1-3Galbeta1-4Glcbeta-Cer(d18:1/24:0)		3.83	2.38E-02

FIG. 18 (cont.)

Candidate Name	candidate_kegg	Log2Fold Change	pvalue
Asclepin	C08849	3.82	1.73E-04
Benzoyl glucuronide (Benzoic acid)	C03033	3.47	5.27E-06
Chlortetracycline	C06571	3.41	1.52E-04
7Z, 10Z, 13Z, 16Z, 19Z-docosapentaenoic acid	C16513	3.37	1.28E-02
L-Urobilinogen	C05789	3.29	4.00E-03
cis-9,10-Epoxy stearic acid	C19418	3.12	7.45E-04
4,4'-Diaponeurosporene	C16145	3.10	9.06E-04
15(S)-HpEDE		3.02	6.24E-03
(9S,10S)-10-hydroxy-9-(phosphonoxy)octadecanoic acid	C15989	3.00	6.18E-03
PS(18:0/20:0)	C02737	2.99	2.01E-02
Tamoxifen	C07108	2.96	1.16E-02
Trehalose-6,6'-dibehenate	C19190	2.72	4.15E-04
2-Methyl-6-solanyl-1,4-benzoquinol	C17570	2.59	6.08E-04
3-alpha-hydroxy-5-alpha-androstane-17-one 3-D-glucuronide	C03033	2.51	2.27E-03
Oligomycin D	C11314	2.47	1.54E-02
Taurochenodeoxycholic acid	C05465	2.41	2.09E-03
Pheophorbide a	C18021	2.40	1.77E-02
		2.28	3.37E-03
gamma-L-Glutamyl-butyrosin B	C18005	2.22	5.84E-04
Sphingosine-1-phosphate	C06124	2.21	7.18E-03
Trp-P-1	C19306	2.16	2.03E-04
Picrasin C	C08776	2.16	1.98E-03
3-Demethylubiquinone-9	C03226	2.12	5.63E-03
Cassaine	C08670	2.08	8.61E-03
(-)-Jasmonic acid	C08491	2.05	4.93E-04
Pregnanediol-3-glucuronide	C03033	2.04	2.54E-04
Epoxy murin-A	C08484	2.03	1.57E-03
L-Lysine	C00047	2.03	8.33E-04

FIG. 19

Candidate Name	candidate_kegg	Log2Fold Change	pvalue
γ-Glutamyl-γ-aminobutyraldehyde	C15700	9.75	2.17E-03
Perfluidone	C19054	9.13	2.32E-02
Oxoadipic acid	C00322	8.70	2.95E-04
(R)-2-Hydroxybutane-1,2,4-tricarboxylate	C01251	8.50	1.91E-04
2-Naphthylmethylsuccinic acid	C14115	8.44	7.25E-04
5-Methyl-5,6,7,8-tetrahydromethanopterin	C04488	8.10	1.24E-03
Salidroside	C06046	8.07	3.87E-03
(R)-S-Lactoylglutathione	C03451	7.80	2.36E-03
PGD2-d4	C00696	7.71	1.77E-03
S-Acetyldihydrolipoamide-E	C16255	7.67	4.53E-03
2,6-Dihydroxypseudoxynicotine	C15986	7.40	1.65E-02
Coumestric acid	C12479	7.36	9.21E-04
2-Hexaprenyl-3-methyl-6-methoxy-1,4 benzoquinone	C05804	7.02	2.90E-03
Rhizoctin A	C17944	6.60	2.92E-03
Indole-3-acetaldehyde oxime	C02937	6.56	9.65E-03
2-deoxyecdysone	C16495	6.52	2.64E-03
2-(5'-Methylthio)pentylmalic acid	C17222	6.51	1.54E-03
D-Saccharic acid	C00818	6.51	2.45E-03
Avermectin A2b	C11960	6.40	2.01E-03
TXB2	C05963	6.31	3.28E-03
Pyridoxamine	C00534	6.28	1.85E-02
Stypandrol	C09971	6.25	2.67E-03
Avermectin B1b monosaccharide	C11965	6.23	1.57E-02
Porphobilinogen	C00931	6.11	1.29E-04
Pseudaminic acid	C20082	6.06	2.63E-03
pregnenolone sulfate	C18044	5.97	1.44E-03
Chenodeoxycholic acid glycine conjugate	C05466	5.94	3.30E-03
Nicotinamide riboside	C03150	5.94	4.46E-04
Zeaxanthin diglucoside	C15969	5.92	2.43E-03
TG(12:0/12:0/12:0)	C00422	5.87	4.20E-03
Polhovide	C09532	5.87	1.81E-03
Avermectin A2a monosaccharide	C11974	5.85	1.03E-02
1-Methoxypyrene-6,7-oxide	C18262	5.84	4.12E-03
Melibiotol	C05399	5.82	2.90E-03
N-Carbamoyl-L-aspartic acid	C00438	5.76	3.15E-04
2'-N-Acetylparomamine	C17582	5.73	1.51E-02
PS(13:0/22:6(4Z,7Z,10Z,13Z,16Z,19Z))		5.63	1.07E-02
Azadirachtin A	C08748	5.57	1.57E-03
PS(22:6(4Z,7Z,10Z,13Z,16Z,19Z)/20:5(5Z,8Z,11Z,14Z,17Z))		5.56	6.42E-02
Demethylalangiside	C11813	5.51	1.15E-02
Urocortisol	C05472	5.49	1.42E-03

FIG. 19 (cont.)

Candidate Name	candidate_kegg	Log2Fold Change	pvalue
Urocortisol	C05472	5.49	1.42E-03
Daunorubicin	C01907	5.49	1.08E-03
Desacetoxyvindoline	C02673	5.44	8.93E-03
Rabelomycin	C12402	5.44	8.83E-04
3',4'-Anhydrovinblastine	C11641	5.41	2.12E-03
Avermectin A2a	C11976	5.34	1.00E-03
Traumatic Acid	C16308	5.34	8.40E-03
Dihydroechinofuran	C18134	5.31	1.37E-03
Se-Adenosylselenomethionine	C05691	5.31	2.68E-03
Myriocin	C19914	5.31	3.92E-04
β-Cryptoxanthin	C08591	5.27	2.90E-01
L-Histidinol phosphate	C01100	5.24	1.15E-03
N-Formyl demecolcine	C16710	5.22	5.59E-03
Thiamine acetic acid	C02892	5.18	9.41E-04
7a,12a-Dihydroxy-3-oxo-4-cholenoic acid	C15568	5.15	1.29E-03
Sarcostin	C17770	5.13	1.29E-04
PS(P-16:0/22:6(4Z,7Z,10Z,13Z,16Z,19Z))		5.12	2.68E-03
N10-Formyltetrahydrofolic acid	C00234	5.10	2.37E-03
Cortol	C05482	5.02	4.57E-03
Linatine	C05939	4.99	4.02E-03
Batrachotoxin	C13750	4.99	2.60E-03
2-Octaprenyl-3-methyl-5-hydroxy-6-methoxy-1,4-benzoquinone	C05815	4.93	2.95E-03
		4.89	1.20E-03
Indoleglycerol phosphate	C03506	4.86	2.77E-03
1,25-hydroxyvitamin D3	C01673	4.82	2.41E-04
Echitovenine	C11784	4.82	2.89E-03
5-Formyltetrahydrofolate	C03479	4.80	3.49E-03
α-Cryptoxanthin	C15981	4.78	6.90E-05
Ribostamycin	C01759	4.72	2.47E-03
LPA(P-16:0e/0:0)	C15646	4.65	2.28E-03
Estrone 3-glucuronide	C11133	4.65	9.43E-03
Staurosporine	C02079	4.58	1.02E-03
Delphinidin 3-O-glucoside	C12138	4.58	4.61E-04
2-Oxoarginine	C03771	4.57	2.13E-03
Estriol-17-glucuronide	C03033	4.47	6.04E-03
Anhydrotetracycline	C02811	4.47	5.62E-03
N-Acetyldemethylphosphinothricin tripeptide	C17950	4.47	1.18E-02
Erythromycin A	C01912	4.46	1.62E-03
Avermectin B2b	C11959	4.46	2.62E-03
Digoxin	C06956	4.42	1.91E-03
Neamine (Neomycin A)	C01441	4.41	3.96E-03
5β-Cyprinolsulfate	C05468	4.41	1.46E-03
Avermectin B2a	C11975	4.38	1.15E-03

FIG. 19 (cont.)

Candidate Name	candidate_kegg	Log2Fold Change	pvalue
Premithramycin B	C12388	4.36	7.73E-03
Cavinine	C08524	4.33	7.40E-03
trans-Cinnamic acid	C00423	4.29	4.04E-04
L-Urobilin	C05793	4.28	3.02E-03
Coproporphyrin	C03263	4.27	3.97E-03
Dehydroisoandrosterone 3-glucuronide	C03033	4.25	6.42E-04
12-oxo-9(Z)-dodecenoic acid	C16311	4.25	1.31E-03
Naphthalene-1,2-diol	C03012	4.24	1.92E-03
Vanillyl alcohol	C06317	4.17	8.40E-05
UDPMurAc(oyl-L-Ala-D-γ-Glu-L-Lys-D-Ala-D-Ala)	C04702	4.17	5.64E-03
Megalomicin B	C11986	4.17	2.62E-04
Chikusetsusaponin IV	C17540	4.15	9.99E-04
1D-1-Guanidino-3-amino-1,3-dideoxy-scylo-inositol	C01298	4.15	5.53E-04
Macrocin	C00744	4.14	8.98E-04
L-Glutamyl 5-phosphate	C03287	4.12	8.26E-03
Tetrahydroaldosterone-3-glucuronide	C03033	4.02	1.52E-03
Dihydromacarpine	C05316	4.02	4.47E-04
Gibberellin A44 diacid	C06095	3.95	2.23E-02
Ritonavir	C07240	3.95	2.45E-05
Glutathionylspermine	C16562	3.88	1.20E-02
Isobenzan	C18960	3.86	2.08E-03
Phenethylamine glucuronide	C03033	3.85	2.02E-03
(S)-N-Methylcoclaurine	C05176	3.85	2.12E-02
Pyruvophenone	C17268	3.82	2.15E-03
9S,11R,15S-trihydroxy-2,3-dinor-13E-prostaenoic acid-cyclo[8S,12R]	C14795	3.80	6.45E-04
L-Cystathionine	C02291	3.79	3.13E-03
Galactosylglycerol	C05401	3.79	1.27E-02
20-hydroxy-LTE4	C03577	3.79	9.91E-04
Cucurbitacin S	C08806	3.76	2.19E-03
Staphyloxanthin	C16148	3.75	7.53E-03
Dihydrodeoxystreptomycin	C03755	3.75	3.42E-03
6-deoxyerythronolide B	C03240	3.69	8.39E-05
2,4-Bis(acetamido)-2,4,6-trideoxy-beta-L-altropyranose	C19972	3.67	1.85E-02
Lithocholic acid	C03990	3.59	6.02E-03
MILTEFOSINE		3.53	2.56E-04
Oleandolide	C11990	3.53	3.03E-03
CAPSAICIN	C06866	3.52	1.40E-03
Sucrose	C00089	3.52	2.53E-03
7-Methylxanthosine	C16352	3.49	6.10E-03
LIMONIN	C03514	3.48	4.16E-03
Abcisate	C06082	3.47	4.49E-03
9alpha-Hydroxyandrost-1,4-diene-3,17-dione	C14909	3.46	3.14E-03
Allocryptopine	C02134	3.45	5.74E-04

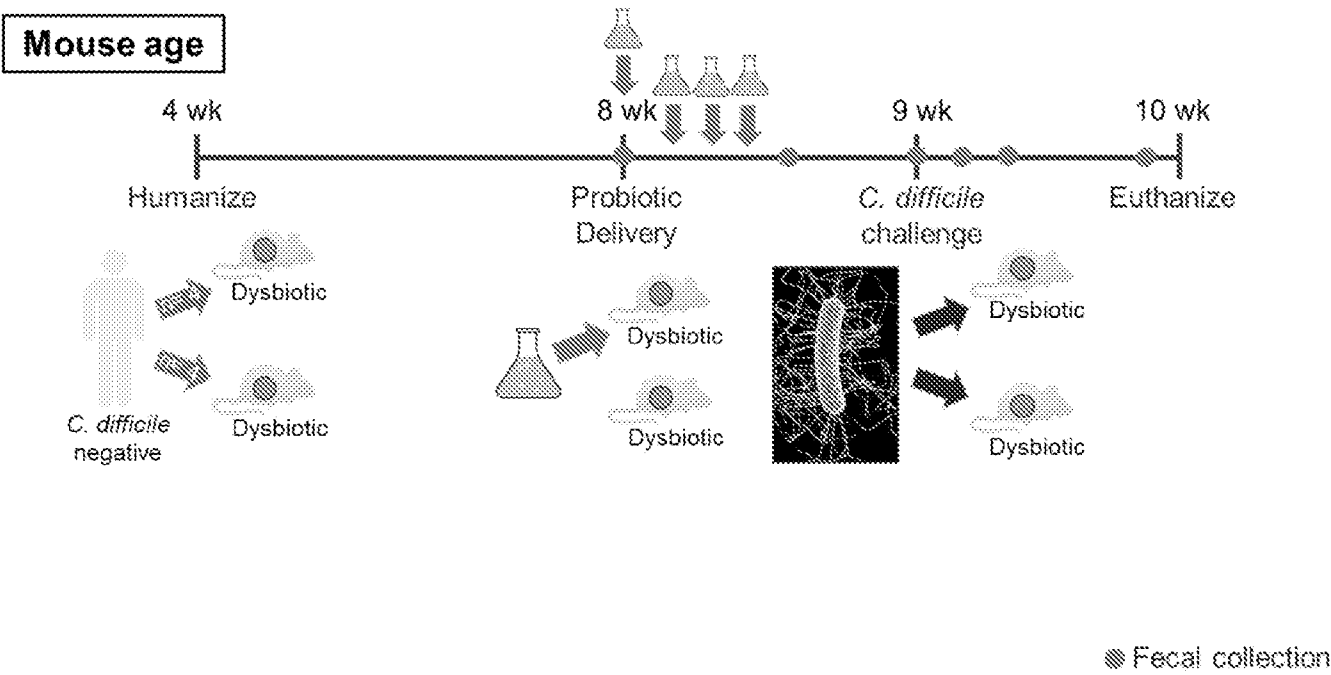
FIG. 19 (cont.)

Candidate Name	candidate_kegg	Log2Fold Change	pvalue
Adenosyl cobinamide	C06508	3.45	6.39E-04
Shikimic acid	C00493	3.41	1.67E-02
Biliverdin IX	C00500	3.37	2.36E-03
Arachidonoyl Ethanolamide	C11695	3.37	1.27E-02
Precorrin 8X	C06408	3.36	4.62E-04
Thebaine	C06173	3.34	3.90E-04
3-Hydroxyethylbacteriochlorophyllide a	C18153	3.34	1.76E-03
Tetrahydrofolic acid	C00101	3.33	1.42E-02
3,7,12-Trioxo-5 β -cholan-24-oic Acid	C13154	3.32	1.13E-02
Prebetanin	C08567	3.31	4.39E-04
Avermectin A1b	C11968	3.31	3.84E-03
Leukotriene A4	C00909	3.30	2.95E-03
		3.29	2.63E-03
Leukotriene E4	C05952	3.29	4.63E-03
Homotrypanothione	C16567	3.26	3.39E-05
Buspirone	C06861	3.25	9.01E-04
7 α -Hydroxycholest-4-en-3-one	C05455	3.23	2.06E-04
FMLP	C11596	3.19	3.29E-03
17-beta-estradiol-3-glucuronide	C03033	3.12	8.42E-03
meso-2,6-Diaminoheptanedioate	C00680	3.12	4.69E-03
Cholesterol	C00187	3.08	4.24E-04
Chondroitin	C00401	3.08	3.83E-03
Z-Gly-Pro-Leu-Gly-Pro	C03183	3.07	6.04E-03
Nopaline	C01682	3.05	3.66E-03
prasterone sulfate	C04555	3.05	5.82E-03
Erythronolide B	C06635	2.99	1.91E-04
Rec-beta-Tocopherol	C14152	2.99	1.90E-03
2-Arachidonoylglycerol	C13856	2.98	1.43E-02
S-Adenosylmethioninamine	C01137	2.96	2.24E-02
Daunorubicin	C01907	2.94	1.39E-02
Epothilone C	C15694	2.93	1.33E-02
O-1,4- α -L-Dihydrostreptosyl-streptidine 6-phosphate	C04767	2.93	4.17E-03
germacradienol	C16143	2.92	2.17E-03
Morphine 3-glucuronide	C16643	2.87	6.70E-03
1-Palmitoyl-2-(5-keto-8-oxo-6-octenoyl)-sn-glycero-3-phosphatidylcholine	C13902	2.86	6.36E-04
(10S)-Juvenile hormone III diol phosphate	C16507	2.86	7.54E-02
Kabiramide B		2.85	1.12E-02
Traumatic acid	C16308	2.85	3.97E-02
3 α ,7 α ,12 α -trihydroxy-5 α -cholan-24-yl sulfate	C16259	2.83	4.70E-03
Urdamycinone B	C12404	2.83	1.56E-03
Gambiridin A1	C17772	2.77	5.33E-03
Phorbol 12,13-dibutanoate	C03634	2.75	3.30E-04
(S)-6-O-Methylnorlaudanosoline	C06517	2.73	2.66E-02

FIG. 19 (cont.)

Candidate Name	candidate_kegg	Log2Fold Change	pvalue
Amikacin	C06820	2.73	3.06E-03
Nicotianamine	C05324	2.73	4.06E-02
Tetracosatetraenoyl CoA	C16171	2.66	7.27E-03
27-O-Demethyl-rifamycin SV	C14727	2.65	2.87E-03
beta-D-Glucosyl crocetin	C19867	2.64	2.60E-03
Iokundjoxide	C08874	2.63	2.01E-03
trans,trans-Farnesyl phosphate	C20121	2.63	1.65E-02
Horhammericine	C11677	2.60	2.25E-03
6,8a-Seco-6,8a-deoxy-5-oxoavermectin "2a" aglycone	C11969	2.55	2.18E-02
Mascaroside	C09132	2.54	7.58E-02
Tylactone	C12000	2.53	1.46E-02
13S-hydroperoxy-9Z,11E,14Z-octadecatrienoic acid	C04785	2.45	8.02E-03
6'-Dehydro-6'-oxoparomamine	C17583	2.43	9.23E-03
Chlorobactane		2.40	1.09E-02
Linamarin	C01594	2.38	2.59E-02
Avermectin A1a monosaccharide	C11982	2.38	2.32E-03
(-)-Menthyl acetate	C09870	2.38	5.13E-03
Glutathionylaminopropylcadaverine	C16566	2.37	7.15E-04
S-Glutaryl dihydroliipoamide	C06157	2.36	1.68E-02
Chlorophyllide b	C16541	2.35	4.90E-03
3-Hydroxy-9,10-secoandrosta-1,3,5(10)-triene-9,17-dione	C19944	2.33	4.13E-02
Ergosta-5,7,22,24(28)-tetraen-3 β , γ -ol	C05440	2.33	9.47E-04
glycochenodeoxycholic acid 7-sulfate	C15559	2.32	2.53E-03
LPA(0:0/16:0)	C00416	2.31	2.88E-04
Cer(d16:1/23:0)		2.31	1.83E-03
N4-(b-N-Acetyl-D-glucosaminy)-L-asparagine	C04540	2.30	8.20E-03
3-Oxo-delta4-steroid	C00619	2.28	8.69E-02
D-Glucosaminide	C06023	2.28	3.31E-03
Dinoprost (prostaglandin F2- α ;))	C00639	2.27	3.71E-03
Protorifamycin I	C12246	2.27	1.51E-03
Pantetheine	C00831	2.27	1.68E-01
8,8a-Deoxyoleandolide	C11989	2.26	6.63E-03
Deoxycytidine	C00881	2.25	9.08E-02
Glycosyl-4,4'-diaponeurosporenoate	C16147	2.24	1.23E-03
Methymycin	C11996	2.22	1.43E-02
Demethylcitalopram	C16608	2.14	2.24E-02
Albomaculine	C08515	2.14	1.42E-02
L-Serine-phosphoethanolamine	C03872	2.10	1.31E-02
L-N2-(2-Carboxyethyl)arginine	C06655	2.05	1.65E-03
(2-Naphthyl)methanol	C02909	2.04	2.73E-02
5-(3'-Carboxy-3'-oxopropenyl)-4,6-dihydroxypicolinate	C05641	2.04	5.81E-02
Ipecac (Emetamine)	C09420	2.02	2.28E-02
PI(17:0/20:4(5Z,8Z,11Z,14Z))		2.01	1.01E-02
Dihydroptericoic acid	C00921	2.01	1.11E-02
Desmosterol	C01802	2.01	6.82E-04

FIG. 20



INTERNATIONAL SEARCH REPORT

International application No.

PCT/US2016/053073

A. CLASSIFICATION OF SUBJECT MATTER IPC(8) - A61K 35/741; A61K 35/742; A61K 35/744; A61K 35/745 (2016.01) CPC - A61K 35/74; A61K 35/741; A61K 35/742; A61K 35/745; A61K 35/747; C12R 1/00 (2016.11) According to International Patent Classification (IPC) or to both national classification and IPC		
B. FIELDS SEARCHED Minimum documentation searched (classification system followed by classification symbols) IPC - A61K 35/741; A61K 35/742; A61K 35/744; A61K 35/745 CPC - A61K 35/74; A61K 35/741; A61K 35/742; A61K 35/745; A61K 35/747; C12R 1/00 Documentation searched other than minimum documentation to the extent that such documents are included in the fields searched USPC - 424/93.41; 424/93.3; 424/93.4 (keyword delimited) Electronic data base consulted during the international search (name of data base and, where practicable, search terms used) Orbit, Google Patents, Google Scholar Search terms used: risk predict Roseburia faecis Faecalibacterium prausnitzii Akkermansia muciniphila		
C. DOCUMENTS CONSIDERED TO BE RELEVANT		
Category*	Citation of document, with indication, where appropriate, of the relevant passages	Relevant to claim No.
X	WO 2014/110493 A1 (BAYLOR COLLEGE OF MEDICINE) 17 July 2014 (17.07.2014) entire document	1-8, 12-14, 23, 24
X	WO 2014/150094 A1 (UNIVERSITY OF FLORIDA RESEARCH FOUNDATION, INC.) 25 September 2014 (25.09.2014) entire document	9, 11, 32, 36, 38
Y		34, 35
X	WO 2015/095241 A2 (SERES HEALTH, INC.) 25 June 2015 (25.06.2015) entire document	15-18
X	US 2014/0296134 A1 (THE BOARD OF REGENTS OF THE UNIVERSITY OF TEXAS SYSTEM) 02 October 2014 (02.10.2014) entire document	19-22, 25-28
Y		29-31
Y	— THERIOT et al. "Antibiotic-induced shifts in the mouse gut microbiome and metabolome increase susceptibility to Clostridium difficile infection," Nature Communications, 20 January 2014 (20.01.2014), Vol. 5, Pgs. 1-10 and Supplemental Information. entire document	29-31
Y	US 2014/0363397 A1 (ALLEN-VERCOE et al) 11 December 2014 (11.12.2014) entire document	34, 35
A	✓ DUBBERKE et al. "Development and validation of a Clostridium difficile infection risk prediction model," Infection Control and Hospital Epidemiology, 04 April 2011 (04.04.2011), Vol. 32, No. 4, Pgs. 360-366. entire document	1-36, 38
A	✓ RIDLON et al. "The human gut sterolbiome: bile acid-microbiome endocrine aspects and therapeutics," Acta Pharmaceutica Sinica B, 09 February 2015 (09.02.2015), Vol. 5, Iss. 2, Pgs. 99-105. entire document	1-36, 38
<input type="checkbox"/> Further documents are listed in the continuation of Box C. <input type="checkbox"/> See patent family annex.		
* Special categories of cited documents: "A" document defining the general state of the art which is not considered to be of particular relevance "E" earlier application or patent but published on or after the international filing date "L" document which may throw doubts on priority claim(s) or which is cited to establish the publication date of another citation or other special reason (as specified) "O" document referring to an oral disclosure, use, exhibition or other means "P" document published prior to the international filing date but later than the priority date claimed "T" later document published after the international filing date or priority date and not in conflict with the application but cited to understand the principle or theory underlying the invention "X" document of particular relevance; the claimed invention cannot be considered novel or cannot be considered to involve an inventive step when the document is taken alone "Y" document of particular relevance; the claimed invention cannot be considered to involve an inventive step when the document is combined with one or more other such documents, such combination being obvious to a person skilled in the art "&" document member of the same patent family		
Date of the actual completion of the international search 09 November 2016		Date of mailing of the international search report 15 DEC 2016
Name and mailing address of the ISA/US Mail Stop PCT, Attn: ISA/US, Commissioner for Patents P.O. Box 1450, Alexandria, VA 22313-1450 Facsimile No. 571-273-8300		Authorized officer Blaine R. Copenheaver PCT Helpdesk: 571-272-4300 PCT OSP: 571-272-7774

INTERNATIONAL SEARCH REPORT

International application No.

PCT/US2016/053073

Box No. II Observations where certain claims were found unsearchable (Continuation of item 2 of first sheet)

This international search report has not been established in respect of certain claims under Article 17(2)(a) for the following reasons:

1. ☐ Claims Nos.:
because they relate to subject matter not required to be searched by this Authority, namely:
2. ☐ Claims Nos.:
because they relate to parts of the international application that do not comply with the prescribed requirements to such an extent that no meaningful international search can be carried out, specifically:
3. ☒ Claims Nos.: 37
because they are dependent claims and are not drafted in accordance with the second and third sentences of Rule 6.4(a).

Box No. III Observations where unity of invention is lacking (Continuation of item 3 of first sheet)

This International Searching Authority found multiple inventions in this international application, as follows:

1. ☐ As all required additional search fees were timely paid by the applicant, this international search report covers all searchable claims.
2. ☐ As all searchable claims could be searched without effort justifying additional fees, this Authority did not invite payment of additional fees.
3. ☐ As only some of the required additional search fees were timely paid by the applicant, this international search report covers only those claims for which fees were paid, specifically claims Nos.:
4. ☐ No required additional search fees were timely paid by the applicant. Consequently, this international search report is restricted to the invention first mentioned in the claims; it is covered by claims Nos.:

Remark on Protest

- ☐ The additional search fees were accompanied by the applicant's protest and, where applicable, the payment of a protest fee.
- ☐ The additional search fees were accompanied by the applicant's protest but the applicable protest fee was not paid within the time limit specified in the invitation.
- ☐ No protest accompanied the payment of additional search fees.